AN ABSTRACT OF THE THESIS OF

J. KIRK McGLOTHLAN for the degree of Master of Science

in Chemistry presented on August 19, 1982.

Title: REDUCTION OF ZIRCONIUM(IV) AT A Pt MICROELECTRODE IN
        FUSED EQUIMOLAR SODIUM CHLORIDE - POTASSIUM CHLORIDE

Abstract approved: <u>_____Redacted for Privacy_____</u>
Dr. Harry Freund

Previous potentiometric studies of zirconium in fused equimolar sodium chloride - potassium chloride eutectic have yielded conflicting formal potentials for the reduction half reactions. Russian investigators report Zr(IV) and Zr(II) to be the only stable species, while Canadian investigators report Zr(IV), Zr(III) and Zr(II) to be stable.

Cyclic voltammetry, differential pulse, normal pulse and DC polarography have been used to study the reduction of Zr(IV) in fused equimolar NaCl-KCl. The studies were carried out at temperatures ranging from 953K to 1123K, and concentrations ranging from 2.5×10^{-5} to 7.4×10^{-4} mole fraction of Zr(IV). It was found that Zr(IV) is reduced by a quasi-reversible two electron step according to the reaction:

$$Zr(IV) + 2e^- \rightleftharpoons Zr(II)$$
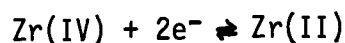
The formal potential observed is -1.25 volts versus a standard Cl_2 electrode at 1013K. The Zr(II) species produced is only slightly soluble in NaCl-KCl eutectic.

REDUCTION OF ZIRCONIUM(IV) AT A Pt MICROELECTRODE

IN FUSED EQUIMOLAR SODIUM CHLORIDE - POTASSIUM CHLORIDE

by

J. Kirk McGlothlan

A THESIS

submitted to

Oregon State University

in partial fulfillment of
the requirements for the
degree of
Master of Science

Commencement June 1983

APPROVED:

Redacted for Privacy

Professor of Chemistry in charge of major

Redacted for Privacy

Chairman of Department of Chemistry

Redacted for Privacy

Dean of Graduate School

Date thesis is presented __August 19, 1982__

Typed by Opal Grossnicklaus for J. Kirk McGlothlan

TABLE OF CONTENTS

LIST OF TABLES

REDUCTION OF ZIRCONIUM(IV) AT A PLATINUM MICROELECTRODE
IN FUSED EQUIMOLAR SODIUM CHLORIDE - POTASSIUM CHLORIDE

Electrochemistry in Fused Salts

The history of modern electrochemistry in fused salts stretches back to an article written in 1912 by Baur and Ehrenberg (5). It describes studies dealing with the use of an oxygen electrode in fused borates, silicates, oxides, carbonates, phosphates, and sulphates. Despite such early interest most of the published work has appeared since 1945. Interest peaked in the late 50's and the 60's, when most work was related to the nuclear industry. The nature of the work has changed in recent years, being directed more towards other types of energy research. The present concern about energy has led to a mild resurgence in fused salt research.

Two monographs on fused salts which were written in the early 60's include chapters on electrochemistry, both coauthored by H. A. Laitinen (6, 45). They cover well the dynamic types of electrochemical measurements done until then, but do not cover emf measurements.

Fused salt electrochemistry has been attractive for both dynamic and static systems for one reason in particular, the high exchange current densities. As a consequence many systems are reversible in fused salts which are often irreversible in aqueous systems. This is especially true for the Ag,Ag(I) systems.

Hamer et al (17) in 1956 collected the available thermodynamic data to calculate a tabulation of theoretical emf's for cells containing a single molten chloride electrolyte. Reversible cells

of the type:

$$M/MCl_n/Cl_{2(g)}(C) \tag{1}$$

Where M is a metallic element in the solid, liquid or gaseous state and MCl_n is the corresponding chloride in the solid or liquid state, the net cell reaction is:

$$M + n/2 \; Cl_2 \; \rightleftarrows \; MCl_n \tag{2}$$

Thus $\Delta G^o = -nFE^o_{cell}$ corresponds to the free energy of formation of MCl_n. Typically the free energy is evaluated from thermochemical information on the temperature dependence of heat of formation. Starting with the fundamental definition:

$$\Delta G^o = \Delta H^o - T\Delta S^o \tag{3}$$

a direct relationship can be developed between ΔG^o and ΔH^o:

$$\frac{\Delta G^o}{T} = \frac{\Delta H^o}{T} - \Delta S^o \tag{4}$$

which may be differentiated at constant pressure and each term reduced to yield:

$$\frac{\partial \left(\frac{\Delta G^o}{T} \right)}{\partial T} = \frac{-\Delta H^o}{T^2} \tag{5}$$

If $\Delta H^o = \Delta H^o_0 + \int_{T_1}^{T_2} \Delta C_p \; dT$ and expressing ΔC_p as a function of T:

$$\Delta C_p = \Delta a + (\Delta b)T + \frac{(\Delta C)}{T^2} \tag{6}$$

leads to:

$$(\Delta H^o)_{T_2} = (\Delta H^o_0)_{T_1} + \int_{T_1}^{T_2}[(\Delta a) + (\Delta b)T + \frac{(\Delta c)}{T_2}]dT \tag{7}$$

Where T_1 is the reference temperature, generally 298K, and T_2 the temperature of interest, substituting into the general equation leads to:

$$\Delta G^{o} = \Delta H_0^{o} - (\Delta a)T \ln T - (\Delta b)T - \frac{(\Delta c)}{2T} + T \qquad (8)$$

Specifically in the case of zirconium chlorides Hamer reports only the limited data shown in Table I.

TABLE I. HAMER'S THEORETICAL E^{o} VALUES

Net Cell Reaction	E^{o} volts	Temp K
$Zr + Cl_2 \rightleftarrows ZrCl_2$ (c)	2.594	723
(m.pt. $ZrCl_2$: 995K)	2.560	773
	2.526	823
	2.508	873
$Zr + 3/2\ Cl_2 \rightleftarrows ZrCl_3$	2.540	673
(m.pt. $ZrCl_3$: 1300K)	2.509	723
	2.492	773

The need during the 1950's for good thermodynamic data lead to the compilation of the Janaf Thermochemical Tables (21). The best data collected for $ZrCl_2$, $ZrCl_3$, and $ZrCl_4$ in the temperature range 700K to 1000K are shown in Table II.

The Janaf Tables and Hamer's tabulations presumably set limits for E^{o} values for no interaction with any solvent is considered. We know that interaction with fused alkali halides occurs and this should make it more difficult to achieve reduction. Hence the experimentally determined E^{o} values for formation will tend to be less positive than the calculated values for the pure compounds.

The 1950's and 1960's saw several attempts to determine emf series for metals in molten alkali halides. Of most lasting value are the tabulations of Laitinen and Liu (27) and Flengas and

TABLE II. THEORETICAL E^o VALUES FROM THE JANAF TABLES

	$G^o_{kcal/mol}$	$E^o volt$	T^oK
$Zr + Cl_2 \rightleftarrows ZrCl_2(c)$	-107.898	2.339	700
	-104.718	2.270	800
	-101.589	2.203	900
	- 98.514	2.136	1000
	- 95.489	2.070	1100
$Zr + Cl_2 \rightleftarrows ZrCl_2(l)$	-106.022	2.299	700
	-103.414	2.242	800
	-100.888	2.187	900
	- 98.436	2.134	1000
	- 95.050	2.082	1100
$Zr + \frac{3}{2}Cl_2 \rightleftarrows ZrCl_3(c)$	-166.377	2.405	700
	-161.038	2.328	800
	-155.765	2.251	900
	-150.555	2.176	1000
	-145.401	2.102	1100
$Zr + 2Cl_2 \rightleftarrows ZrCl_4(c)$	-183.811	1.993	700
	-176.962	1.918	800
	-170.188	1.845	900
	-163.488	1.772	1000
	-156.850	1.700	1100
$Zr + 2Cl_2 \rightleftarrows ZrCl_4(g)$	-187.895	2.037	700
	-185.213	2.008	800
	-182.531	1.979	900
	-179.854	1.950	1000
	-177.178	1.921	1100

Ingraham (15). Use of these tabulations is complicated by the methods of reporting results. Thus there are $E^o_{molarity}$, $E^o_{molality}$, and $E^o_{mole\ fraction}$, and measurements are reported versus AgCl,Ag, $PtCl_2$, Pt and Cl_2,Cl- reference electrodes. The relationship among the three E^o scales depends on the specific reference electrode employed.

It is of particular importance to be able to compare the AgCl,Ag reference electrode to the fundamental Cl_2,Cl- reference electrode. Flengas (15) reports:

Net Cell Reaction	E^{o*}mole fraction volts	Temp. K
AgCl + Cl- $\rightleftarrows$ Ag + ½Cl$_2$ -.845		973
1:1		
NaCl , KCl -.820		1073
-.795		1173

Hamby and Scott (18) performed experiments in the 1:1 NaCl-KCl eutectic with Ag,AgCl and Cl_2,Cl- electrodes. They confirmed the results of Flengas and devised several types of Ag,AgCl reference electrodes.

The linear least squares plot for the temperature dependence of the AgCl,Ag formal potential as proposed by Flengas is:

$$E^{o*}_{AgCl,Ag} \quad in \ 1:1 \quad = \quad -0.900 \ volt$$
$$vs \quad NaCl-KCl$$
$$Cl_2,Cl-$$

Laitinen and Liu report at 723K for LiCl-KCl eutectic:

Measurement vs PtCl$_2$, Pt in LiCl-KCl Eutectic	$E^o_{mole\ fraction,723K}$,volt
Cl$_2$,Cl-	+0.216
AgCl,Ag	-0.637

Hence $E^o_{mole\ fraction,723K}$ for AgCl,Ag vs Cl_2,Cl- is calculated to be -0.853 volt. Considering the different solvents and the extrapolation the agreement is reasonable with the somewhat more negative value as expected being found in the NaCl-KCl solvent.

Introduction

The electrochemistry of zirconium in fused alkali chlorides has been the subject of many studies. The results of these studies are not always compatible. Not only are the formal potentials different (Table III), but the studies do not agree with respect to the cell reactions involved. The disagreement in the reactions involved is centered around whether zirconium(III) is involved in the reaction steps. The two major articles were written by Komarov, Smirnov, and Baraboshkin (22), and by Swaroop and Flengas (49).

The potentiometric study of equilibria between metals and their ions in various oxidation states in molten alkali halides has been developed generally by M. V. Smirnov and co-workers (41) and also specifically with respect to zirconium and zirconium halides (22,42).

The researches of Flengas and his co-workers (49) relate both to the thermodynamic interpretation of cells containing zirconium metal in equilibrium with its chlorides and to the preparation and properties of lower valent zirconium halides (12, 28, 47, 49). Studies by Struss and Corbett on lower valence zirconium halides present additional data (43, 44). Other investigations were conducted by Yang and Hudson (51, 52), Suzuki (46), Baboian, Hill, and Bailey (3), and by Eon, Pommier, and Fondanaïche (13).

Despite the key papers just cited, together with dozens of supporting papers from the Russian (Smirnov et al) and Canadian (Flengas et al) laboratories, the nature of the zirconium-zirconium halide systems remains confused, and with unresolved conflicts. Unfortunately the Russian papers are very difficult to review

TABLE III. FORMAL POTENTIALS

REACTIONS	POTENTIALS (volts vs $Cl_2,Cl-$)		

1. SWAROOP AND FLENGAS (49)   (NaCl-KCl)

	943K	973K	1013K
$Zr(II) + 2e- \rightleftarrows Zr$	-2.225	-2.200	-2.166
$Zr(III) + e- \rightleftarrows Zr(II)$	-1.837	-1.813	-1.784
$Zr(IV) + e- \rightleftarrows Zr(III)$	-1.266	-1.240	-1.205
$Zr(III) + 3e- \rightleftarrows Zr$	-2.096	-2.071	-2.039
$Zr(IV) + 4e- \rightleftarrows Zr$	-1.888	-1.863	-1.830

2. T. SUZUKI (46)   (LiCl-KCl)

	723K
$Zr(IV) + 4e- \rightleftarrows Zr$	-2.07

3. KOMOROV, SMIRNOV, BARABOSHKIN (22)   (NaCl-KCl)

$Zr(II) + 2e- \rightleftarrows Zr$	$-2.55 + 6.7 \times 10^{-4}T$
$Zr(IV) + 4e- \rightleftarrows Zr$	$-2.62 + 6.7 \times 10^{-4}T$
$Zr(IV) + 2e- \rightleftarrows Zr(II)$	$-2.69 + 6.7 \times 10^{-4}T$

4. BABOIAN, HILL, BAILEY (3)   (LiCl-KCl)

	723K	823K
$Zr(II) + 2e- \rightleftarrows Zr$	-1.86	-
$Zr(IV) + 4e- \rightleftarrows Zr$	-	-1.77

5. EON, POMMIER, FONDANAICHE (13)   (LiCl-KCl)

	973K
$Zr(IV) + 2e- \rightleftarrows Zr(II)$	-1.850
$Zr(II) + 2e- \rightleftarrows Zr$	-2.150

critically, for in translation (presumably) errors both of substance and typography may have occured. The following sections of this thesis include independent theoretical and mathematical developments to the extent possible, with the objective of clarifying the results described in the Russian and Canadian papers.

High temperature equilibria between metals and their ions involve soluble species, often in various oxidation states.

In the specific case of zirconium such abbreviated reactions could be described:

$$Zr(IV) + 4e- \rightleftarrows Zr_{(c)} \qquad (9)$$

$$Zr(IV) + 1e- \rightleftarrows Zr(III) \qquad (10)$$

$$Zr(III) + 1e- \rightleftarrows Zr(II) \qquad (11)$$

Zr(I) has not been observed in fused alkali halides, and conflicting evidence has been reported for the existence of Zr(II) and Zr(III). Smirnov and Kudyakov (41) consider the system to be described completely by:

$$Zr(IV) + 4e- \rightleftarrows Zr_{(c)} \qquad (12)$$

$$Zr(IV) + 2e- \rightleftarrows Zr(II) \qquad (13)$$

This work will examine and attempt to explain the differences and to resolve the conflict. The work done by Komarov, Smirnov and Baraboshkin, and that done by Swaroop and Flengas will be discussed in some detail.

Historical

Komarov, Smirnov and Baraboshkin ("the Russians") prepared all of their solutions by anodic dissolution of zirconium metal into the molten electrolyte. The composition of the melt was determined by "the amount of electric energy passed through it, and by chemical analysis of the material in the crucible after the experiment." They prepared three solutions. Their three solutions had reported compositions of 0.16%, 1.24%, and 6.8% zirconium by weight in 1:1 molar NaCl-KCl. They give the mole fractions of zirconium for the 0.16% and 6.8% zirconium solutions as 5.83×10^{-4} and 2.46×10^{-2} respectively. They did not publish any mole fraction for the 1.24% zirconium solution. We calculated mole fractions for these solutions to be 1.17×10^{-3} for the 0.16% solution, 9.07×10^{-3} for the 1.24% solution and 5.05×10^{-2} for the 6.8% zirconium solution. These mole fractions were calculated assuming that the percentages of zirconium given are correct and that the Russians corrected for the amount of sodium or potassium reduced out of the melt when the zirconium was anodically disolved. However, even if they did not, the difference between these values and the true values would be small. There is no way to ascertain whether the inconsistency is due to an error in the reported weight percent or mole fraction.

Their cell is shown in Figure 1. The zirconium melt was contained in a baked zirconium dioxide crucible, suspended in the melt by molybdenum wires. The potential of a zirconium electrode in the melt was measured versus a chlorine reference electrode, at a series of temperatures ranging from 943K to 1253K. For each solution
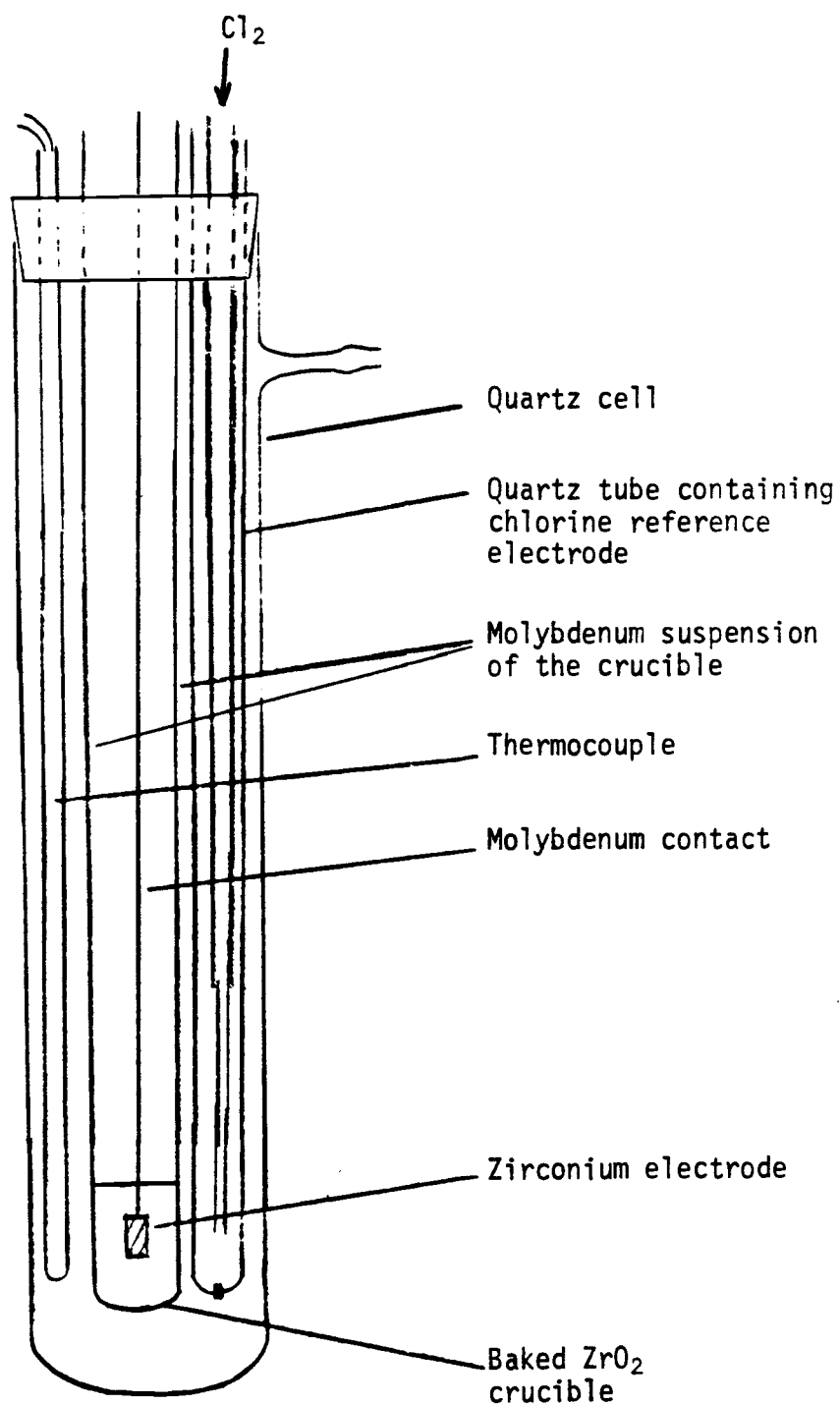
Figure 1. Cell of Komarov, Smirnov and Baraboshkin.

a least squares fit of the data points yields an empirical equation
relating temperature and cell potential. The equations the
Russians obtained, corrected for the thermal emf's are:

0.16%Zr
$$E = -2.552 + 3.45 \times 10^{-4}T \text{ volts} \tag{14}$$

1.24% Zr
$$E = -2.579 + 4.55 \times 10^{-4}T \text{ volts} \tag{15}$$

6.8% Zr
$$E = -2.579 + 5.26 \times 10^{-4}T \text{ volts} \tag{16}$$

Using these three equations isotherms relating cell potential and
zirconium concentration were constructed. Three points were used to
determine the line. Isotherms were constructed at 1000K, 1050K,
1150K and 1200K. Figure 2 shows the 1000K isotherm, using the mole
fractions we calculated, and the Russians' mole fraction.

The slope of the isotherm at the 0.16% zirconium point corre-
sponds to a Nernstian slope for a two electron reaction. Therefore
it was assumed only zirconium(II) was present. Assuming only zir-
conium(II) present, in the solution and in equilibrium with the
Zr metal electrode, equation 14 can be related to the Nernstian
expression for the cell potential.

$$-2.552 + 3.45 \times 10^{-4}T = E^{o\prime} + 0.992 \times 10^{-4}T \log(Zr^{2+}) \tag{17}$$

Using the Russians' value for the mole fraction the equation for the
formal potential becomes:

$$E^{o\prime}_{Zr(II),Zr} = -2.55 + 6.7 \times 10^{-4}T \tag{18}$$

Using our value for the mole fraction it becomes:

$$E^{o\prime}_{Zr(II), Zr} = -2.55 + 6.4 \times 10^{-4}T \tag{19}$$

This difference will not nearly account for the discrepancies
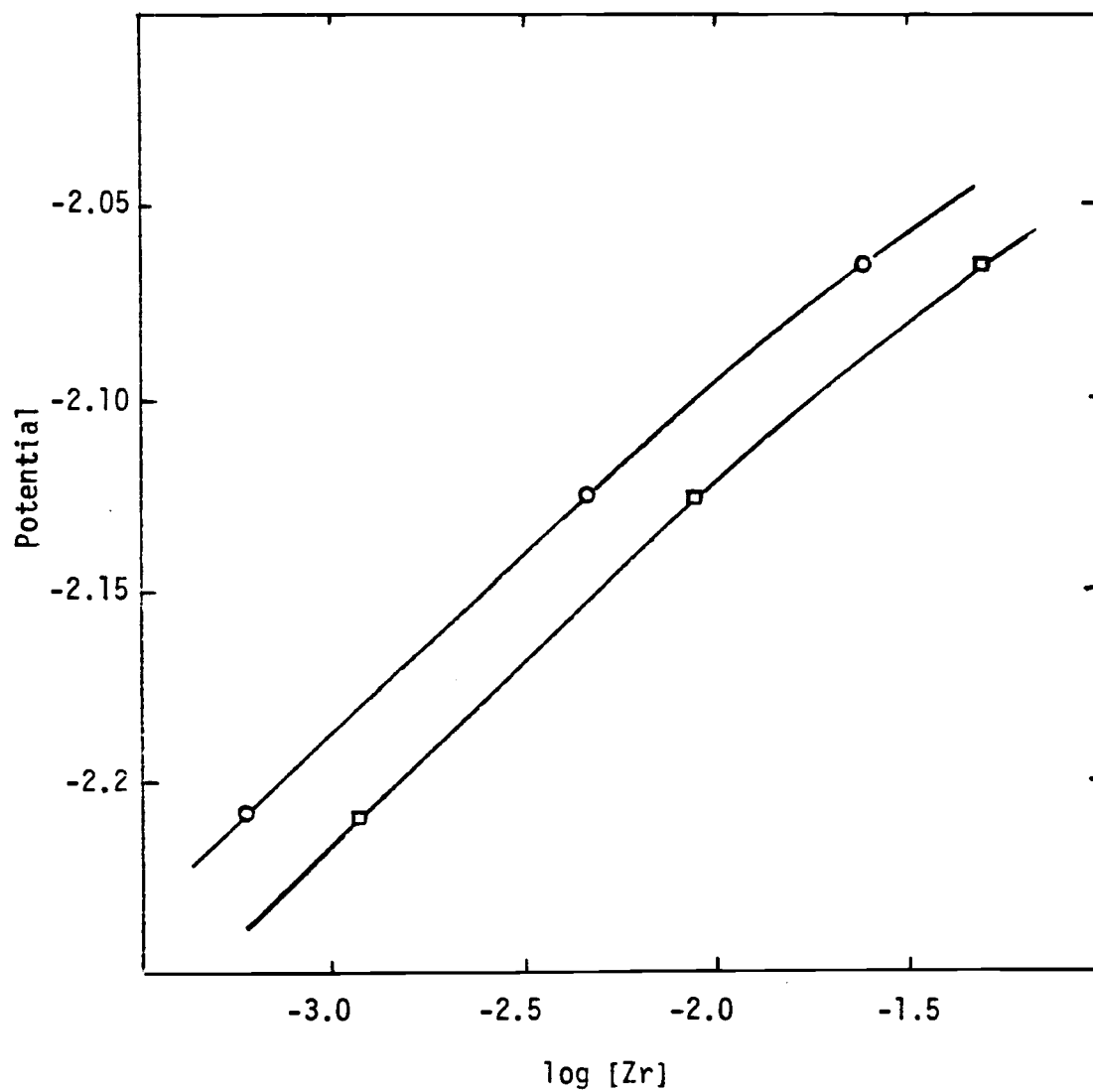
Figure 2. 1000°K Isotherm using Komanov et al.'s data.

o = Komanov et al's mole fractions

□ = Our calculated mole fractions

mentioned earlier. The slope of the isotherm where the zirconium concentration is 6.8% gives an n value greater than two. The Russians assumed that zirconium(III) was not present in the melt. They based this assumption on the findings of Larson and Leddy (25) that pure zirconium trichloride dissociates above 723K. Assuming then that only zirconium(IV) and zirconium(II) are present in the melt the fraction of zirconium(IV) in the melt can be found using equation 21. Equation 21 is derived by equating the total number of coulombs (nF $mole_{(Zr)}$) with the sum of the coulombs due to Zr(II), and due to the Zr(IV).

$$n_{ave}F[M_{Zr(T)}] = 2F \, [M_{Zr(II)}] + 4F \; [M_{Zr(IV)}] \qquad (20)$$

cancelling, and substituting $\quad [M_{Zr(II)}] = [M_{Zr_{(T)}}] - [M_{Zr(IV)}]$

$$n_{ave} \, [M_{Zr(T)}] - 2 \, [M_{Zr(T)}] - [M_{Zr(IV)}] + 4F \, [M_{Zr(IV)}]$$

$$\frac{n_{ave}-2}{2} = \frac{M_{Zr(IV)}}{M_{Zr(T)}}$$

$$X = (n_{ave}-2)/2 \qquad (21)$$

X is the fraction of the total zirconium which is Zr(IV).

Each isotherm gives a different slope and a slightly different X value. Because of this the cell potential cannot simply be related to the Nernstian expression. By relating the cell potential and the fraction of zirconium(IV) at each temperature, a series of formal potentials is obtained. A least squares fit of these points yields an equation for the formal potential of the zirconium (IV) zirconium couple.

$$E^{o'}_{Zr(IV),Zr} = -2.62 + 6.7 \times 10^{-4}T \text{ volts} \qquad (22)$$

This equation was obtained using the Russians' values for the mole fractions and X values.

The zirconium(II), Zirconium(IV) formal potential can then be calculated from the formal potentials for zirconium(II), zirconium and zirconium(IV), zirconium, and is:

$$E^{\circ\prime}_{Zr(IV),Zr(II)} = -2.69 + 6.7 \times 10^{-4} T \text{ volts} \tag{23}$$

Using this value for the formal potential for the reaction:

$$Zr(IV) + Zr \rightleftharpoons 2 Zr(II) \tag{24}$$

The equilibrium constant (K) can be calculated from equation 25.

$$\Delta G = -RT \ln K \tag{25}$$

This yields a value for K of 0.0388 at 1000K. For this value of K and at a total mole fraction of zirconium of 2.46×10^{-2}, the fraction of zirconium(IV) that is predicted to be in the melt is 0.306. The fraction of zirconium(IV) that they calculated from the slope of the isotherm is 0.18 at 1000K.

The Russians' technique of analyzing their data is questionable. They use three points on a plot of potential versus log $[Zr_{(T)}]$ to determine two different slopes. The three points are determined by empirical equations, and not by direct experimental results. The use of the equation inserts more uncertainty into the potential data. In addition each solution containing a given concentration of zirconium was apparently prepared only once, and the temperature versus cell potential data taken only once for each solution. The problems associated with fused salt work make single determinations suspect. Even if their data analysis is suspect, the potentials they measured are not in the range of those measured by Swaroop and Flengas (49).

Swaroop and Flengas (49) ("the Canadians") prepared their solutions by two different techniques. The first was by direct addition of previously prepared salts. The preparation of these salts is described in several articles (28, 47, 48). The second method of preparation was by the direct reaction of zirconium and zirconium(III) in the melt to produce zirconium(II).

$$Zr_s + 2(ZrCl_3) = 3(ZrCl_2) \qquad (26)$$

The weight loss of the zirconium electrode was followed by measuring the extension of a quartz spring incorporated into the cell. Some weight loss of the rod was seen after the loss of weight from the zirconium rod reached the point where all the zirconium(III) had been reduced. 5×10^{-5} to 1×10^{-4} mole fraction of excess metal was dissolved in the melt. No explanation for this was given. The zirconium,zirconium(II) systems were prepared by both methods while the zirconium(III) and zirconium(IV) systems were prepared only by direct addition. The cell used is shown in Figure 3. The melt was contained in a platinum crucible.

The Canadians used a two electrode system, for which the reference electrode was a Ag,AgCl type electrode (14). Two measuring electrodes were used. First, for the Zr,Zr(II) systems, a Zr rod was used with a sliding seal to enable it to be inserted into or removed from the melt. The platinum crucible in which the melt was contained was used as the measuring electrode for the redox systems. Six zirconium(II) solutions were prepared, ranging in concentration from 0.925×10^{-3} to 6.81×10^{-3} mole fraction of zirconium. The zirconium(III) and zirconium(IV) concentrations were all in the range of 0.6×10^{-4} to 6×10^{-3} mole fraction. The potential of the platinum
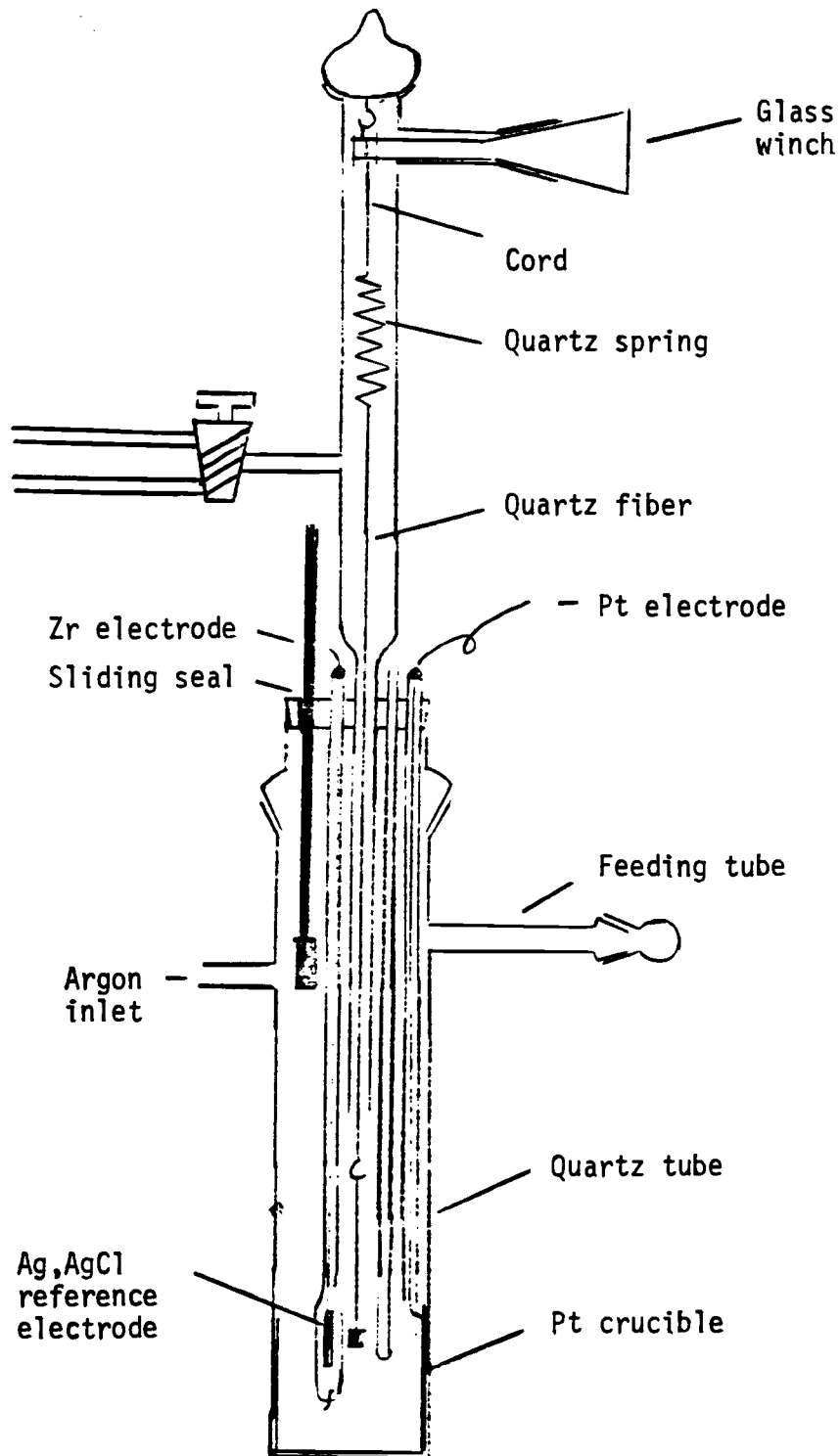
Figure 3. Cell of Swaroop and Flengas

electrode was measured versus Ag,AgCl in the temperature range of 943K to 1023K. They report that above 1023K the potential readings become unstable. Below 1023K the potentials became steady in three to six hours. The potentials were observed for another three hours to ensure that stability had been reached. The Canadians also performed an experiment in which a zirconium electrode was placed in a solution containing 8.5×10^{-3} mole fraction of zirconium(IV). The potentials of both the zirconium electrode and a platinum electrode were measured. The two potentials were not equal at the start of the experiment. They remained reasonably constant for about five hours, then started to change. The potential of the platinum electrode approached that of the zirconium electrode. It took 20 to 25 hours for the two electrodes to have equal potentials. Until the potentials became equal the system was reacting, was not at equilibrium, and no simple expression can be used to predict the potentials.

The Canadians also determined the liquidus curves of $NaCl-ZrCl_2$, $KCl-ZrCl_2$, $NaCl-ZrCl_3$, and $KCl-ZrCl_3$. They found that zirconium trichloride disproportionated in a NaCl melt, but was stable for at least 24 hours in both KCl and NaCl-KCl melts.

Other groups also have performed experiments on the zirconium-fused chlorides systems. Yang and Hudson (51, 52) carried out measurements of the potential of a zirconium bar in a zirconium(IV)-KCl-LiCl melt, and obtained a curve for the variation of potential with concentration. The varying slope indicated an n value changing from one to three, depending on the concentration. In a separate experiment they obtained a line with a slope indicating an n value

of 0.9. The system was apparently reacting during this series of measurements.

Suzuki (46) reported potential measurements on zirconium-LiCl-KCl systems in which the zirconium was added by anodic dissolution of a zirconium bar. Zirconium(IV) was reported to have formed at 723K in the melt, while a mixture of zirconium(IV) and zirconium(II) was formed at higher temperatures. Coulombs and the weight loss of the zirconium bar were compared in order to obtain n values. Above 723K increasing amounts of zirconium(II) were found in the melt.

In 1965 Baboian, Hill, and Bailey (3) described polarographic work on zirconium and hafnium in fused KCl-LiCl. They found that at 723K anodic dissolution of a zirconium bar yielded zirconium(IV), but at 823K anodic dissolution yielded mostly zirconium(II). Their polarograms of zirconium(IV) at 723K had the shape of a Heyrovsky-Ilkovic type wave, i.e. the plots of $\log(i/i_d-i)$ versus E were linear and the slopes indicated a four electron reaction. Their conclusion was that zirconium metal must have alloyed with the platinum microelectrode. They found no evidence of zirconium(III) in the melt. They detected zirconium tetrachloride in the argon stream used for stirring the melt when solutions of more than about 10^{-3} mole fraction of zirconium(IV) were used. At 723K the polarograms they obtained for zirconium(II) were indistinct, and not reproducible. The polarograms they obtained at 723K for zirconium(IV) were reproducible, and gave a single wave. At 823K two waves appear for the zirconium(IV) solutions, but they are not reproducible, and are indistinct. The two waves are at approximately -1.8 and -2.1 volts versus the chlorine reference electrode.

In 1969 Eon, Pommier, and Fondanaiche (13) reported cyclic voltammetric studies of zirconium in fused LiCl-KCl. Their article describes the electrochemical experiments as linear chronoamperometry. However, examination of the curves published shows that the experiments run were cyclic voltammetry. They used a Danner-Ray type reference electrode (10), with a carbon rod counter electrode and a dipping type tungsten working electrode. The working electrode was a straight cylinder of tungsten, four millimeters in diameter. They dried the LiCl-KCl eutectic by vacuum heat treatment, followed by HCl treatment as the temperature was raised and the salt melted. Argon was bubbled through the melt to remove the excess HCl gas. They found that at 773K zirconium(II) was formed by the anodic dissolution of zirconium. At 673K zirconium(IV) is formed by anodic dissolution of zirconium. Solutions of zirconium tetrachloride were prepared by addition of potassium hexachlorozirconate to the melt, in the concentration range between 4×10^{-4} and 1.2×10^{-3} mole fraction. At 673K only one reduction wave was found, corresponding to the reaction:

$$Zr(IV) + 2e- = Zr(II) \tag{27}$$
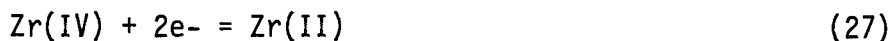
The zirconium(II) was deposited on the electrode in the form of the black shell that Bockris and his collaborators had reported earlier (20). This deposit of zirconium(II) could not be further reduced. At 973K two waves were observed, corresponding to the reactions:

$$Zr(IV) + 2e- = Zr(II) \tag{28}$$

$$Zr(II) + 2e- = Zr \tag{29}$$

The waves at 973K were distorted because of some deposition of the black zirconium dichloride species. They found the reaction of

zirconium(IV) forming zirconium(II) to be "highly irreversible."

Electrodes

Reference electrodes are not commercially available for fused salt systems, and must be individually constructed for each system used. Many types of reference electrodes have been used. The most popular electrodes being the metal, metal ion types. Gas electrodes, particularly the chlorine reference electrode have also been used. The most popular electrodes used in the chloride melts have been the Ag,Ag(I) and Pt,Pt(II) systems, along with the chlorine reference electrode. These electrodes have been described by many people (14, 29, 40).

The indicator or working electrode used is also the subject of much interest. At the high temperatures used in much of fused salt research the problems are compounded because of the near impossibility of sealing platinum into the quartz or vycor glasses used. Dipping, "bubbling," and electrodes sealed in ceramics have all been used. Platinum, tungsten, and molybdenum are the most popular electrode materials. Dipping electrodes consist of a piece of wire inserted into the melt. Problems are encountered with stability and noise, due to fluctuations in the length of wire inserted into the melt. However, dipping electrodes are often used because of their extreme simplicity. "Bubbling" electrodes are an attempt to improve the dipping type of electrode. For this type of electrode the wire that is to be dipped into the melt is passed through a tube. Inert gas is bubbled through the tube during the experiment, causing the wire electrode to be alternately inserted and removed from the melt as bubbles form and burst. The curves obtained with this type of

electrode are much like those obtained with the DME. The choice of reference and working electrode used is generally made by finding which of the possible electrodes works for the particular system and for the particular researcher involved. More often, choices in fused salt research are made for experimental rather than theoretical reasons.

Fused Salt Purification

One of the most significant problems encountered in working with fused salts is purification of the melt. Particularly important is hydroxide and oxygen removal. The oxygen is removed the same way as in aqueous systems, by bubbling with an inert gas, usually argon. Two of the more prominent articles on hydroxide removal were written by Maricle and Hume (31) and by Laitinen, Ferguson, and Osteryoung (26).

The technique proposed by Laitinen et al is long and arduous, requiring several days of predrying, and elaborate techniques. The method of Maricle and Hume is to bubble chlorine through a melt which hasn't been especially prepared in any other way. The chlorine is then removed by bubbling the melt with argon for 20 minutes or more. The chlorine is rather difficult to remove and attacks platinum if any is left in the melt.

Fredericks, Shuerman and Lewis (16) have conducted a series of experiments on methods for removing hydroxide from alkali halides. The method found to be the most effective was the treatment of the salt with a reactive gas at a series of temperatures up to the fusion temperature of the salt. The reactive gas used was HCl for chloride melts and HBr for bromide melts.

Once the melt is purified and a suitable working and reference electrode are found, electrochemical experimentation can begin.

Electrochemical Techniques

The electrochemical techniques used in this research were cyclic voltammetry, differential pulse polarography, and some DC and pulse polarography.

Cyclic Voltammetry

The paper by Nicholson and Shain (32) is the classic work dealing with cyclic voltammetry. Delahay's "New Instrumental Methods in Electrochemistry" (11) includes a chapter on cyclic voltammetry, as does Adams' "Electrochemistry at Solid Electrodes" (1).

Cyclic voltammetric experiments are carried out with a system qualitatively similar to that employed for DC polarography. The difference is that the applied potential has a higher scan rate, and is normally reversed to scan back to the original potential. The scan rates range from 5 mv/sec to 500 mv/sec. A scan rate of 5 mv/sec is often too slow and a DC type of wave is obtained. Scan rates higher than 500 mv/sec generally require instrumentation with improved response time characteristics. The applied potential wave form and the resultant voltammetric wave are shown in Figure 4. The shape of the cyclic voltammogram with its characteristic peak comes from the condition that the scan rate is fast enough so that diffusion control is not attained before the rate constant becomes large. The faster the scan the larger the rate constant becomes (and consequently the current) before the diffusion layer is depleted and the current becomes diffusion controlled. When the current becomes diffusion controlled, the observed current drops nearly to the diffusion current obtained from a DC polarogram, the difference
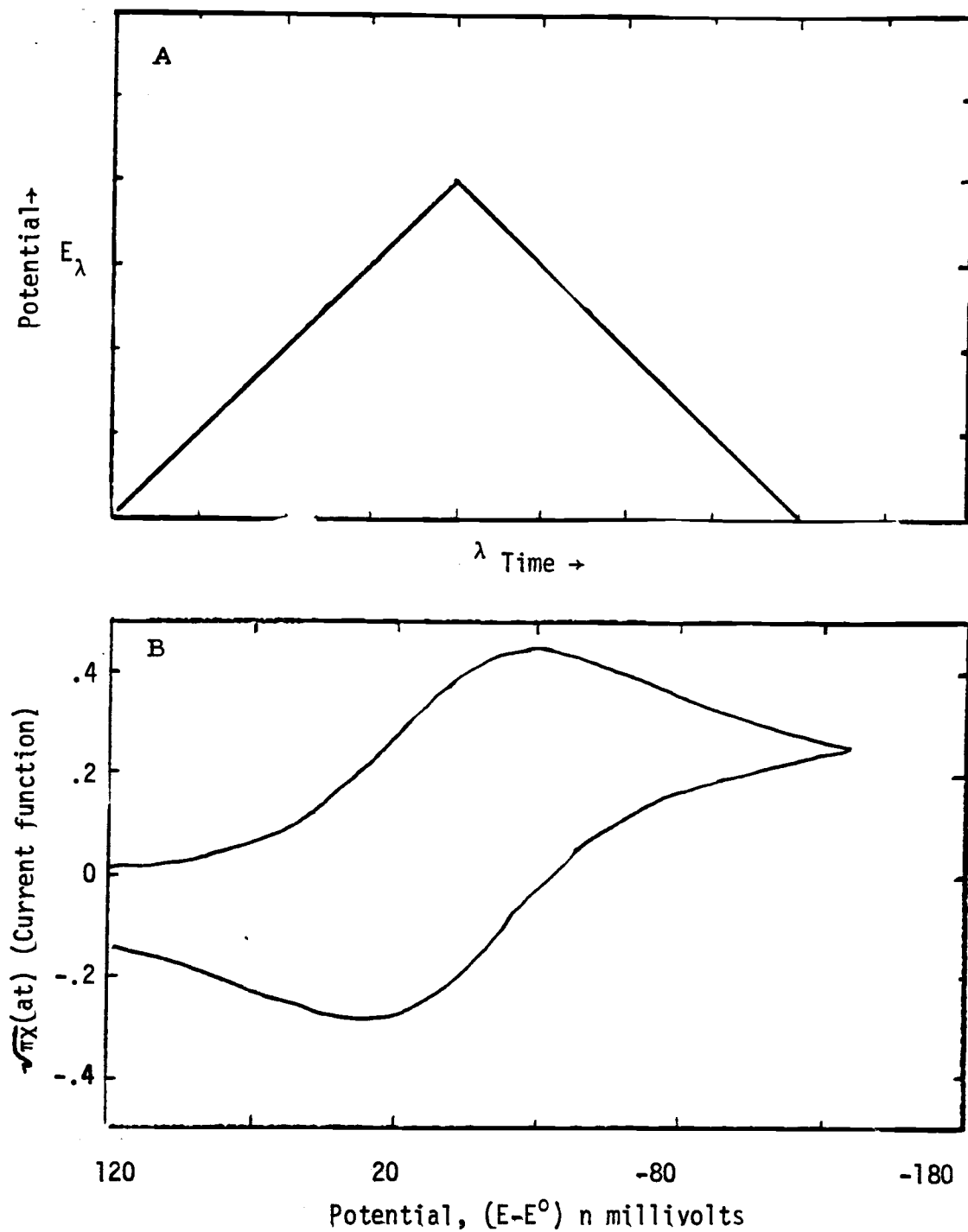
Figure 4.

A. Potential-time waveform for cyclic voltammetry.

B. Cyclic polarogram, E_λ = -141.3 mv

being due to capacitive charging effects.

In some cases where cyclic voltammetry is the intent of the experiment, the wave is a DC shaped wave and can be treated by the classical techniques. Any time that the scan rate, diffusion co-efficients, and concentration are such that the current is diffusion limited throughout the last section of the wave a characteristic S shaped DC type wave is obtained, rather than a wave exhibiting a current maxima.

Cyclic voltammetry can be used to gain a qualitative and quan-titative insight into the electrochemical reactions of interest. The way a wave shape changes as the scan rate is increased can tell much about the reversibility of a reaction, and can give insight into competing reactions and problems caused by deposition or preci-pitation of the reduced species. If a reaction is reversible the peak potential will not change as the scan rate is increased. For an irreversible reaction the cathodic peak will move negatively, the anodic peak will move in the positive direction along the potential axis, and both waves will be drawn out and lowered. For a completely irreversible reaction no peak will be seen on the reverse scan. The changes in a wave as the scan rate is changed can be analyzed to yield information about preceeding and following chemical reactions, catalytic electrode reactions and ECE (electro, chemical, electro) type reactions.

Nicholson has mathematically solved the Fick's law expression with the appropriate boundary conditions and tabulated the results. The cases for which Nicholson solved the Fick's law expression are shown in Table IV. The equation for the reversible reaction,

TABLE IV. THE EIGHT CASES FOR CYCLIC VOLTAMMETRY

Case	Reaction	Description
I	$O + ne \rightleftarrows R$	Uncomplicated reversible charge transfer.
II	$O + ne \overset{k}{\rightleftarrows} R$	Uncomplicated irreversible charge transfer.
III	$Z \overset{k_f}{\underset{k_b}{\rightleftarrows}} O$ $O + ne \overset{k}{\rightleftarrows} R$	Preceding reversible chemical reaction, irreversible charge transfer.
IV	$Z \overset{k_f}{\underset{k_b}{\rightleftarrows}} O$ $O + ne \overset{k}{\rightarrow} R$	Preceding reversible chemical reaction, irreversible charge transfer.
V	$O + ne \rightleftarrows R$ $R \overset{k_f}{\underset{k_b}{\rightleftarrows}} Z$	Reversible charge transfer followed by a reversible chemical reaction.
VI	$O + ne \rightleftarrows R$ $R \overset{k_f}{\rightarrow} Z$	Reversible charge transfer followed by an irreversible chemical reaction.
VII	$O + ne \rightleftarrows R$ $R + Z \overset{k_f}{\rightarrow} O$	Catalytic reaction with reversible charge transfer.
VIII	$O + ne \overset{k}{\rightarrow} R$ $R + Z \overset{k_f}{\rightarrow} O$	Catalytic reaction with irreversible charge transfer.

resulting from Fick's law and the proper boundary conditions is:

$$i = 602n^{3/2}A\sqrt{D}\,\gamma\,C_{ox}^{*}\,(\sqrt{\pi}\,\chi(a,t) + 0.16\,(\sqrt{D}_{ox}/\delta o)\,\Phi(a,t))$$

$$(30)$$

where:

γ = scan rate, volts/sec

A = electrode area, cm^2

D_{ox} = diffusion coefficient, cm^2/sec

C_{ox}^{*} = bulk concentration, oxidized species

δo = radius of electrode, cm

$\chi(a,t)$ is the current function for a planar electrode, and $\Phi(a,t)$ is the correction factor for spherical diffusion. The two current functions were solved by numerical integration.

The current, potential data which Nicholson had tabulated for each of the cases is based on several assumptions. First it is assumed that both the oxidized and reduced species are soluble, second that diffusion is the only mass transport mechanism, and third that the reaction rate is very much faster than the mass transfer rate (Petcoff Pg. 40, 41). The cyclic voltammogram will be distorted any time one or more of these assumptions is not valid. If the reduced species is insoluble the Fick's second law expression for the change in the concentration at the electrode of the reduced species with time will not be dependent on the diffusion coefficient of the reduced species.

The resultant curve, like the Koltoff-Lingane type DC polarograms, will be steeper. The reverse scan in such a case would yield a sharp peak because of the high activity of the reduced species at the electrode surface, and the non-dependence on diffusion mass transport.

Nicholson has developed a set of experimental diagnostic criteria for identifying the type of system involved in an electrode reaction. The diagnostic criteria consist of three graphs. The first graph is peak current/ scan rate versus the scan rate (Figure 5). The second graph is $E_{p/2}/\Delta \log v$ versus the scan rate (Figure 6). $E_{p/2}$ is the potential at 1/2 the peak current. The third graph is i_{ap}/i_{cp} versus the scan rate (Figure 7). Each case yields a distinct set of the curves. In the case of an experiment for which none of the above cases holds, other evidence is needed to ascertain the type of reaction involved.

Various relationships between the current and the potential can be used to obtain n values for the electrode reaction. The relationships between the peak potentials, $E_{cp} - E_{ap} = 2.22RT/nF$, and the peak and half peak potential, $E_{cp} - E_{cp/2} = 2.20RT/nF$, involve an n value term, enabling it to be calculated. As suggested by Reinmuth (37) a graph of log $(\sqrt{i_p} -i/i)$ versus E for the rising portion of the wave will yield a straight line with the slope equal to $2.3RT/nF$ for a reversible wave, and a slope of $2.3RT/\alpha nF$ for an irreversible wave. Petcoff (35) tried several current relationships suggested by various authors for determining n values, and has found this one to be the most satisfactory. It is linear over more of the curve, and the experimental data agree with the theory. Petcoff includes in his thesis graphs of current versus potential which are more like the voltammetric waves expected experimentally than those previously published. The waves that Nicholson shows do not include the dependence of the current on the scan rate. They
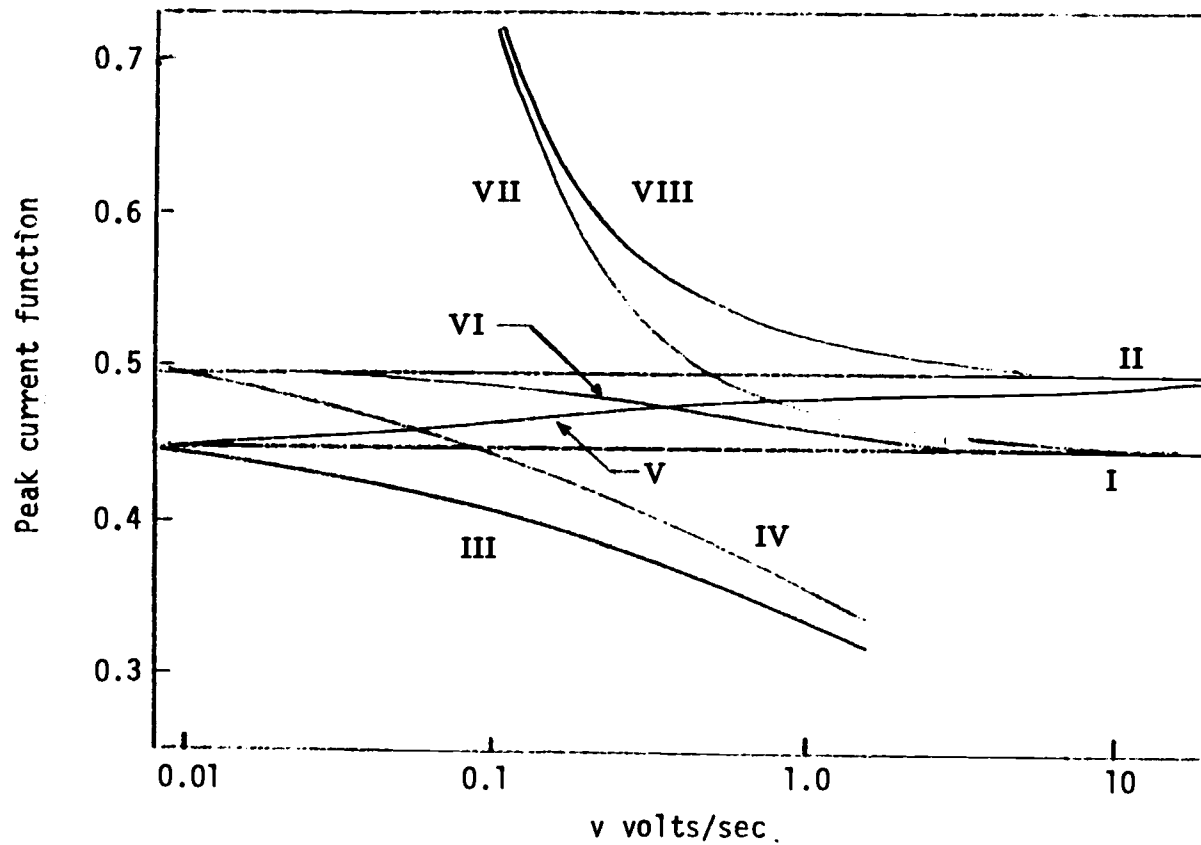
Figure 5. Variations of the peak current functions with rate of voltage scan.
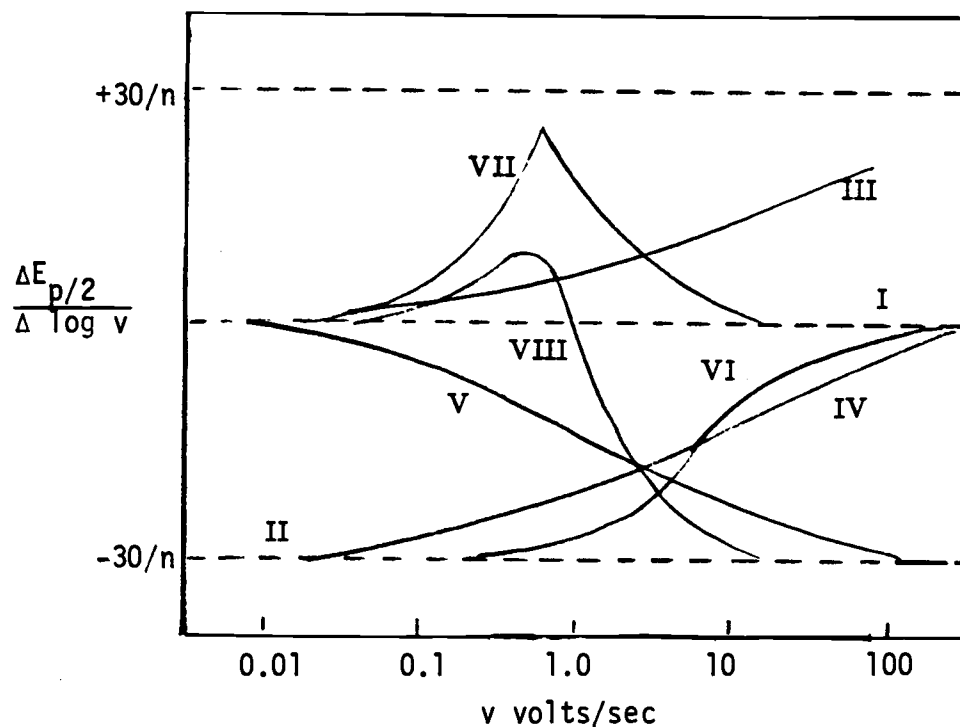
Figure 6. Rate of shift of potential as a function of scan rate.
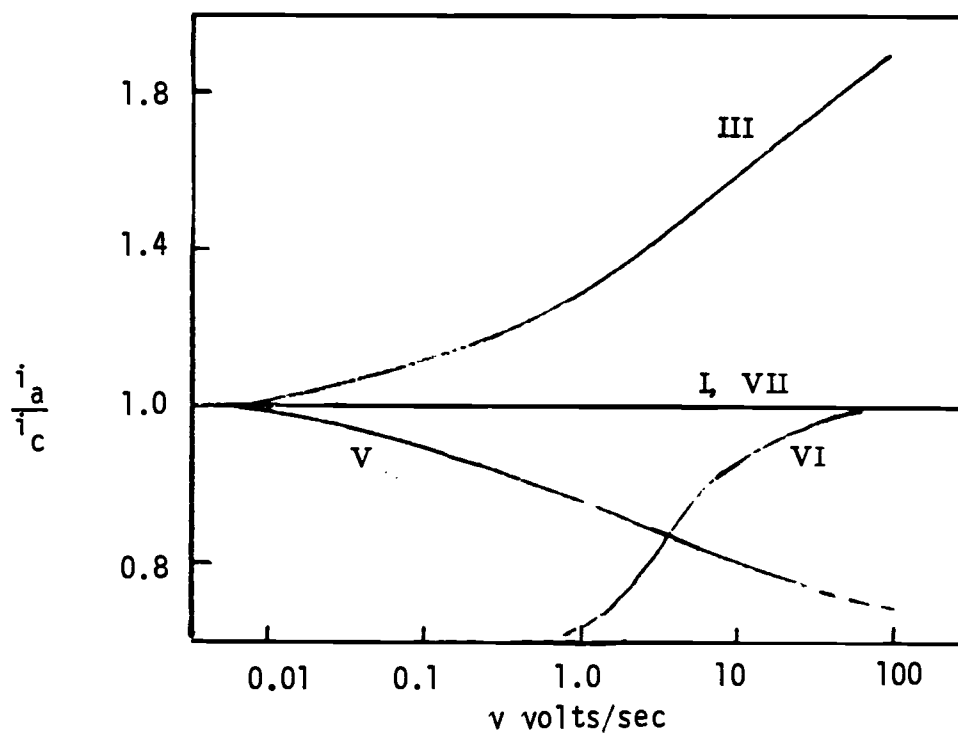
Figure 7. Ratio of anodic to cathodic peak currents as a
function of rate of voltage scan.

have the shape expected, but do not have the current relationships between different scan rates found experimentally. Petcoff's curves are very useful when qualitatively examining waves.

Differential Pulse Polarography

Differential pulse polarography was developed originally by Barker (4) as an extension of his work with square wave polarography. An article written by Parry and Osteryoung (34) condenses the theory of pulse polarography, and confirms it with experimental results. A later article by Burge (8) describes the techniques of differential and integral or normal pulse polarography, and describes the three commercial instruments available as of 1970.

In differential pulse polarography a voltage ramp is applied to the working electrode of a cell system, much the same as in DC polarography. Superimposed on this ramp are a series of pulses identical in height and duration. They are from 0.5 to 5 seconds apart, and are typically 5 to 100 mv in amplitude. The pulse is generally 57 msecs in duration. The current is sampled just prior to the pulse and during the last portion of the pulse. The current sampling time is generally 16.7 or 33 msecs long, covering one or two complete cycles of the 60 cycle line voltage. Figure 8 shows the applied potential wave form, the current wave forms during the pulses, and the observed polarogram. The current observed is the difference between the current before the pulse, and the current during the last portion of the pulse.

There is a sensitivity-resolution tradeoff in selecting the proper pulse height. The current increases as the pulse height increases, but the resolution decreases. The curve obtained is
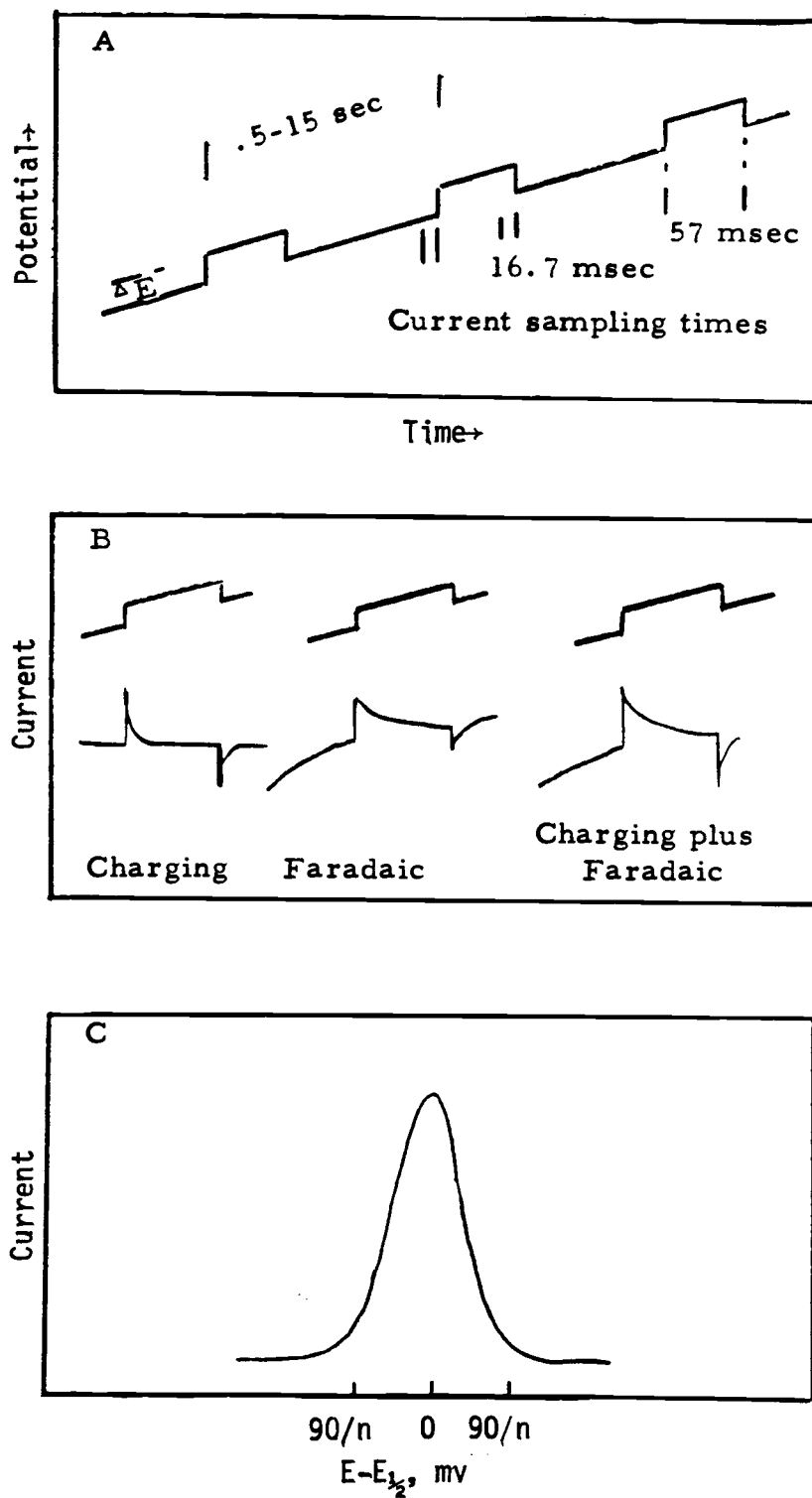
Figure 8. Differential pulse polarography.
A. Applied potential waveforms
B. Current waveforms
C. Observed polarographic curve

the derivative of a normal DC type polarographic wave for small values of the pulse height (less than RT/nf according to Barker). The current, potential relationship for differential pulse polarography can be found by differentiating the current, potential expression for DC polarography.

$$i = i_d \left[\frac{1}{1-\exp((E-E_{\frac{1}{2}})\, nF/RT)} \right] \tag{31}$$

The Cottrell expression is substituted for i_d in the derivative, and equation 32 results.

$$\Delta i = (n^2 F^2/RT) A C \Delta E \sqrt{D/\pi t} \;\; (P/(1+P)^2) \tag{32}$$

where $P = \exp(E-E_{\frac{1}{2}}) nF/RT$. Since Δi is a maximum when $P = 1$, the expression for the maximum current is:

$$\Delta i_{max} = (n^2 F^2/4RT) A C \Delta E \sqrt{D/\pi t} \tag{33}$$

Substituting $\Delta i_{max}/2$ for Δi in equation (32) yields two possible potentials. The difference between these two potentials yields the expression for the half width of the polarographic wave.

$$W_{\frac{1}{2}} = 3.52 \; RT/nF \tag{34}$$

Similarly the width where Δi equals $\Delta i_{max}/4$ is:

$$W_{\frac{1}{4}} = 5.27 \; RT/nf \tag{35}$$

For infinitely small pulse heights E_p equals $E_{\frac{1}{2}}$. For finite pulse heights equation 36 holds:

$$E_{\frac{1}{2}} = E_p - \Delta E/2 \tag{36}$$

i.e., for a cathodic scan the peak occurs $\Delta E/2$ volts before the true half wave potential, where ΔE is the pulse height.

These expressions are all derived assuming that the system is reversible, and that both the reduced and oxidized species are soluble. If the expression for the polarographic wave obtained

from a system with an insoluble reduced species (equation 37) is differentiated, an expression is obtained describing the differential pulse polarogram expected (equation 38).

$$i = i_d - e^{(nF/RT (E-E_{\frac{1}{2}} + (RT/nF) \ln(i_d/2)))} \qquad (37)$$

$$\Delta i = \Delta E \frac{nF}{RT} e^{\left(\frac{nF}{RT} (E-E_{\frac{1}{2}} + \frac{RT}{nF} \ln(nFAC\sqrt{D/\pi t}))\right)} \qquad (38)$$

The expression derived is only valid negative of the potential at which the current of the DC polarogram goes to zero. Positive of this point the derivative is zero. This boundary requirement results in a wave like that shown in Figure 9. The differential pulse polarogram from a normal system is also shown for comparison. Several things are to be noticed; first, as with the DC wave, the discontinuity, and the steep initial portion of the wave changes potential as the concentration changes. Second, the wave is narrower than the normal differential pulse polarogram. The narrowing of the peak will result in larger diagnostic n values if expressions derived from the normal expression for the differential pulse polarogram are used. Also note that the wave is unsymmetrical. The waves shown in Figure 9 were calculated assuming i_d to be 10 μamps, n = 1, T = 298K, ΔE = .010 volts, and $E_{\frac{1}{2}}$ = -1.000 volts.

Normal Pulse Polarography

In normal or integral pulse polarography a series of pulses of increasing amplitude is applied to the working electrode. The potential is returned to the original potential between the pulses. This technique has the advantage that any deposited reduced species is removed between the pulses, so the electrode surface remains the same throughout the scan. For a reaction where the reduced species
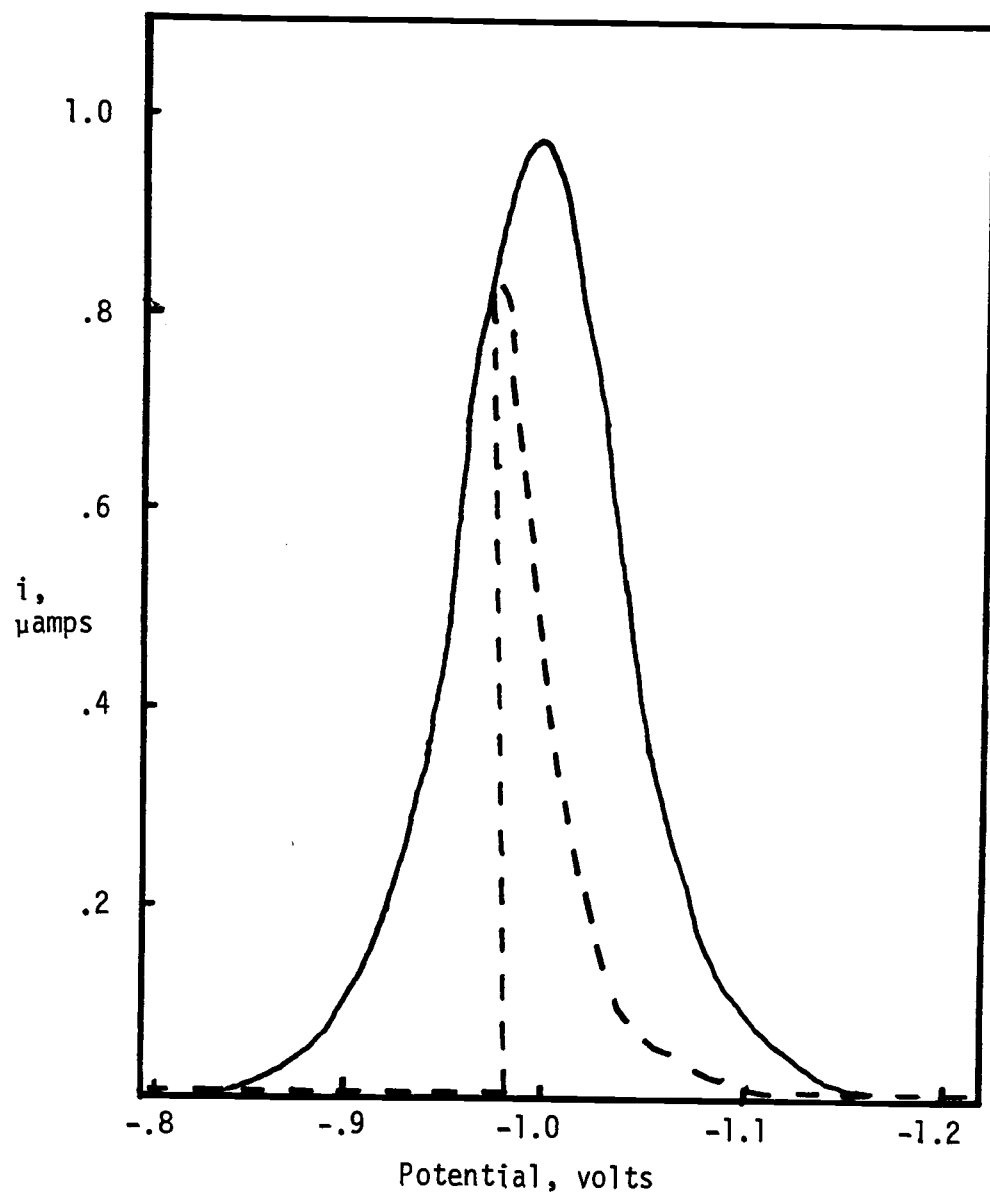
Figure 9. Calculated Differential Pulse Polarographic Waves from Soluble and Insoluble Reduced Species

is only slightly soluble a normal pulse polarogram will yield an
ideal wave, if all other conditions are ideal. For the same situa-
tion DC polarography would give a distorted wave. The pulse widths
and current sampling times are identical to those used in differen-
tial pulse polarography. Figure 10 shows the applied potential
waveform, and the observed polarographic wave. The wave has the
same shape as the normal DC polarographic wave, and is described by
the same current, potential relationships.
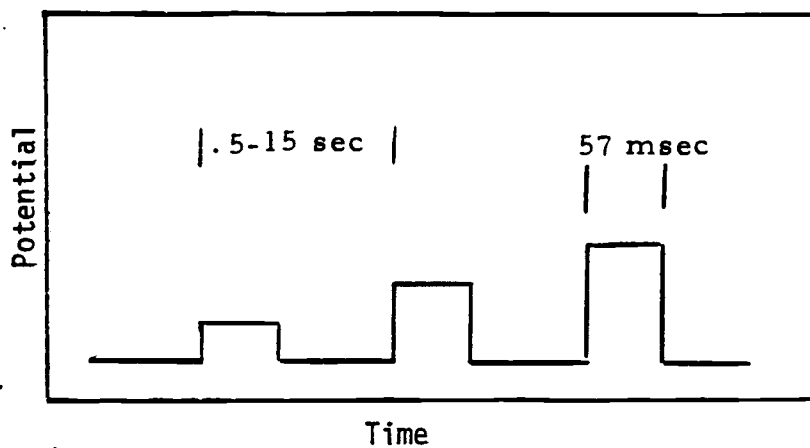
A. Applied potential waveform
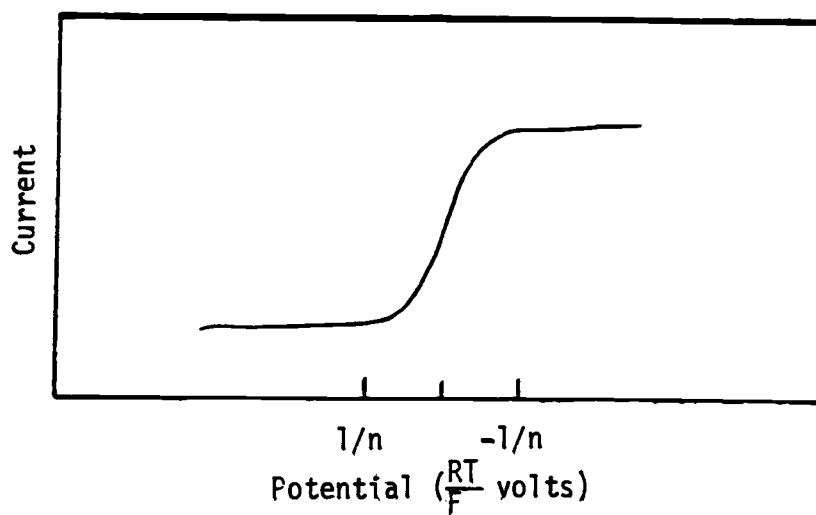
B. Observed waveform

Figure 10. Waveforms for integral or normal pulse polarography.

Experimental

Apparatus

The electrochemical measurements were performed either with a PAR model 174A Polarographic Analyzer or a PAR model 173 Potentiostat/Galvanostat equipped with a model 179 Digital Coulometer.

Par 174A Polarographic Analyzer

The principal instrument was the Polarographic Analyzer. A Varian Associates model F80 XY recorder, or a Tektronix 564B storage oscilloscope equipped with two 3A6 amplifiers were the most commonly used output devices. The 174A Polarographic Analyzer is capable of operating in DC, sampled DC, pulse, and differential pulse polarographic modes, and is equipped with push buttons for forward and reverse scans, enabling its use for cyclic voltammetry. The polarographs' scan rates range from 0.1 mv/sec to 500 mv/sec in a 1,2,5,10 sequence. These scan rates were enhanced by utilization of an external sawtooth generator and a digital gate attached to the external potential input on the instrument. The PAR Polarographic Analyzer has a 57 msec pulse width with a 16.7 msec sample time. The time between pulses was chosen to be 0.5 sec.

PAR 179 Digital Coulometer

The model 179 Digital Coulometer provides a four digit coulombs display with a two digit exponent. The instrument has a front panel 25 pin connector supplying BCD numbers of the six digits and the two signs (coulombs and exponent), along with pins to provide a reset and a pin to "freeze" the display for reading purposes. The coulometer was interfaced with a DEC PDP 11-20 computer. The

details of the circuits and programs used are in appendix 1. The computer provides experimental control, data acquisition and data readout. It also performs the needed calculations and logic decisions.

Sawtooth Generator and Digital Gate

The scanning circuit used with the Polarographic Analyzer was constructed in this laboratory. It consists of two sections, a variable sawtooth generator and a digital gate. Figure 11 shows the circuit diagram for both the digital gate and the sawtooth generator. Box A in Figure 11 encloses the sawtooth generator.

The sawtooth generator circuit works by applying alternately positive and negative potentials to an operational amplifier. Operational Amplifier number one (Op Amp 1) is a simple integrator. Op Amp 1 has its input current provided by Operational Amplifier number three (Op Amp 3). The current, and therefore the rate of charging of the integrator is controlled by resistor R1. R1 is a 300K variable resistor. Switch S4 and the 300K fixed resistor provide for high and low range operations. Op Amp 3 has as its input the +/- 15 volt output limits of Operational Amplifier number two (Op Amp 2). Op Amp 2 is wired as a comparator. The comparator inputs are the output of Op Amp 1, and a voltage divider from its own output. When the output voltage of Op Amp 1 reaches the voltage from the divider, the output of Op Amp 2 changes sign. The change in sign of the output voltage changes the sign of the input voltage to Op Amp 1, causing it to integrate in the opposite direction. The sign of the voltage from the divider circuit also

Figure 11. Programmable cyclic scan circuit.

Components	Wave form (assuming four waves)
TIMING PULSES	
Counter JK Flip Flop 1	
JK Flip Flop 2	
JK Flip Flop 3	
4/INPUT NAND	
NAND 1	
NAND 2	
FET GATE	
START	
JK Flip Flop 4	
SAWTOOTH OUTPUT	
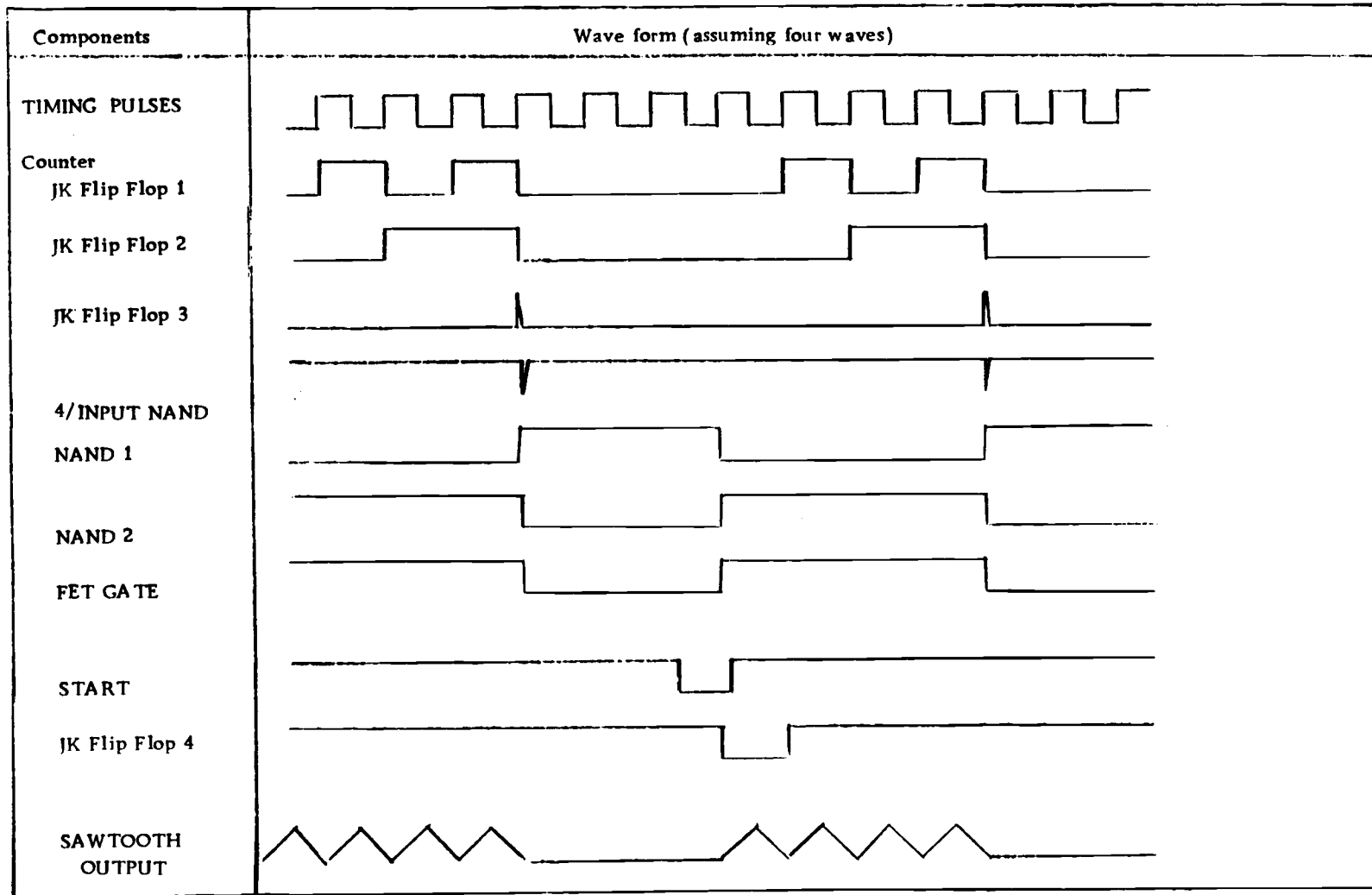
Figure 12. Timing diagram following text description.

changes. This change in sign resets the comparator, so that Op Amp
1 is again integrating towards the divider voltage. Resistor R2
forms the divider circuit and controls the voltage limits of the
sawtooth wave.

Figure 12 shows a timing diagram following this description of
the operation of the digital gate. The logic circuit utilizes the
square wave output of Op Amp 2 to provide the timing and count
pulses. The transistor on the output of Op Amp 2 acts as a buffer,
providing the zero to five volt square wave necessary to operate
the digital devices. JK Flip Flops 1, 2 and 3 act as a simple
binary counter. Switches 1, 2 and 3 program the number of scans
allowed through the gate. These switches form a binary sequence.
These three Flip Flops and switches allow for programming from one
to seven waves to be allowed through the gate. When a Q output
from the JK Flip Flops is high for each switch closed the output of
the four input Nand gate goes to zero. The zero output of the four
input Nand gate causes Nand gate 1 to go high. Nand gate 1 and Nand
gate 2 together form a simple flip flop. When Nand gate 1 is high
it closes the FET gate, so that no more sawtooth waves are allowed
through. The next series of sawtooth waves is started by closing
the start switch. Closing the start switch applies a logic zero to
the K input of JK Flip Flop 4. When a logic zero is applied to the
K input a clock pulse will move this zero to the Q output of JK
Flip Flop 4. This Q output is connected to an input of Nand gate 2.
When the Q output of JK Flip Flop 4 goes to zero the Nand gate flip
flop is forced to the state with Nand gate 1 having a logic zero
output. The logic zero Nand gate 1 opens the FET gate, allowing

sawtooth waves from the sawtooth generator to be present across the 100K output resistor.

Furnace and Controller

The temperature dependence of standard potentials and emf's necessitates accurate and precise temperature control for any electrochemical measurements in fused salts. The system that provides this control consists of a Lindberg Heviduty Furnace Controller, model number 59344, and a Heviduty Electric Company Furnace, type 86. A Platinum, Platinel (II) thermocouple provides the temperature measurement for the feedback circuit. Temperature measurements in the fused salt using a Chromel-Alumel thermocouple showed gradients and fluctuations of less than two degrees. The thermocouples are enclosed in a quartz sheath.

The high temperatures used in this work (933K to 1173K) require the use of quartz for all cells and electrode sheaths. The cell is shown in Figure 13. It is a quartz tube 55mm in diameter by 170mm high, closed at one end, and flanged on the other. The pyrex cell cover is also flanged. The cover flange and the cell flange are both flat ground, allowing them to be sealed with a small amount of silicone High Vacuum grease. A length of copper tubing was bent to fit, and connected to a cold water tap to provide cooling for the cover and the flanges.

Cell

The cell cover (Figure 13) has five openings provided for electrodes and thermocouples. These openings are short sections of glass tubing sealed into the top of the cell cover. The electrodes and the thermocouple sheaths are sealed to the cell by

Thermocouple sheath

Gas Bubbling
tube

Access Port

O-ring
groove

Gas
outlet

Spoon for adding
samples

Working electrode

Ag,AgCl Reference
electrode

Carbon rod
counter electrode

Quartz frit counter
electrode compartment
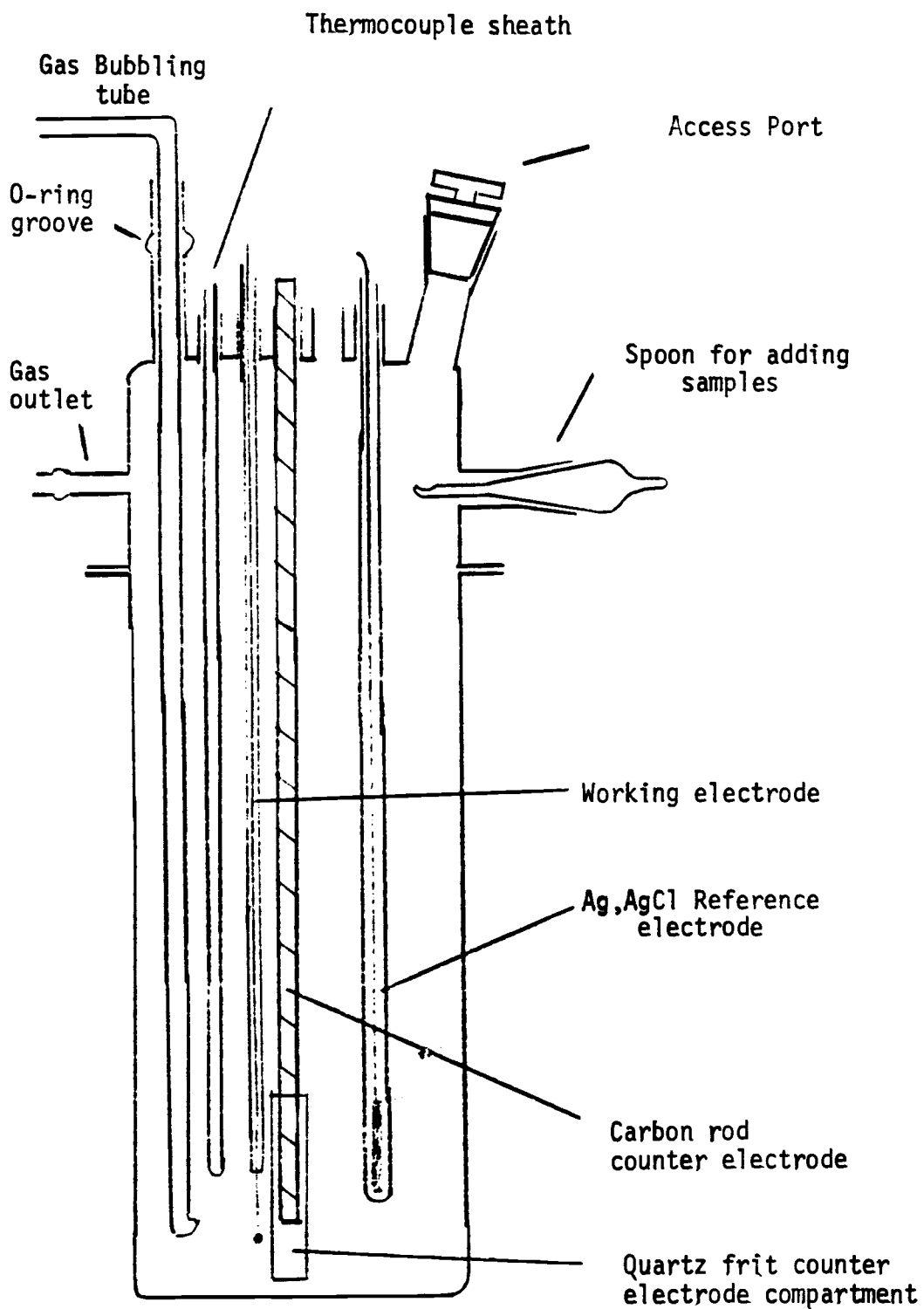
Figure 13. The cell and cell cover.

pushing them through a serum stopper. The larger portion of the serum stopper is easily pushed over the access tube. Any unused access tubes are sealed by serum stoppers that haven't had holes punched through them.

The sliding joint for the gas inlet tube is shown in Figure 13. It is constructed of a pyrex tube with an o-ring groove blown into it. Viton o-rings are used because of their ability to withstand higher temperatures than ordinary o-rings. The sliding joint allows the inlet gases to either be bubbled through the melt, or passed over it. Other accesses provided on the cell cover are for taking melt samples, introducing samples from a sampling spoon, and an outlet for gases. The exhausted gases are bubbled through a sulfuric acid trap.

Electrodes

The counter electrode is a spectrographic grade carbon rod six mm in diameter and 30 cm long. Its lower end is inserted into a quartz tube that has a medium porosity fritted disc on the bottom. This electrode assembly is dipped into the melt.

The working electrode for the cyclic voltammetry and the differential pulse polarography is a "platinum drop" electrode. A piece of 0.005 inch diameter (0.13 mm) platinum wire was heated until a small drop of platinum had formed on the end. This drop typically had a diameter of 1 mm. The large size of the drop in comparison to the wire makes it possible to consider it a spherical electrode. The small diameter platinum wire was melted to a ten inch section of 20 guage Platinum wire, which was passed out of the cell through a 4 mm quartz tube. The quartz tube was sealed

to the top of the cell with a serum stopper, allowing it to be
lowered towards the melt just until the drop is submerged. The top
of the 4 mm quartz tube was sealed with another serum stopper.
This design eliminates the problems associated with sealing plati-
num into a ceramic. At 1013K many ceramics begin to conduct elec-
tricity. It also eliminates the problems with noise normally
found in dipping types of electrodes. The surface area of the drop
is large enough so that small changes in the amount of platinum
wire dipped into the melt do not have a large effect on the total
area of the electrode.

The reference electrode was originally patterned after that
of R. Littlewood (30). Since the temperatures were above the limits
of the Jena Supremax glass used by Littlewood, the electrode was
necessarily constructed of quartz. The method of S. N. Flengas and
T. R. Ingraham of sealing an asbestos fiber into the end of a quartz
tube was originally employed. This worked very well for a time,
but repeated use caused small cracks in the quartz and eventual
failure. Since Littlewood had found that Jena Supremax glass had
a low resistance at the temperature he used, and since the PAR
instruments require a very small input current (femtoamps) a solid
quartz reference electrode was tried. A six mm O.D. quartz tube,
sealed at one end, was used. Comparison of that electrode with
ones of the asbestos fiber construction showed no difference in
potential. The solid quartz reference electrode also produced
polarograms identical to those obtained using the asbestos fiber
type reference electrodes. The solid quartz reference electrode
is much stronger and could be used many times before small cracks

would appear. This design was used throughout the research.

The potential of the reference electrode versus the chlorine reference can be calculated from Ag,AgCl standard electrode potential data, and an approximation of the junction potential. The formal potential at each temperature was derived from formal potential data given by Flengas and Ingraham (14). The formal potentials used are shown in Table V.

TABLE V. Ag,AgCl STANDARD ELECTRODE POTENTIALS

Temperature	E^o (Ag,AgCl)
953K	-.848 V
973K	-.843 V
993K	-.839 V
1013K	-.834 V
1043K	-.837 V
1073K	-.820 V
1123K	-.809 V

The mole fraction of AgCl used was 0.0753.

The junction potential is described by equation 39 (30).

$$E_{junct} = \sum_i (t_i) \frac{2.303RT}{nF} \log \frac{[X_i]_1}{[X_i]_2} \tag{39}$$

Since the conductance across the quartz is mainly by sodium transport the junction potential can be approximated by equation 40.

$$E_{junct} = \frac{2.303RT}{nF} \log \frac{[Na][ref]}{[Na] cell} \tag{40}$$

Using equation 40, and sodium mole fractions of 0.4996 in the melt, and 0.4623 in the electrode, the junction potentials were calculated. They are shown in Table VI.

TABLE VI.   JUNCTION POTENTIALS

Temperature	Junction Potential
953K	.0064 volts
973K	.0065 volts
993K	.0066 volts
1013K	.0068 volts
1043K	.0070 volts
1073K	.0072 volts
1123K	.0075 volts

Equation 41 is used to calculate the potential of the reference electrode versus the chlorine reference.

$$E_{ref} = E^o_{Ag,AgCl} + \frac{2.303RT}{nF} \; \log \, [Ag] + E_{junct} \qquad (41)$$

The calculated potentials for the Ag,AgCl reference electrode used are shown in Table VII.

TABLE VII.   POTENTIALS OF THE Ag,AgCl
REFERENCE ELECTRODE

Temperature	E_{ref}
953K	-1.054 volts
973K	-1.053 volts
993K	-1.053 volts
1013K	-1.053 volts
1043K	-1.052 volts
1073K	-1.052 volts
1123K	-1.052 volts

Procedures

To complete an experiment several steps are involved:

1) Melt purification

2) Testing for melt purity

3) Addition of zirconium

4) Polarograms or cyclic voltammograms taken

The success of an electrochemical experiment in fused salts is largely dependent on the purity of the melt. Hydroxide contamination from moisture is the most damaging, and the hardest to remove. The first technique used for hydroxide removal was that of Maricle and Hume (31). They dried the salt in a vacuum oven, fused the salt at 1013K, and then bubbled chlorine through the melt for 20 minutes. Argon was then passed until all traces of chlorine were removed. This method worked for removing most of the hydroxide impurities. It seemed to leave some traces of hydroxide. Wetting of the quartz by the melt indicated small amounts of hydroxide were present. W. J. Fredericks (16) has developed techniques for growing hydroxide free crystals. Discussions with Dr. Fredericks led to developing a new method for hydroxide removal. The method now used for hydroxide removal is to put HCl gas over the salt several times at several temperatures. The initial temperature at which HCl is passed over the salt is 523K. After HCl is allowed to stand over the salt for 15 minutes it is removed by a vacuum aspirator. The HCl gas is again bled into the cell, left for 15 minutes and removed by the vacuum aspirator. After this second treatment the temperature of the salt is raised to 623K while the salt remains under vacuum. The HCl treatment is repeated at 723K, 773K, 823K, 873K, 923K and finally on the melt. The HCl gas is readily removed by a short vacuum treatment followed by bubbling argon through the melt. This procedure provides for a hydroxide free melt as evidenced by the failure of the melt to wet quartz, and by superior

low residual current polarograms. Dr. W. J. Fredericks also pointed out the phenomenon of the hydroxide free melt not wetting quartz. Amounts of hydroxide whose effects are hard to see polarographically can be detected by noticing the quartz-melt interface.

A look at the cause of hydroxide impurities will explain the effectiveness of this procedure. The reaction for hydrolytic decomposition (Laitinen, Ferguson, and Osteryoung) is responsible for the hydroxide impurity (26).

$$H_2O + Cl^- \rightleftharpoons OH^- + HCl \qquad (42)$$

The addition of HCl to the system shifts the equilibrium of the reaction to the left, and it carries the water off from the melt. The technique of repeated HCl treatments at a series of temperatures takes advantage of the fact that the rate constant for the hydrolytic decomposition reaction is low at the lower temperatures. It is much easier to remove the water before it forms the hydroxide than to remove the hydroxide. The small amount of hydroxide formed is removed by the HCl treatment at the higher temperatures.

The HCl and argon gases are brought to the cell through a glass manifold, and a short piece of rubber tubing. The argon is dried and oxygen removed by passing it over a bed of copper filings at 723K, and then a bed of Linde 5A molecular sieve. The HCl or Cl_2 gas is dried by passing it over a bed of $MgClO_4$. Drying of the HCl and Cl_2 is a precautionary measure, since experiments done by Dr. W. J. Fredericks have shown it to be unnecessary. The gases are passed out of the cell through a H_2SO_4 trap.

A hydroxide free melt will show a useable potential range of -0.7 volts to -2.4 volts versus the chlorine reference and will not

wet quartz. Hydroxide in the melt will produce a breakdown or wave at -1.6 volts.

$ZrCl_4:NaCl:KCl$

The NaCl:KCl eutectic containing zirconium tetrachloride was prepared at the Teledyne Wah Chang Research Laboratory, Albany, Oregon. Dr. Joe Megy generously made available his specially constructed dry box, nickel crucibles, and a supply of reactor grade zirconium tetrachloride. The dry box is large, and has a well furnace suitable for preparing the $ZrCl_4:NaCl:KCl$ melt. The dry box can be evacuated, and dry argon run in. It has a system to recirculate the argon through a bed of hot zirconium filings, which removes any oxygen. This system maintains a clean, dry and oxygen free atmosphere.

The high vapor pressure of zirconium tetrachloride requires special techniques to keep it from all ending up deposited on the walls of the dry box. Zirconium tetrachloride is mixed in approximately one to two proportions (molar) with dry-mixed NaCl:KCl eutectic. This mixture is placed in a nickel crucible and covered by a layer of NaCl:KCl eutectic. The crucible is placed in the well furnace and covered by a nickel plate. The mixture is heated until it melts, then immediately allowed to cool. Carbon impurities from the zirconium tetrachloride float to the top, and are easily cracked off of the solidified salt. The salt mixture is broken up and placed in a poly bottle. The bottle is then closed and sealed with tape. This $ZrCl_4:NaCl:KCl$ mixture is not highly volatile, like the pure zirconium tetrachloride. Precautions were taken as a margin of safety. The bottle was stored in a glove box, with portions

transfered to weighing bottles to be weighed and added to the melt as needed. Two batches of the $ZrCl_4$:NaCl:KCl salt mixture were made. The first showed a composition of 1.42×10^{-3} moles of zirconium per gram of salt mixture. The second batch showed a composition of 1.27×10^{-3} moles of zirconium per gram of salt.

The zirconium determinations were carried out by precipitation with mandelic acid from an aqueous solution acidified with HCl, following the procedure developed by Kumins (24). The precipitate was fired at 1173K for several hours to decompose the zirconium mandelate to zirconium oxide. The firing at 1173K was repeated several times to insure complete decomposition. Analysis of aqueous solutions of zirconium(IV), and of zirconium(IV) in a concentrated NaCl:KCl solution showed the method to be accurate and reliable in the concentrated salt solutions.

The melt compositions used for the differential pulse polarography and the cyclic voltammetry were in the range of 5×10^{-5} to 2×10^{-4} mole fraction of zirconium.

Preliminary investigations using differential pulse polarography showed two peaks, one at approximately -0.37 volts, and the second at approximately -1.12 volts versus the Ag,AgCl reference electrode. Measured against the chlorine reference electrode these voltages would be -1.31, and -2.06 volts. Subsequent scans done minutes later on the same salt showed only the first peak, with a breakdown potential of approximately -0.8 volts versus the Ag,AgCl reference electrode. If an initial potential of +0.1 volts is reset and held for 45 minutes to an hour or more the scan will return to the original form with two peaks. This problem introduced by scanning

over the second peak was avoided for this work by simply scanning over the first peak and reversing or stopping the scan. The stopping or reversing potential was -0.6 volts versus the Ag,AgCl reference electrode.

Cyclic voltammograms were started at 0.0 volts versus the Ag,AgCl reference electrode. The scans were allowed to reach -0.6 volts, where they were reversed and allowed to scan back to the original potential.

Cyclic Voltammetry Results

In order to simplify understanding the significance of the results and to avoid confusion between the electrochemical techniques the results of each technique will be discussed separately. Keep in mind however that some of the techniques and conditions employed during much of the experimental work are based on conclusions obtained from the first set of cyclic voltammograms and differential pulse polarograms done at 1013K.

Two sets of voltammograms are shown in Figures 14, 15 and 16. The scans shown in Figures 14 and 15 show the changes seen as the scan rate is increased from 10 mv/sec to 100 mv/sec. The mole fraction of zirconium(IV) for these scans was 6.2×10^{-5}. The scans in Figure 16 overlap the first set, showing the changes as the scan rate is increased from 50 mv/sec to 500 mv/sec. The mole fraction of zirconium for these scans was 1.7×10^{-4}. The voltammogram shown in each case is one of many nearly identical scans. They are shown just as taken, without the benefit of any smoothing.

Table VIII shows the average values for the peak potentials (E_{cp} and E_{ap}), the half peak potentials ($E_{cp/2}$) and the peak currents obtained from the voltammograms.

Table IX shows the diagnostic apparent n values calculated from the peak potential separation, and the peak and half peak potential separation. It also shows diagnostic apparent n values obtained from graphs of $\log(\sqrt{i_p}-i/i)$ versus E. The graphs are shown in Figures 17 to 22. The significance and validity of these values will be examined in the discussion section.
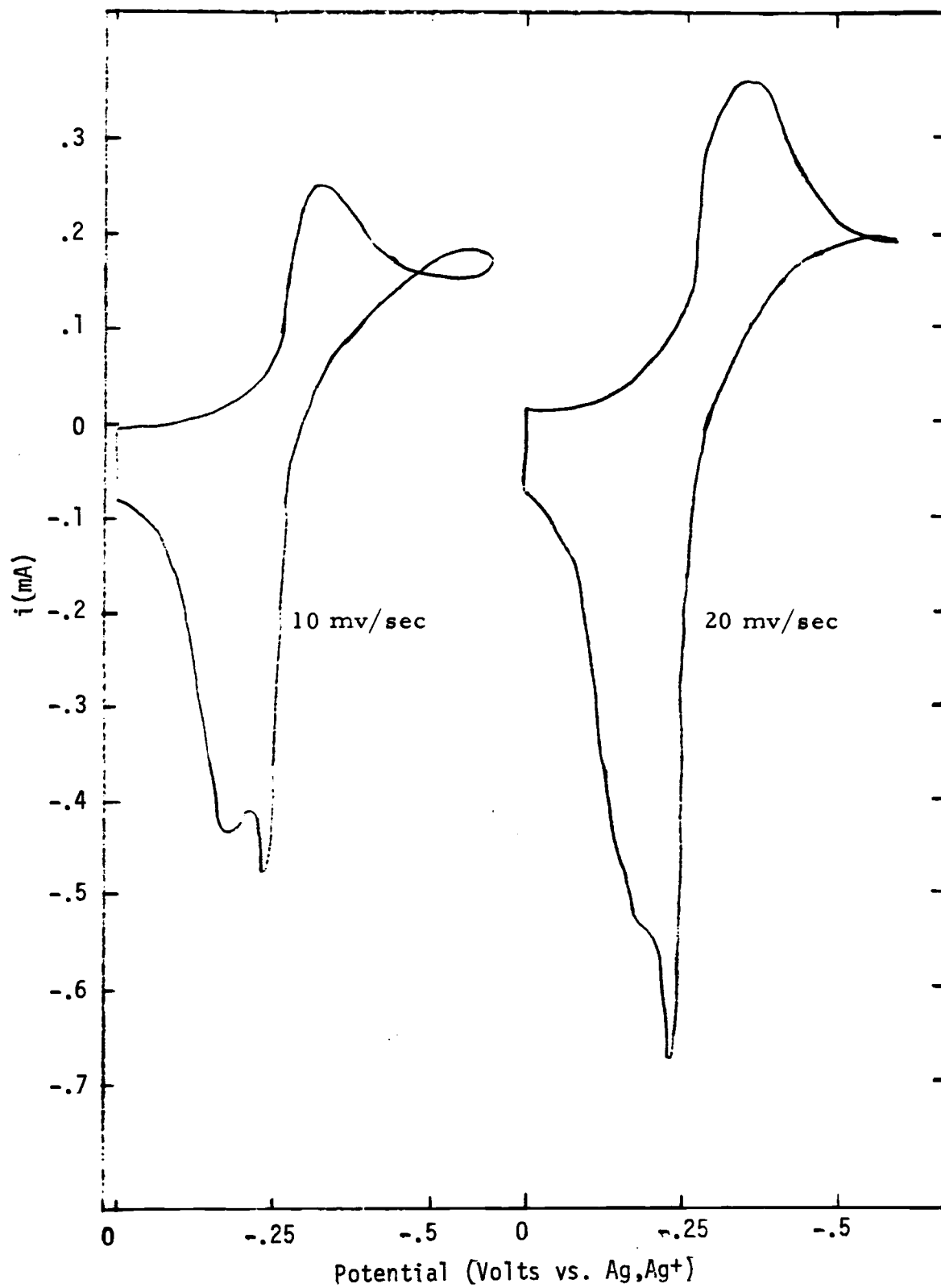
Figure 14. Cyclic voltammograms.
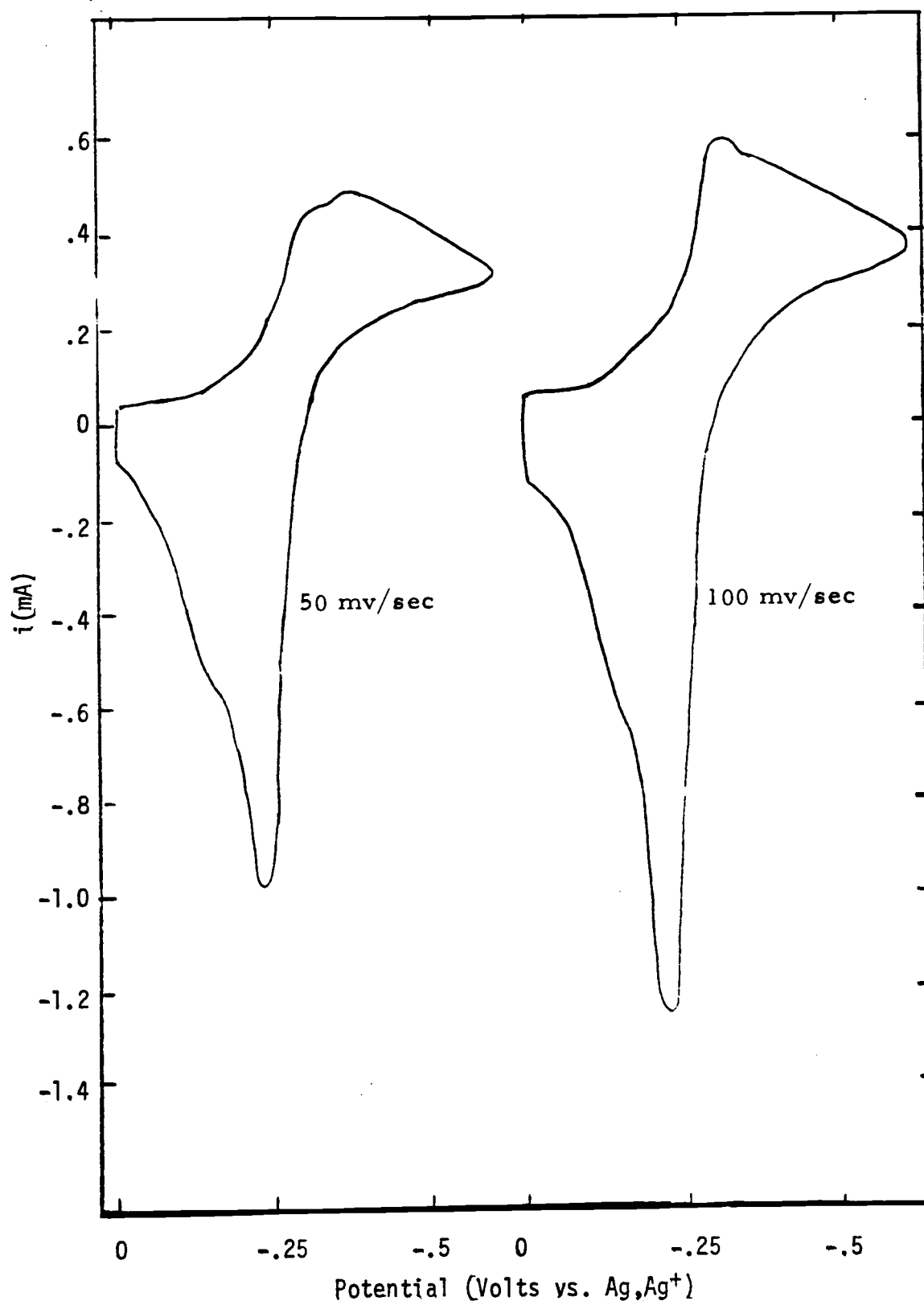
Figure 15. Cyclic voltammograms.
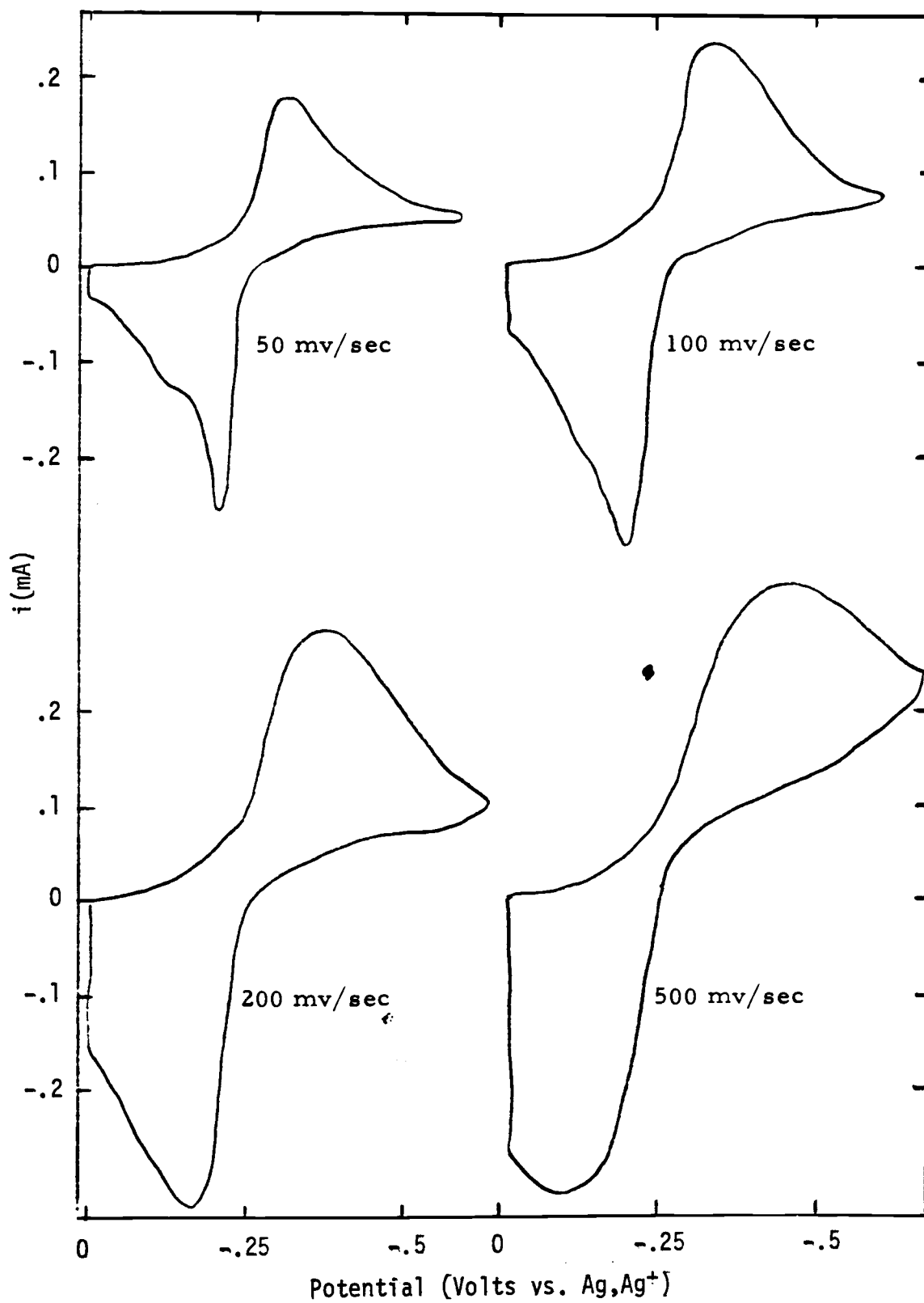
Figure 16. Cyclic voltammograms.

TABLE VIII. CYCLIC VOLTAMMETRIC DATA

Scan Rate	Cathodic Peak E	Cathodic ½ Peak E	Anodic Peak E	Cathodic Peak i	Anodic Peak i
10 mv/sec	-.320 V	-.258 V	-.177 V	.240 mA	.300 mA
20 mv/sec	-.340 V	-.251 V	-.244 V	.358 mA	.480 mA
50 mv/sec	-.333 V	-.252 V	-.226 V	.500 mA	.690 mA
100 mv/sec	-.320 V	-.248 V	-.215 V	.598 mA	1.160 mA
200 mv/sec	-.325 V	-.231 V	-.187 V	.740 mA	1.400 mA
500 mv/sec	-.455 V	-.299 V	-.097 V	.325 mA	.313 mA

TABLE IX. DIAGNOSTIC APPARENT n VALUES FROM VOLTAMMETRIC DATA

Scan Rate	$E_{cp}-E_{\frac{1}{2}cp}$	"n"	$E_{cp}-E_{ap}$	"n"	"αn" from graphs
10 mv/sec	.062 V	3.09	.143 V	1.36	0.88
20 mv/sec	.088 V	2.17	.096 V	2.02	1.18
50 mv/sec	.081 V	2.37	.107 V	1.81	1.32
100 mv/sec	.071 V	2.70	.105 V	1.85	1.43
200 mv/sec	.094 V	2.04	.138 V	1.40	1.53
500 mv/sec	.146 V	1.31	.358 V	0.54	1.21
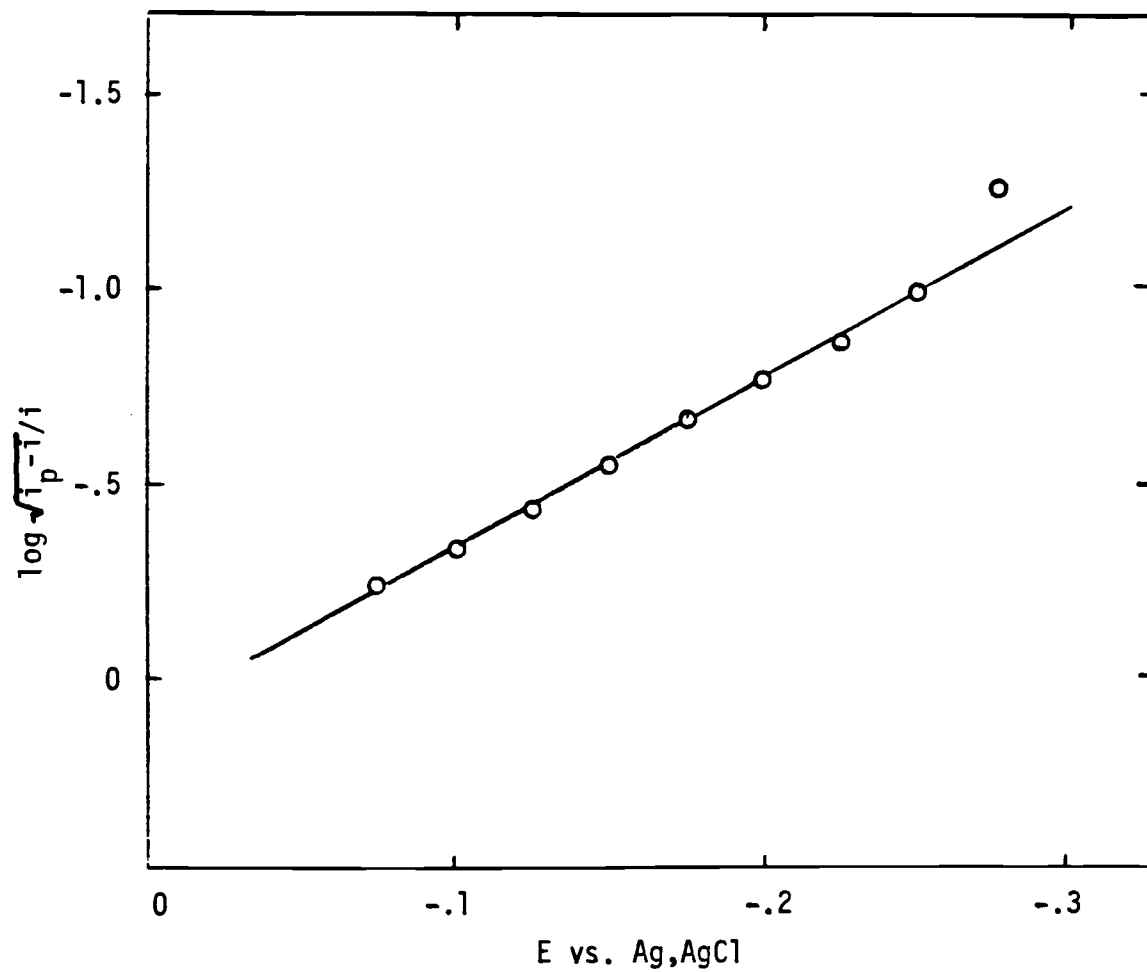
Figure 17. $\log \sqrt{i_p-i}/i$ vs. E
$v = 10$ my/sec
slope = 0.227
$\alpha n = 0.88$
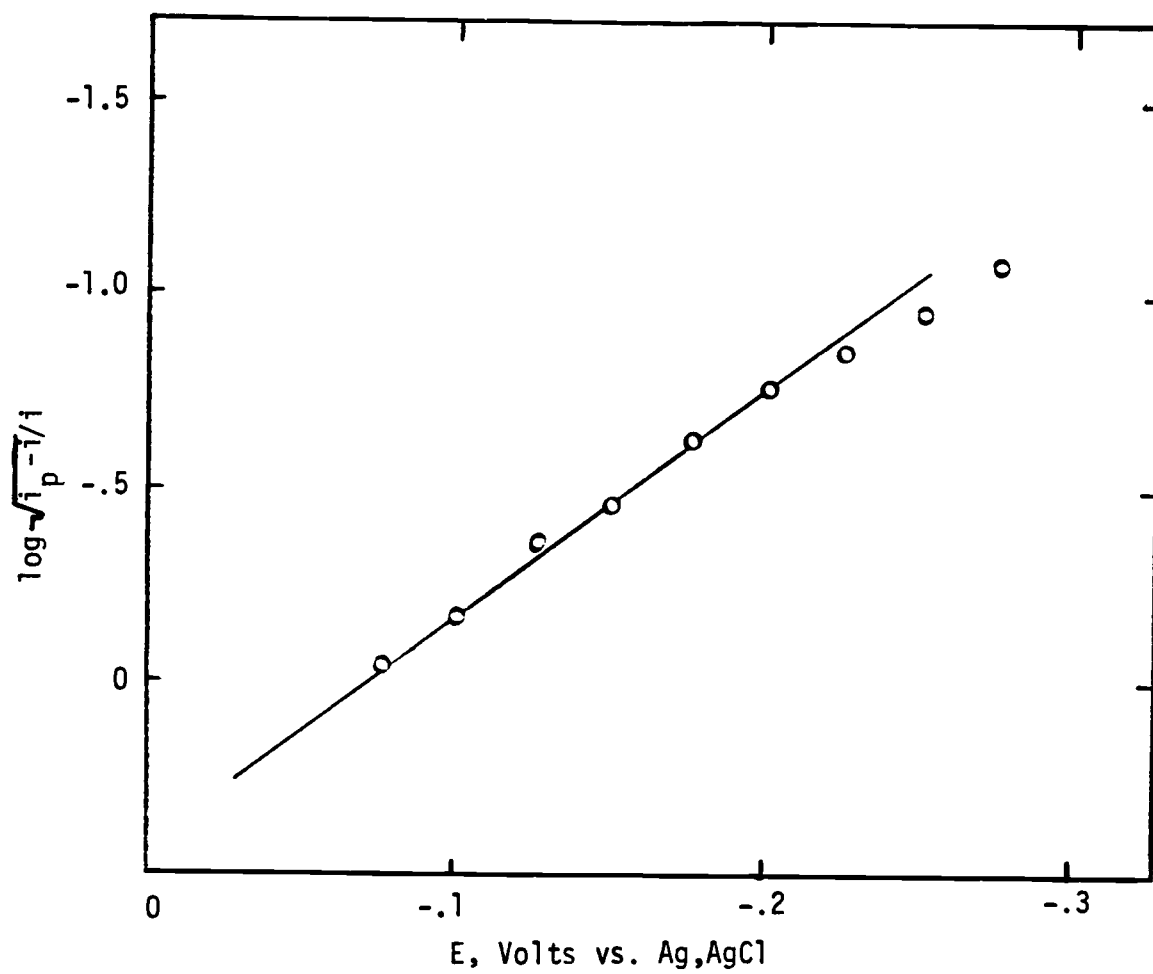
Figure 18. $\log \sqrt{i_p - i}/i$ vs. E

v = 20 mv/sec
slope = 0.170
αn = 1.18
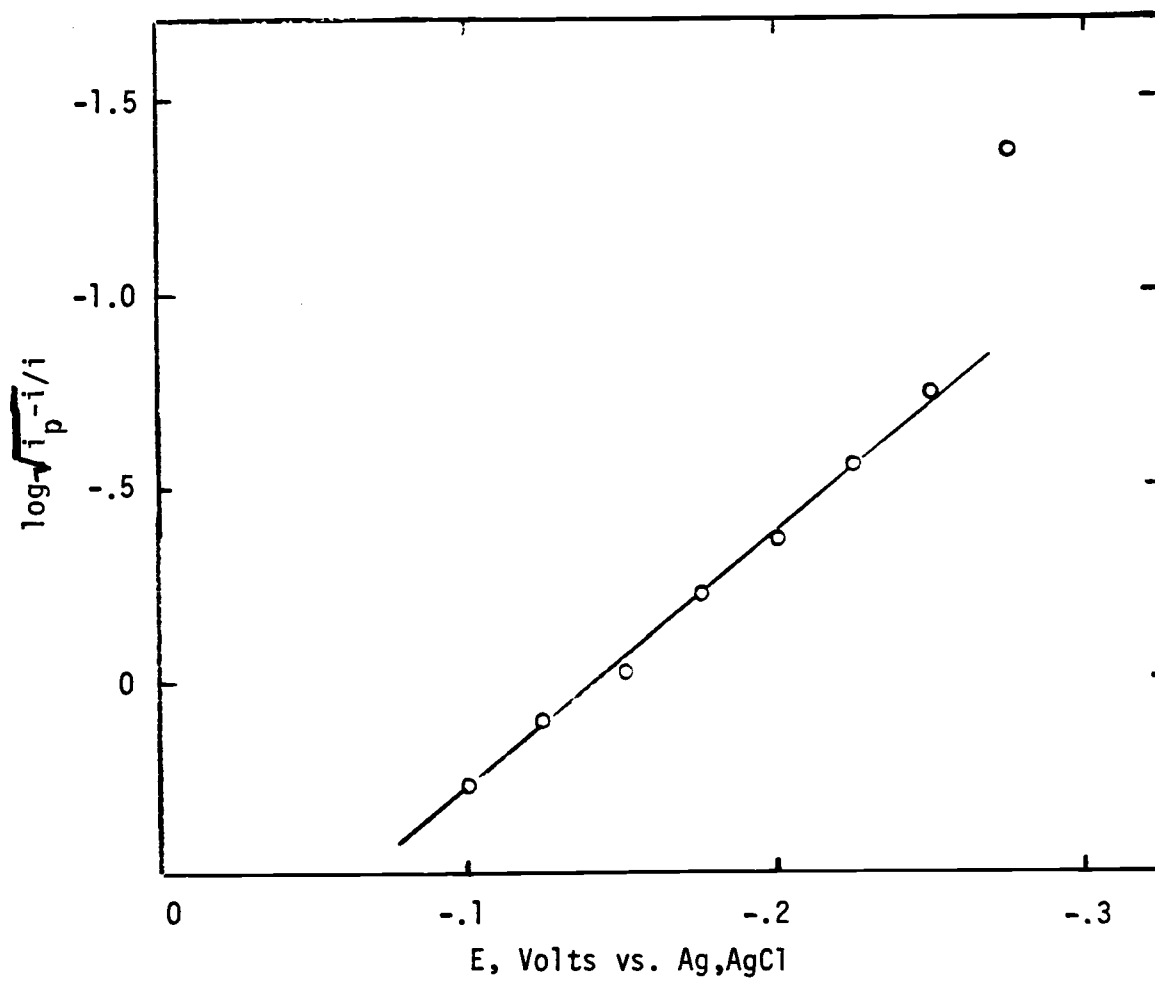
Figure 19. $\log\sqrt{i_p - i}/i$ vs. E

$v = 50$ mv/sec
slope = 0.153
$\alpha n = 1.32$
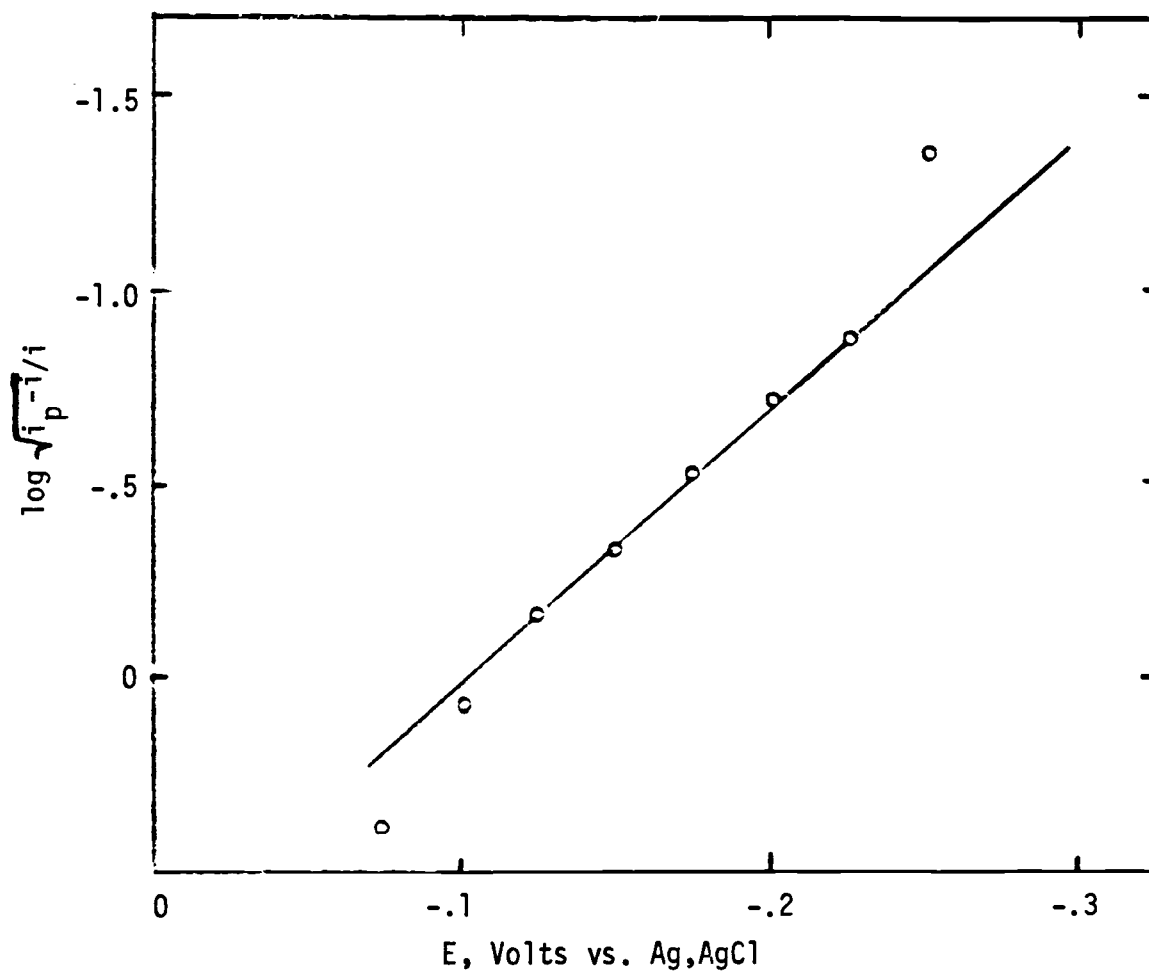
Figure 20. $\log \sqrt{i_p^{-1}}/i$ vs. E

$v = 100$ mv/sec
slope = 0.141
$\alpha n = 1.43$
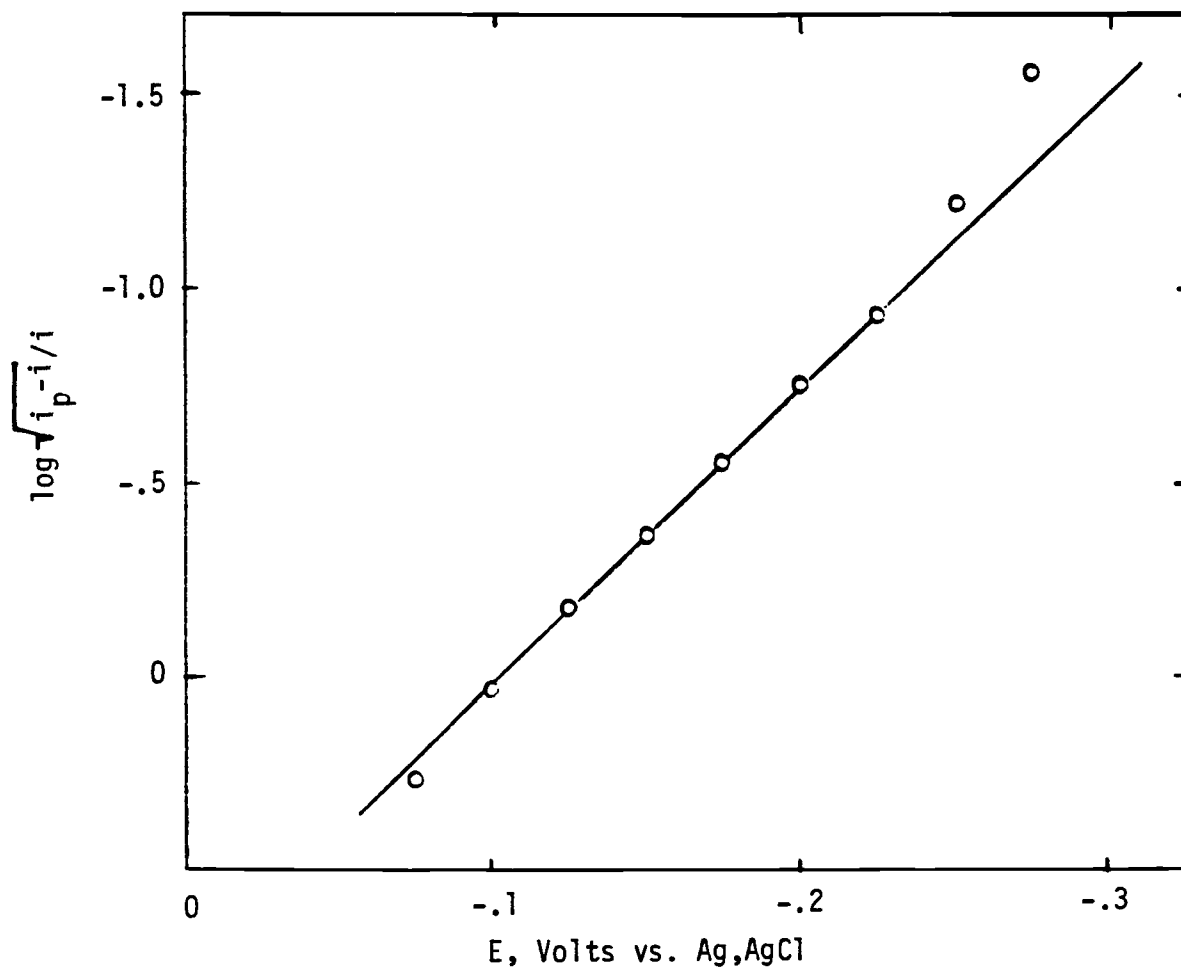
Figure 21. $\log \sqrt{i_p - i/i}$ vs. E

v = 200 mv/sec
slope = 0.131
αn = 1.53
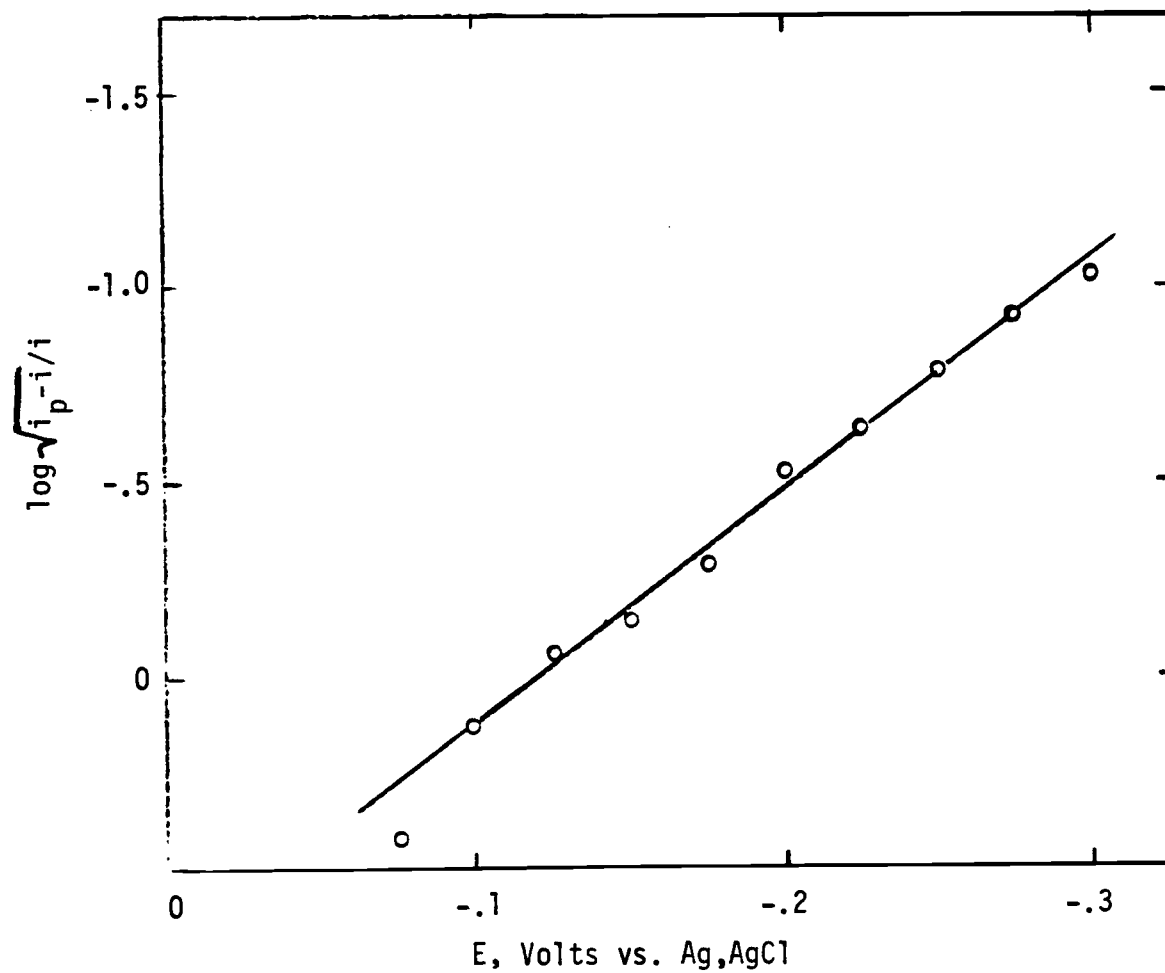
Figure 22. $\log \sqrt{i_p - i}/i$ vs. E

v = 500 mv/sec
slope = 0.162
n = 1.21

Discussion and Conclusions

Analysis of the results of the experiments may be simplified to considering reactions that are most likely and the voltametric characteristics of these reactions. If the presence of Zr(I) is eliminated as a possibility there are three remaining reactions that could account for the first reaction step, assuming there are no preliminary or post reactions complicating the situation.

$$Zr(IV) + e- \rightleftarrows Zr(III) \tag{43}$$

$$Zr(IV) + 2e- \rightleftarrows Zr(II) \tag{44}$$

$$Zr(IV) + 4e- \rightleftarrows Zr(0) \tag{45}$$

The three differ in n value and in the nature of the reduced species. The four electron reaction would result in deposition of the metal and a voltammogram related to the Koltoff-Lingane type of polarogram. The reverse scan of a cyclic voltammogram would be a sharp unsymmetrical peak.

The two and one electron reactions would each have the same shape of voltammetric wave; however, the two electron wave would be steeper.

All of the theory developed for cyclic voltammetry is based on the assumption that the reduced species is soluble. If the reduced species is not soluble, or only slightly soluble, the waves will appear distorted. As is shown in the theoretical section, if the reduced species forms a deposit that has a constant activity, then the DC wave, and consequently the cyclic voltammograms will be steeper. It was also shown that as a consequence of this the differential pulse polarogram will be narrower, and will be asymmetric.

Any degree of irreversibility will broaden the waves and

cause the apparent n values to be smaller.

Thus, two factors can affect the apparent n values. First, irreversibility will make the apparent n values smaller, and second, an insoluble reduced species that results in a deposit that has a constant activity will make the apparent n values larger.

The effects of both irreversibility and precipitation can be minimized by the proper choice of experimental conditions. If the reduced species is slightly soluble the concentration of Zr(IV) used can be decreased to a level low enough to prevent precipitation of the reduced species, while still high enough for successful measurement. The distortion in the cyclic voltammograms due to irreversibility can be minimized by slow scan rates.

A low concentration of Zr(IV) will affect the cyclic voltammograms because diffusion control will be attained more rapidly. Because of the somewhat higher diffusion coefficients in fused salts than in water, low concentrations have an even greater effect, so that at very low concentrations diffusion can be the current limiting factor at practically all of the scan rates used. The waves obtained when the current is diffusion controlled will have the form of a normal S shaped form of the DC wave, and will be unuseable for cyclic voltammetric interpretation, although they can be analyzed by normal polarographic techniques. The fast scan rates will spread the forward and reverse waves if the reaction is quasi-reversible.

If the electrochemical rate constant is low, the kinetics will partially or entirely control the current. When the current is kinetically controlled the voltammogram will be spread and lowered. Spreading of the waves will decrease the calculated apparent n

values, if the estimation is based on the reversible case. The equations derived for the irreversible case can only be used when the reaction is totally irreversible.

The first experiments utilizing cyclic voltammetry run at 1013K and with concentrations between 6.2×10^{-5} and 1.7×10^{-4} mole fraction of zirconium, showed characteristics expected of a quasi-reversible reaction, and of a slightly soluble reaction product. For the cyclic voltammetric waves the separation of the peak potentials increases with scan rate, indicating quasi-reversibility. The anodic scan shows an initial very sharp peak at the lower scan rates, which disappears as the scan rate is increased. The faster scan rates yield smaller amounts of the reaction product, because of the shorter reaction times. The smaller amounts of reduced species mean a smaller percentage of the reduced species is deposited, and therefore the sharp stripping wave disappears.

Because of the complications introduced by the quasi-reversibility and the deposition, all of the n values calculated will be called diagnostic apparent n values, to emphasize that they are to be used only for analyzing what the most probable n value is, and are not to be taken as exact n values.

The comparison of the diagnostic apparent n values in Table IX requires careful consideration of the effects of precipitation of the reduced species and of quasi-reversibility on the diagnostic apparent n values. The various methods of analyzing for the diagnostic apparent n values are affected differently by the complications.

The first column of diagnostic apparent n values in Table IX

comes from the difference between the cathodic peak potential and the potential at one half of the peak current. This method of measuring the diagnostic apparent n value depends only on the characteristics of the cyclic voltammetric wave between E_{cp} and $E_{cp/2}$. The first part of the curve does not affect the diagnostic **apparent n** value, nor does the anodic wave.

The diagnostic apparent n value comes from a balance of the effects of deposition, and the quasi-reversibility. The true n value would be observed only when the solution conditions are such that the scan rate is fast enough to prevent deposition, yet slow enough for the wave to be nearly reversible. With the experimental curves, the only curve that comes close to these requirements is the 200 mv/sec scan in Figure 16. The diagnostic apparent n value of 2.04 obtained for this wave is therefore the most reliable of these values.

The second column of diagnostic apparent n values in Table IX are calculated from the difference between the cathodic and anodic peak potentials. The separation of the peaks is affected by both the anodic and cathodic scans. The quasi-reversibility of the reaction has a much greater effect on this diagnostic apparent n value because the peak separation increases faster than peak and half peak potential separation. For these measurements the increased separation results in a decreased diagnostic apparent n value, especially after the scan rate is increased to where deposition does not occur. The effect is most dramatic when the scan rate is increased from 200 mv/sec to 500 mv/sec. Even with the kinetic problems all of the diagnostic apparent n values except at 500

mv/sec are greater than one. The conclusion to be reached from these results is that the actual n value must be greater than one.

The next column of diagnostic apparent n values in Table IX is obtained from graphs of $\log(\sqrt{i_p}-i)/i$. The graphs of $\log(\sqrt{i_p}-i)/i$ (Figures 17 to 21) all cover the first rising portion of the wave. Data from this first rising portion of the wave yields diagnostic apparent an values ranging from 0.88 to 1.53. The data are taken from the earliest portion of the curve, where the effects of deposition should be the least. Irreversibility has a great effect on this portion of the curve. The effects of irreversibility on this portion of the curve are more difficult to understand than the way deposition and irreversibility affect the other portions of the curve, and consequently the other diagnostic apparent n values.

Since the peak current is dependent on the square root of the scan rate and the current at the foot of the wave is not, the graphs of $\log(\sqrt{i_p}-i)/i$ necessarily change as the scan rate changes. For this reason the application of these graphs needs careful consideration as to which regions of the curve it is valid.

The current in the rising or middle section of the wave changes with scan rate in the irreversible case. The graphs of $\log(\sqrt{i_p}-i)/i$ are applicable in this region for the irreversible case; however, in the case of the reduction of Zr(IV), that region is distorted by deposition of the reduced species.

The true an value then lies somewhere between 0.88 and 1.53. Since Zr(I) has not been found in fused halides we have eliminated the three electron transfer. From this data then, the two electron transfer remains the choice.

The cyclic voltammetric data taken at 740 C indicate a quasi-reversible two electron step according to reaction 46.

$$Zr(IV) + 2e- \rightleftarrows Zr(II) \tag{46}$$

The Zr(II) product is only slightly soluble.

The solubility of the reduced species can be estimated from these curves by calculating the amount of zirconium produced during the slowest scan which does not show the effects of deposition. The 200 mv/sec scan in Figure 15 shows the wave form expected for cyclic reduction and oxidation in a homogeneous system, and will be used for the following calculation.

The number of coulombs passed during the scan is found by graphical integration. The number of moles of zirconium(II) produced may then be calculated from the number of coulombs. The number of coulombs passed is 7.2×10^{-4}, and consequently the number of moles of zirconium(II) produced is 3.7×10^{-9} moles. The volume in which this Zr(II) is dissolved is approximately the volume of the sphere of diffusion minus the volume of the Pt drop electrode. The sphere of diffusion can be estimated from the diffusion coefficient for Zr(II), and the time between when Zr(II) was first produced and when it was last produced. The diffusion coefficient for Zr(II) in fused NaCl-KCl found by Sakakura (38) is 5.4×10^{-3} cm^2/sec. The time of diffusion is 5.1 seconds. The Einstein-Smoluchowski equation (7) for the mean square distance of diffusion is used to estimate the distance Zr(II) will diffuse from the surface of the electrode.

$$X^2 = 2Dt \tag{47}$$

Using equation 47 the x value is 0.23 cm. Remembering that this is a diffusion distance, the radius of the sphere of diffusion becomes 0.28 cm when the radius of the Pt drop microelectrode is included.

The volume that the Zr(II) is dissolved in is therefore found by equation 48.

$$V = 4/3 \ (0.28 \ cm)^3 - 4/3 \ (0.05 \ cm)^3 \qquad (48)$$

The volume is 0.095 cm^3 or approximately 0.095 ml. This yields a molar concentration of 3.9×10^{-5} moles/liter. The mole fraction is found by estimating the molar volume of the NaCl-KCl eutectic. The molar volume of the eutectic is estimated to be one half the sum of the molar volumes of KCl and NaCl. The molar volumes of NaCl and KCl are given by Sundheim (45). The estimated mole fraction solubility of Zr(II) is 1.6×10^{-6} in a solution whose total mole fraction of zirconium is 1.7×10^{-4}.

The limited solubility of the reaction product is confirming evidence that it is Zr(II).

The analysis of the initial cyclic voltammograms showed several principles to apply in subsequent experiments. First, the limited solubility of the reduction product, coupled with the relatively high currents observed suggests the use of much lower concentrations of zirconium(IV). If the zirconium concentration is sufficiently low the concentration of the zirconium(II) may not exceed its solubility. The low concentration may also enhance the reversibility, perhaps making it possible to get a reversible polarographic wave. Second, the first series of experiments showed that there was a

window in the range of possible scan rates in which the effects of deposition of the reduced species and of the quasi-reversibility are minimized. For this reason, only the scans that fall within this window will be analyzed. The initial scans showed a scan rate of 200 mv/sec to fall within this window. Also needed are scans at a series of temperatures, yielding the temperature dependance for the formal potential. Several changes other than the shift of the formal potential are to be expected as the temperature is increased. First, the kinetics will become faster, and second, zirconium dichloride melts at 995K. This may change the shape of the waves. The liquid zirconium dichloride could coat the electrode in a different way than the solid, or it may run off and not coat the electrode at all. The liquid may have an enhanced solubility. The 200 mv/sec scans taken with these ideas in mind are shown in Figures 23 to 26. The data from these scans are in Tables X and XI. The second series of experiments were run at a range of temperatures (953K, 973K, 993K, 1013K, 1043K, 1973K, and 1123K) and at a range of concentrations. The first scans of this second series were run at 953K and a Zr(IV) mole fraction of 1.9×10^{-4}. Subsequent scans at the higher temperatures were all done at higher concentrations than the first. The Zr(IV) concentration in the melt drops continuously during the experiments. There are two probable reasons for this. The first is loss of zirconium tetrachloride due to its high vapor pressure. The zirconium tetrachloride that enters the vapor phase over the melt condenses on the cooler cell cover, effectively pumping it out of the melt. The second way in which zirconium is lost is by the precipitation of zirconium dichloride as it is produced at
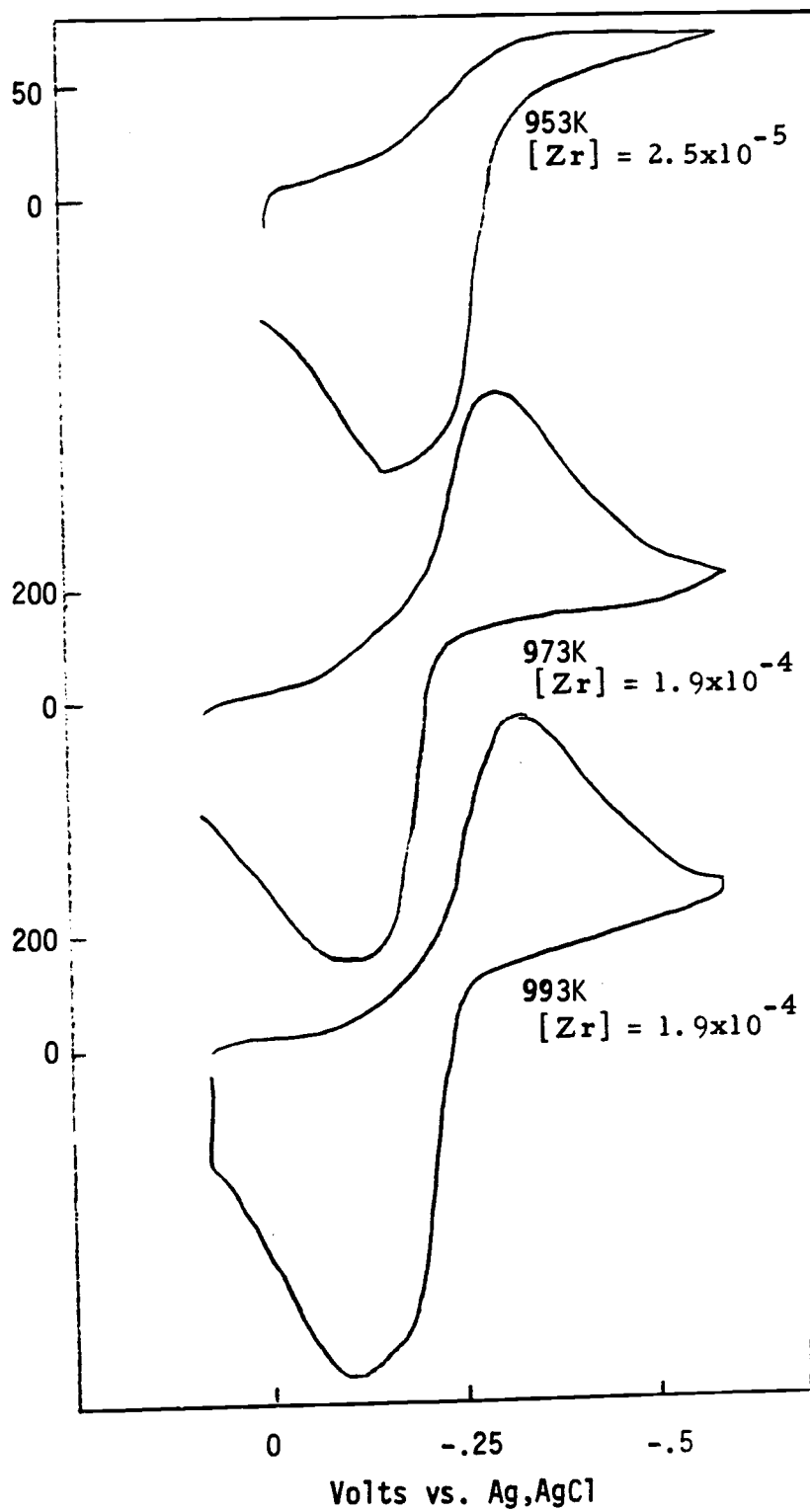
Figure 23. Cyclic voltammograms, 200 mv/sec
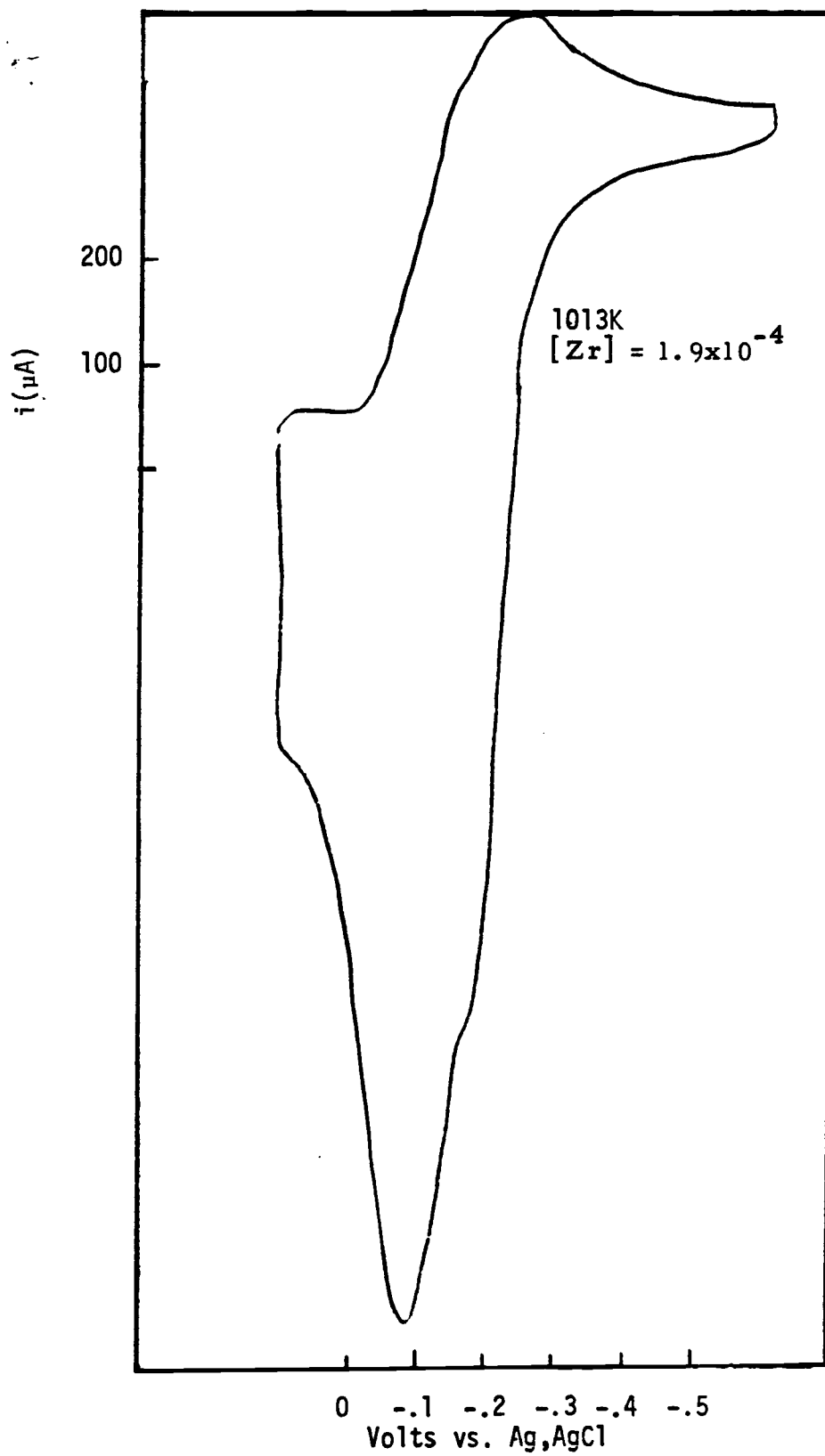
Figure 24. Cyclic Voltammograms.   200 mv/sec

100 μA

i, μA

1043K
$[Zr] = 1.9 \times 10^{-4}$

100

1123K
$[Zr]$ 1.9×10^{-4}

Volts vs. Ag,AgCl
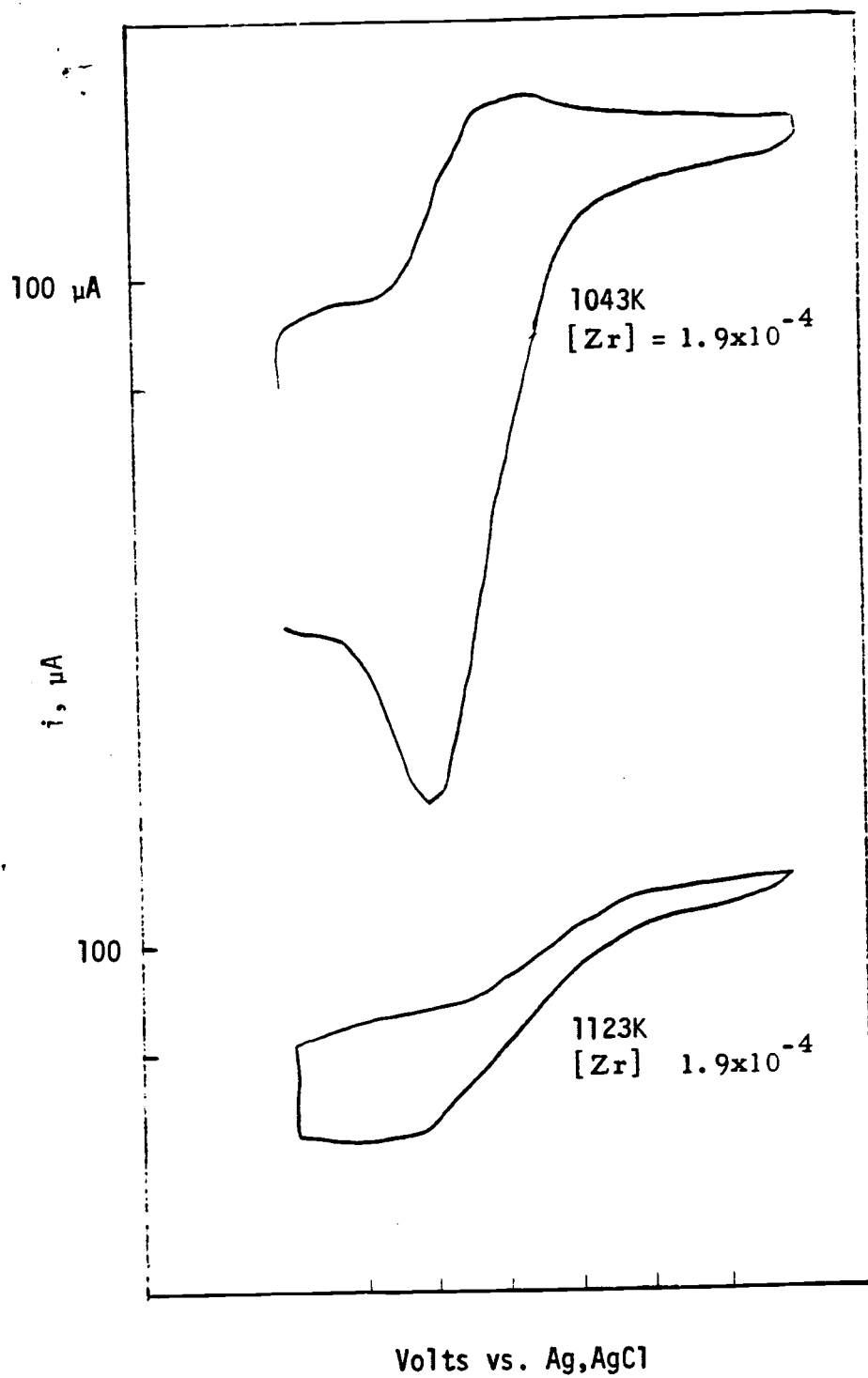
Figure 25. Cyclic voltammograms, 200 mv/sec
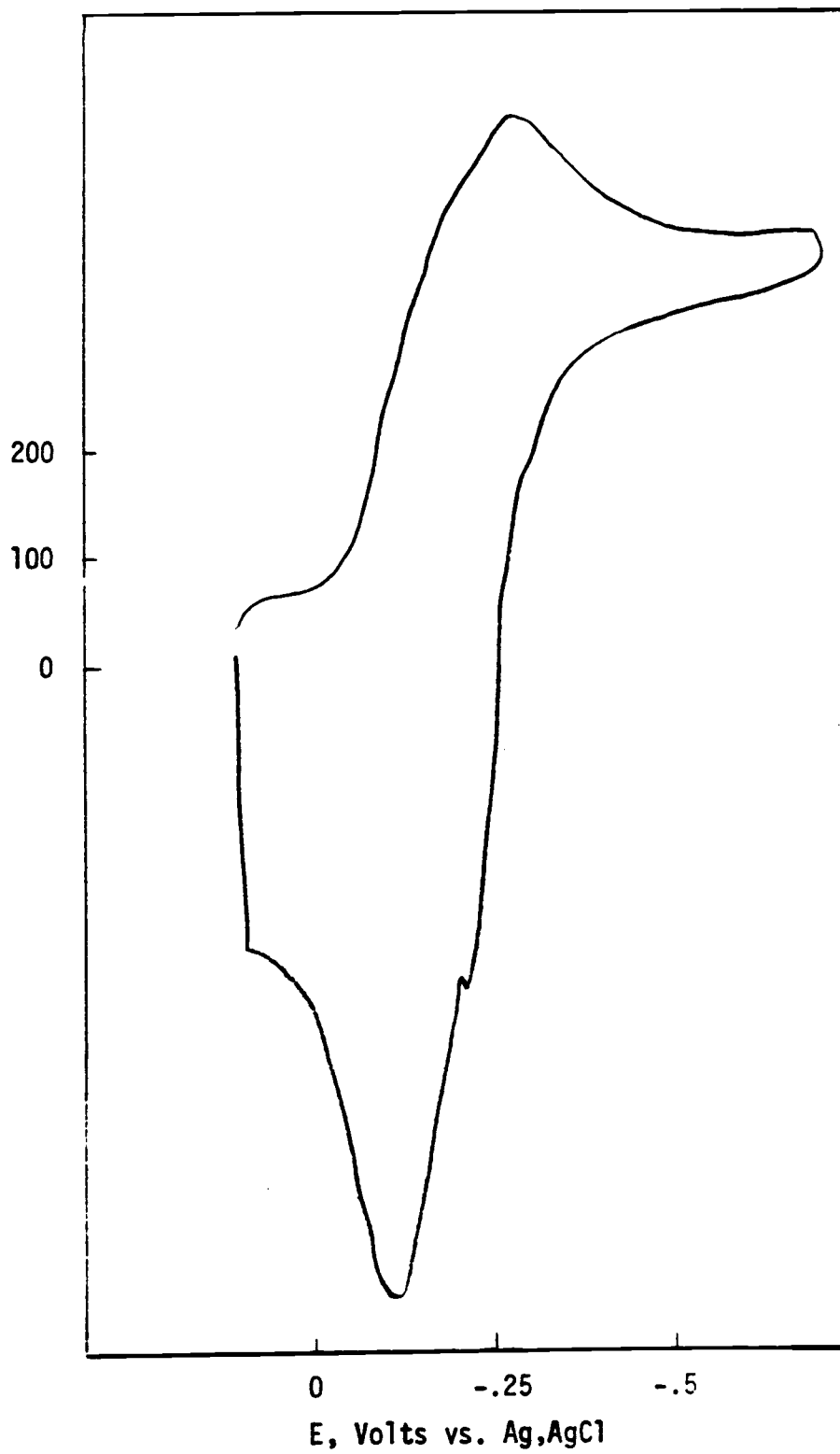
Figure 26. Cyclic voltammogram.   200 mv/sec
[Zr] < 1.9x10^{-4}.   1073K

TABLE X. DATA FROM CYCLIC VOLTAMMOGRAMS TAKEN AT 200 mv/sec

Temp.	Concentration	E_{cp}	$E_{cp/2}$	E_{ap}	i_{cp} (mA)	i_{ap} (mA)
953K	$<2.5 \times 10^{-5}$	-.330	-.230	-.150	70.8	133
973K	1.9×10^{-4}	-.290	-.212	-.105	533	433
993K	$<1.9 \times 10^{-4}$	-.325	-.237	-.100	577	567
1013K	$<1.9 \times 10^{-4}$	-.250	-.105	-.080	440	833
1043K	$<1.9 \times 10^{-4}$	-.225	-.212	-.090	267	392
1073K	$<1.9 \times 10^{-4}$	-.285	-.120	-.115	500	617
1123K	$<1.9 \times 10^{-4}$	-----	-.265	-----	150	---

TABLE XI. DIAGNOSTIC APPARENT n VALUES FROM CYCLIC VOLTAMMOGRAMS
SCAN RATE = 200 mv/sec

Temp.	Concentration, Mole Fraction	$E_{cp}-E_{cp/2}$	"n"	$E_{cp}-E_{ap}$	"n"
953K	2.5×10^{-5}	.100	1.8	.235	0.77
973K	1.9×10^{-4}	.078	2.36	.185	1.00
993K	1.9×10^{-4}	.088	2.14	.225	0.84
1013K	1.9×10^{-4}	.145	1.32	.170	1.13
1043K	1.9×10^{-4}	.018	15.2	.135	1.47
1073K	1.9×10^{-4}	.165	1.23	.170	1.20

the working electrode. Because of this loss of zirconium(IV) its concentration cannot be maintained at a constant level in the melt. Therefore Zr(IV) must be added to the melt several times during the experiments.

The shape of the cyclic voltammograms taken at 953K and 2.5×10^{-5} mole fraction of zirconium(IV) indicate that deposition is taking place even at this low concentration. (Figure 27) The anodic scan shows the sharp peak exhibited when stripping of a deposited product takes place. The cathodic scan is generally a cleaner wave than is seen at higher concentrations. The concentration could be reduced further, but the difficulty in keeping the zirconium in the solution would be magnified. In addition the currents seen at 2.5×10^{-5} mole fraction, while high by aqueous standards, are low by fused salt standards.

The cyclic voltammograms are still quasi-reversible at 2.5×10^{-5} mole fraction of zirconium(IV). The curves are diffusion controlled at each scan rate because of the low concentrations. The data obtained from these curves must then be DC polarographic type data, since a value for the cathodic peak potential cannot be taken from these curves. The scans taken at higher concentrations can be analyzed by cyclic voltammetric techniques.
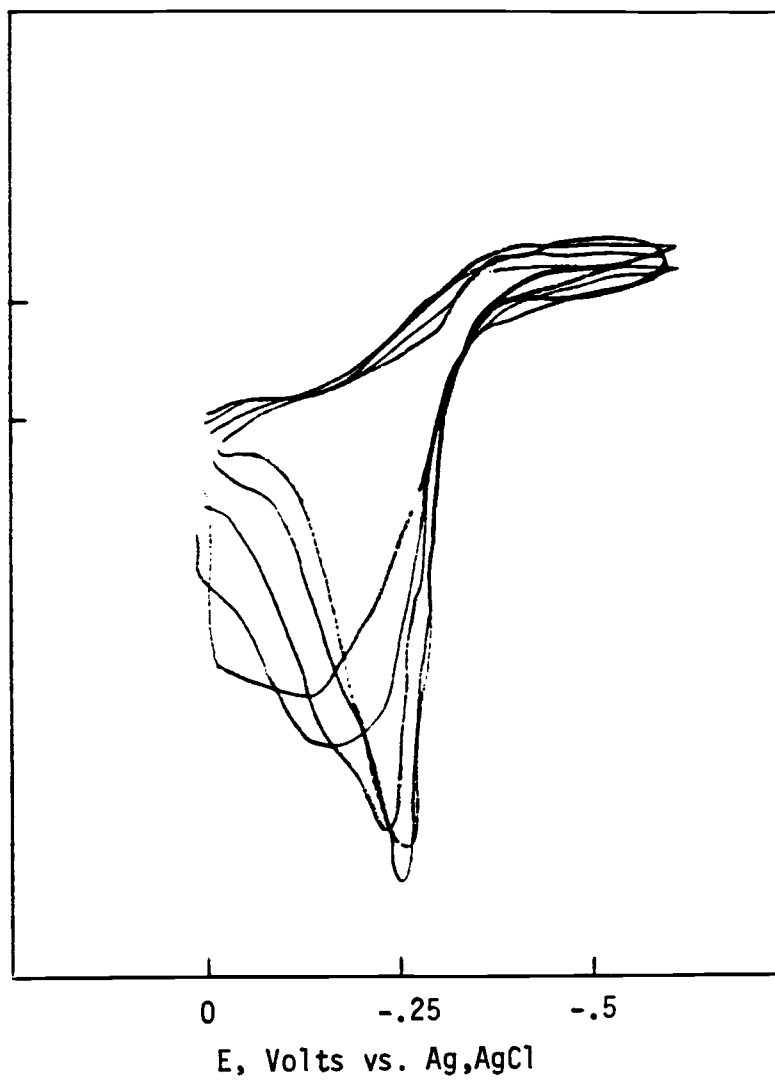
Figure 27. Low concentration cyclic voltammograms
[Zr] = 2.5×10^{-5}
Temp. = 953K

Differential Pulse Polarography

Examples of the initial differential pulse polarograms are shown in Figures 28 and 29. The voltage range over which the polarogram was taken markedly affected the polarograms run after it in the same melt. Figure 28A shows a polarogram run immediately after immersing the platinum drop microelectrode, and addition of zirconium(IV). Figure 28B shows the type of polarogram found after a scan like that shown in Figure 28A is run. If the potential is set positive of the first wave (+.1 volts vs Ag,AgCl) and allowed to remain there for 45 minutes to an hour a polarogram like that in figure 28A is again obtained. To eliminate the problems found from scanning past the first wave most scans were halted at -0.6 volts. The polarograms in Figure 29B are examples of this type of polarogram. The differential pulse polarograms were analyzed for the thermodynamic data they contained.

The differential pulse polarograms taken show an elbow on the positive side of the peak, corresponding to the one seen on the cyclic voltammograms. The half widths and quarter widths of the polarograms average to be 112 mv and 180 mv respectively. The diagnostic apparent n values are expected to be larger than the actual value because deposition makes the normal wave steeper, and consequently the differential pulse polarogram's peak narrower, as we saw in the theoretical section. Since the reduced species is slightly soluble we expect the initial part of the wave to show more of the characteristics expected from a soluble species, and to show less narrowing of the peak. The width at the quarter height does show
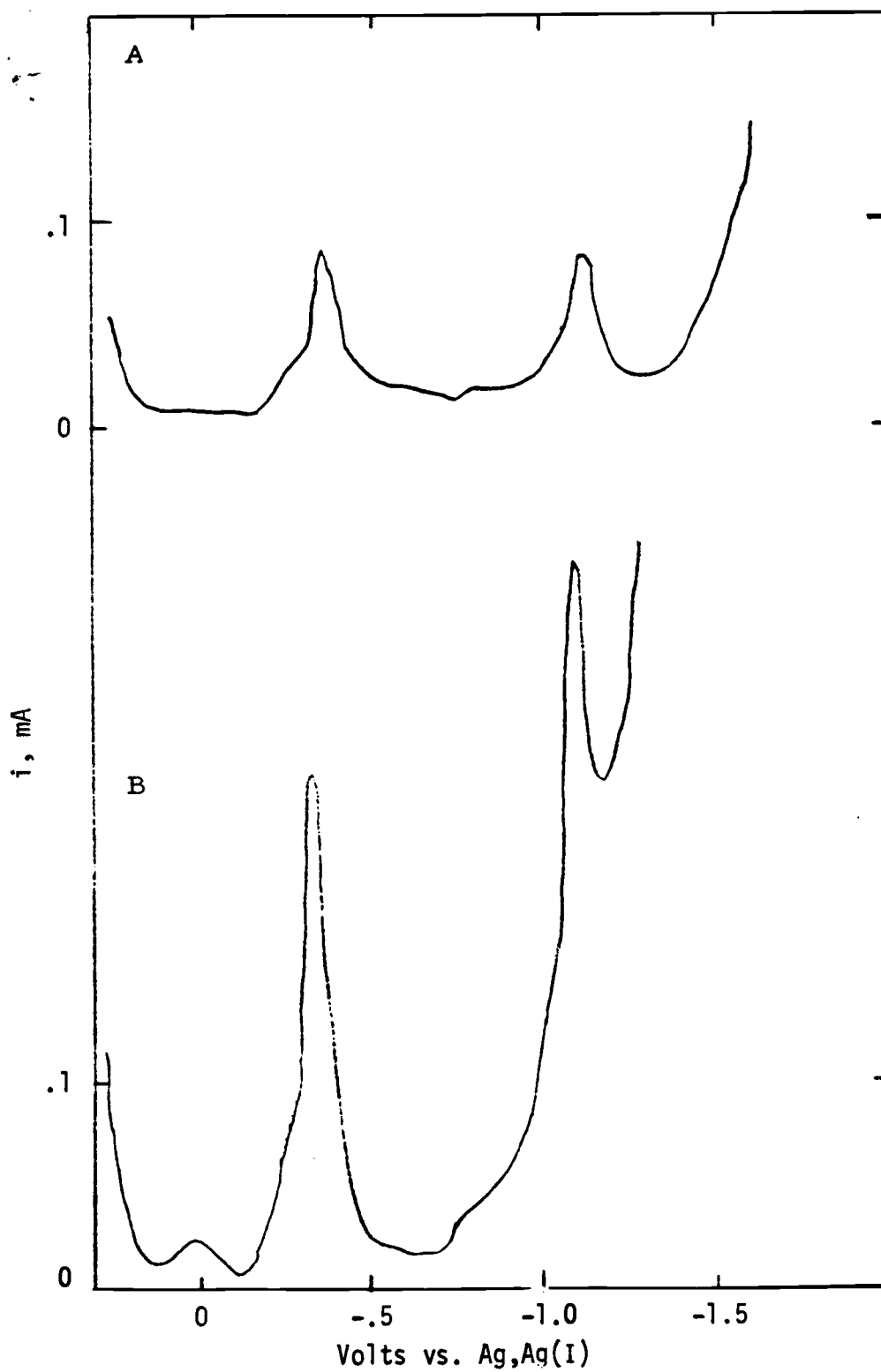
Figure 28. Differential pulse polarograms.
A. Initial wave
B. Wave found after A is run
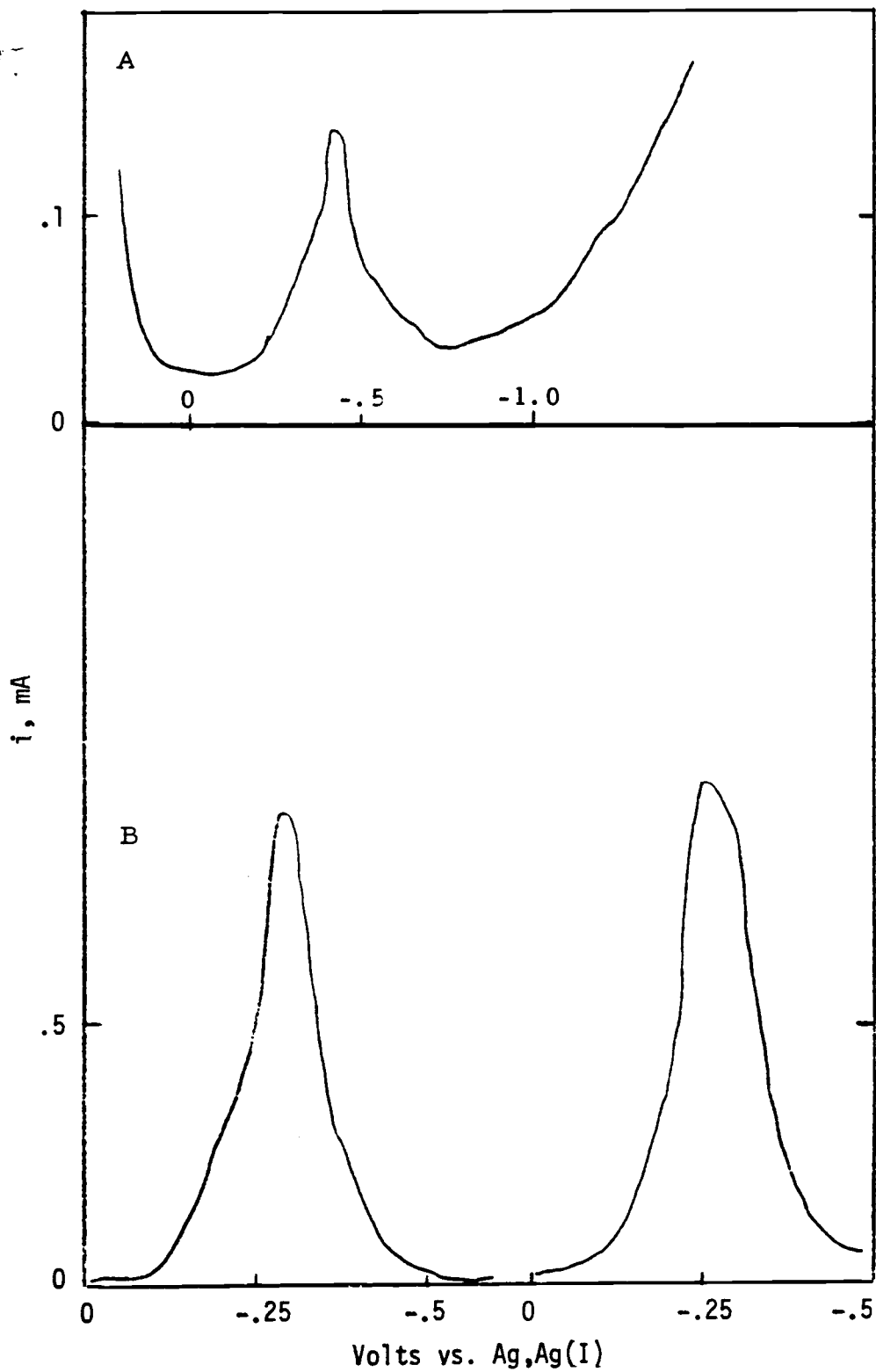
Figure 29. A type found after a Figure 22B type scan is run.
B two scans 0 to -0.6V

less narrowing, and consequently a smaller diagnostic n value. The
diagnostic apparent n values obtained from the widths are 2.74 from
the half height, and 2.55 from the quarter height. The peak poten-
tial is $\Delta E/2$ volts more positive than the half wave potential. The
half wave potential would be equal to the formal potential if no
quasi-reversibility were present, and the activity coefficients of
the two species were equal.

The average peak potential found in these experiments is -0.279
volts. The half wave potential and formal potential is -0.292 volts.
This potential versus the standard chlorine electrode is -1.35 volts.

Data for peak potentials, half wave potentials and half widths
were taken from the polarograms which were scanned at 10 mv/sec,
with a 25 mv pulse height. The polarograms which were scanned past
the second wave showed similar results.

Differential pulse polarograms were also run at the same series
of temperatures that the cyclic voltammograms were run at. (953K,
973K, 993K, 1013K, 1043K, 1073K, and 1123K)

The differential pulse polarograms run at 953K and 2.5×10^{-5}
mole fraction of zirconium(IV) (Figure 30) show very low currents
and wide peaks. At 973K and 1.9×10^{-4} mole fraction of zirconium(IV)
the current is much larger, the peak is narrower and has the "elbow"
that is characteristic of the slightly soluble reduction product.
At 993K the peak has the same shape as the one at 973K, but has
shifted more positive. The concentration of zirconium(IV) constantly
decreases throughout the experiment because of loss by volatiliza-
tion of zirconium tetrachloride and precipitation of zirconium
dichloride. As the temperature is raised the volatility of zirconium

tetrachloride increases and it is lost at a faster rate. For the scans taken at 1013K and 1043K the concentration of zirconium has dropped to a point where the waves are less distorted than those found at higher concentrations. The peaks at 1073K and at 1132K are wider, but still distorted, indicating deposition and quasi-reversibility are still problems. The data and diagnostic apparent n values are shown in Tables XII and XIII.
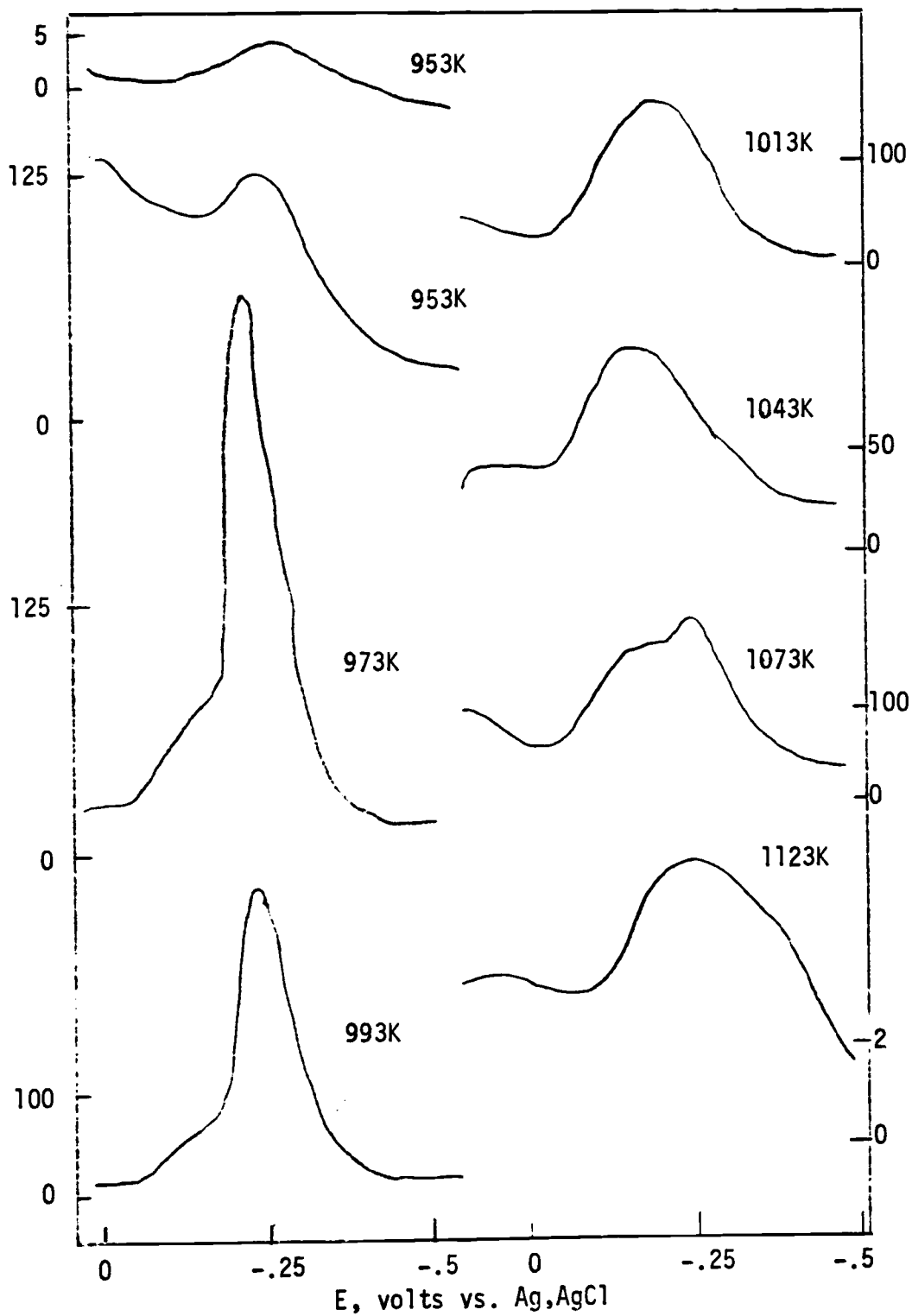
Figure 30. Differential pulse polarograms
[Zr] = 2.5×10^{-5} at 680°; 1.9×10^{-4} at all other temp.

TABLE XII. DIFFERENTIAL PULSE POLAROGRAPHY

Temp.	Concentration	Scan Rate/ Pulse Ht.	E_p,V	$E^{0'}$, V	$w_{\frac{1}{2}}$, V	$w_{\frac{1}{4}}$, V
953K	2.5×10^{-5}	10 / 10	-.265	-.270	-----	-----
953K	2.5×10^{-5}	10 / 25	-.275	-.287	.150	
953K	$<2.5 \times 10^{-5}$	10 / 25	-.250	-.262	.140	
973K	1.9×10^{-4}	10 / 25	-.220	-.232	.087	.135
993K	$<1.9 \times 10^{-4}$	10 / 25	-.235	-.247	.100	.150
1013K	$<1.9 \times 10^{-4}$	10 / 25	-.185	-.197	.182	.237
1043K	$<1.9 \times 10^{-4}$	10 / 25	-.162	-.174	.167	.250
1073K	$<1.9 \times 10^{-4}$	10 / 25	-.237 -.185	-.239 -.197	.200	.257
1123K	$<1.9 \times 10^{-4}$	5 / 5	-.237	-.249	.225	.287

TABLE XIII. DIAGNOSTIC APPARENT n VALUES FROM DIFFERENTIAL PULSE POLAROGRAPHY

Temp.	Scan Rate/ Pulse Ht.	$W_{1/2}$	"n"	$W_{1/4}$	"n"
953K	10 / 25	.150	1.93		
953K	10 / 25	.140	2.06		
973K	10 / 25	.087	3.39	.135	3.27
993K	10 / 25	.100	3.01	.150	3.00
1013K	10 / 25	.182	1.69	.237	1.94
1043K	10 / 25	.167	1.89	.250	1.89
1073K	10 / 25	.200	1.63	.257	1.85
1123K	5 / 25	.225	1.51	.287	1.78

DC Polarography

If the conclusion reached from the cyclic voltammetry and differential pulse polarography that the reduced species is slightly soluble is valid, coverage of the microelectrode by the reduced species will cause a decrease in the diffusion currents of the DC polarograms after the diffusion current is initially reached.

The DC polarograms show interesting characteristics (Figure 31). At 953K and 2.5×10^{-5} mole fraction of zirconium(IV) the diffusion current is constant after the plateau is reached. At 953K and 1.9×10^{-4} mole fraction of zirconium(IV) there is a distinct peak in the polarogram. The current constantly decreases after the diffusion peak is reached. This is the characteristic expected if the reduced species is deposited on the electrode as a non-conducting species. If zirconium metal were being deposited, the electrode area would increase rather than decrease, and an increase in current would be seen. The reduced species must then be zirconium(II) since zirconium(III) is a soluble species. The data are shown in Table XIV. At 1043K the DC polarograms show constant current after the diffusion plateau is reached. This is the temperature at which zirconium dichloride was expected to be molten, and changes in the polarograms were expected.
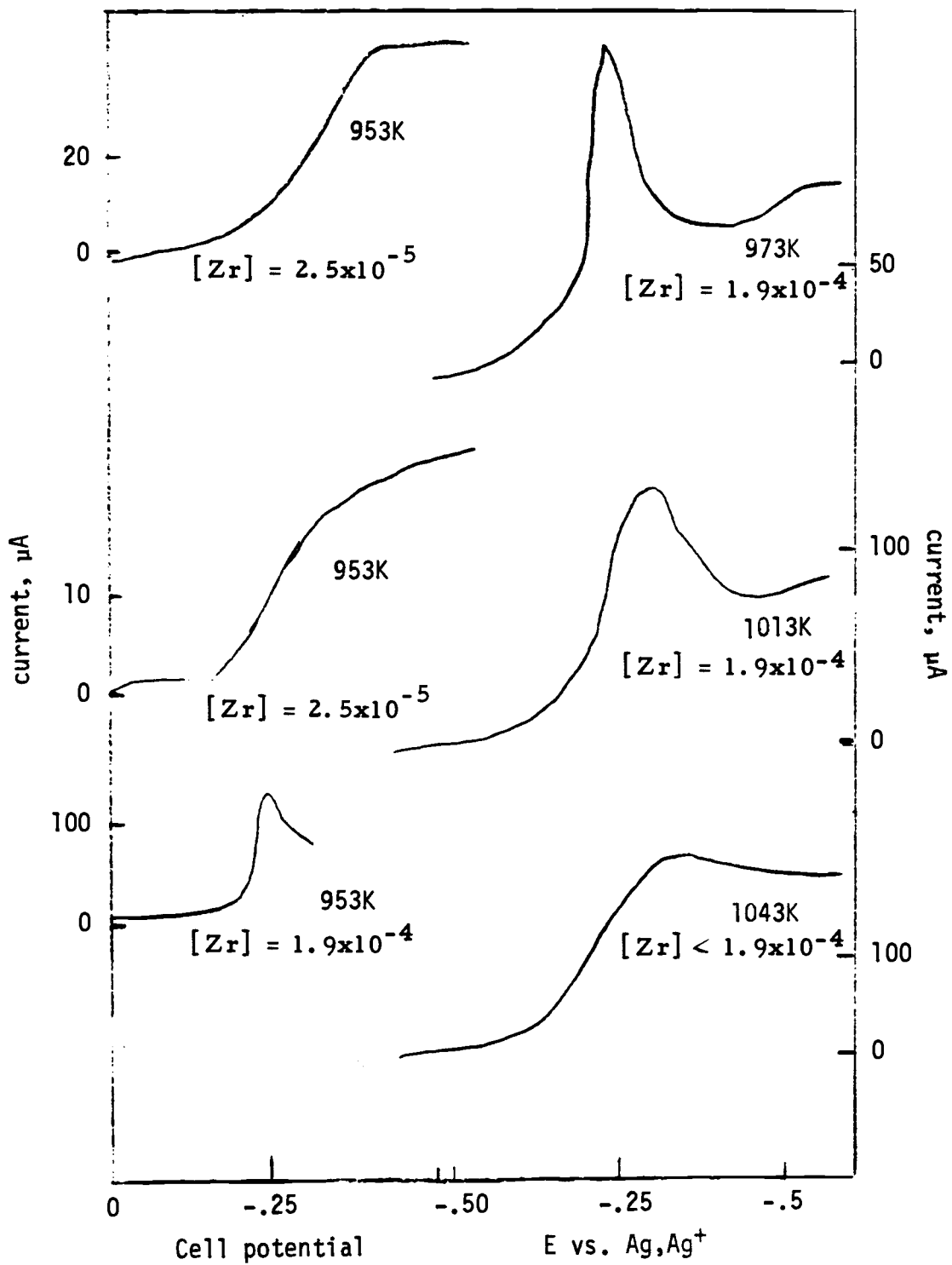
Figure 31. DC polarograms. 2 mv/sec

TABLE XIV. DC POLAROGRAPHY

Temp.	Concentration, Mole Fraction	Scan Rate	$E_{\frac{1}{2}}$,V	i_d	E_p,V	$E_{cp/2}$,V
953K	25×10^{-5}	5 mv/sec	-.315	$50 \mu A$		
953K	25×10^{-5}	2 mv/sec	-.313	$43.3 \mu A$		
953K	1.9×10^{-4}	2 mv/sec		$133 \mu A$	-.245	-.225
973K	1.9×10^{-4}	2 mv/sec		$162.5 \mu A$	-.220	-.200
993K	$<1.9 \times 10^{-4}$	5 mv/sec		$166 \mu A$	-.235	-.210
1013K	$<1.9 \times 10^{-4}$	2 mv/sec		$133 \mu A$	-.300	-.220
1043K	$<1.9 \times 10^{-4}$	2 mv/sec	-.200	$200 \mu A$		
1073K	$<1.9 \times 10^{-4}$	10 mv/sec	-.225	$300 \mu A$		

Normal Pulse Polarography

In contrast to DC polarography, normal pulse polarography should yield waves free from most of the effects of deposition. Since for the pulse polarographic scan the potential is held at a point where the reduced species will be reoxidized (with short pulses causing reduction to take place), at the start of each pulse the electrode should be free of deposited reduced species. The quasi-reversibility of the system will cause distortion of the normal pulse polarographic wave. The wave will be broadened in the same way that a DC wave is.

The pulse polarograms (Figure 32) at 953K to 993K do show a less distorted shape than the DC polarograms, as expected. The normal pulse polarographic technique does remove, or minimize the problems caused by deposition of a slightly soluble species. At 1013K and above the pulse polarographic waves start to broaden until at 1043K and 1123K the wave disappears into the background. The differential pulse polarogram at 1123K did show a peak however. It is broadened, but still has a much narrower peak than would be expected from a one electron reaction. For this reason, not only is the two electron reaction confirmed, but it also indicates that the broadening and disappearance of the normal pulse polarogram must be due to complications peculiar to normal pulse polarography. The data is given in Table XV.
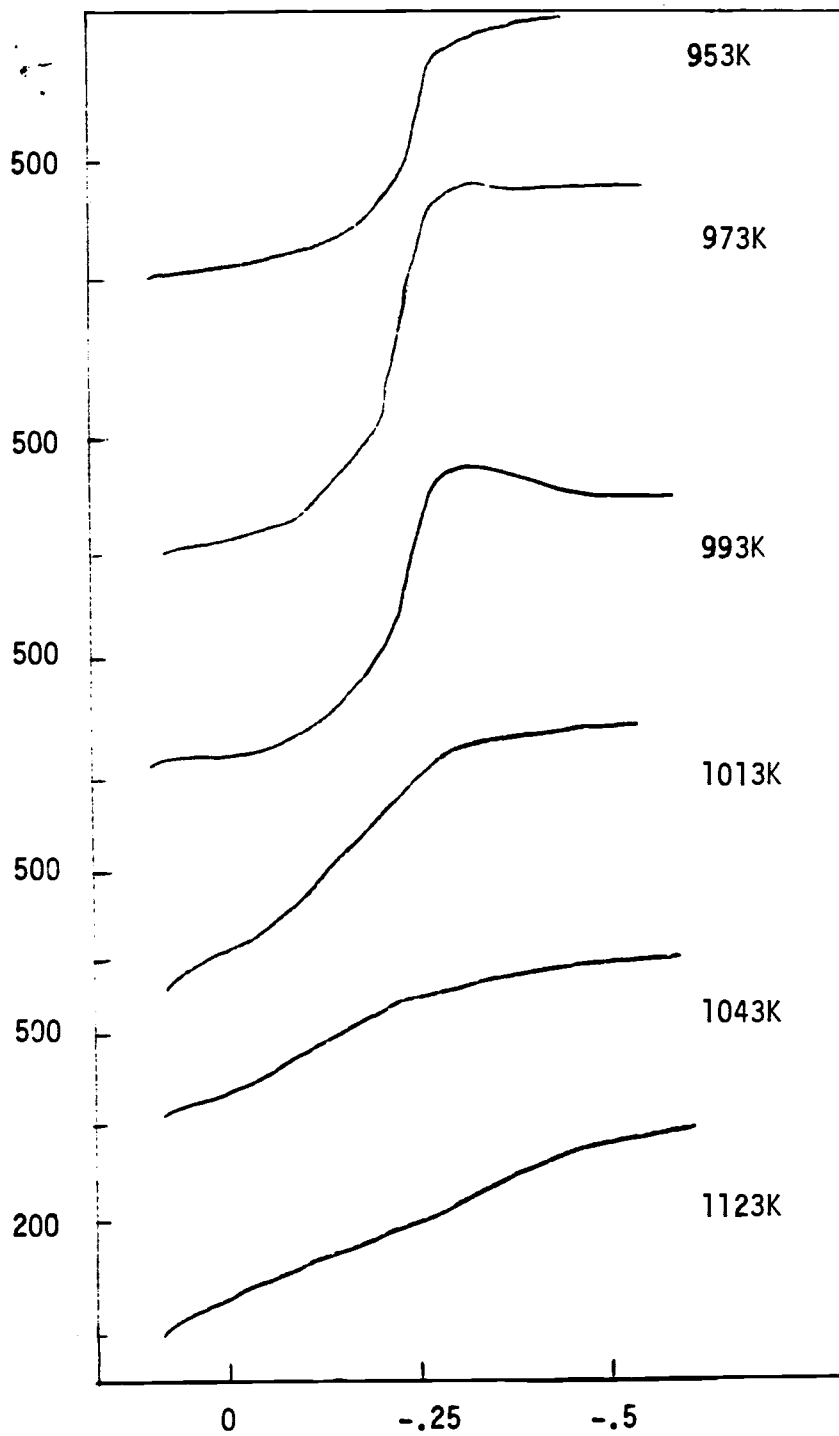
Figure 32. Normal pulse polarograms.
Pulse 5 mv/sec
$[Zr] = 1.9 \times 10^{-4}$

TABLE XV. NORMAL PULSE POLAROGRAPHY

Temp.	Conc. [Zr]	Scan Rate	$E_{\frac{1}{2}}$, V	i_d, mA
953K	1.9×10^{-4}	5 mv/sec	-.237	1.08
973K	1.9×10^{-4}	5 mv/sec	-.225	1.50
973K	$<1.9 \times 10^{-4}$	10 mv/sec	-.225	1.58
993K	$<1.9 \times 10^{-4}$	5 mv/sec	-.225	1.33
993K	$<1.9 \times 10^{-4}$	5 mv/sec	-.230	1.31
1013K	1.9×10^{-4}	5 mv/sec	-.137	1.08
1013K	1.9×10^{-4}	5 mv/sec	-.162	0.90

Fluoride Additions to the Melt

The addition of fluoride to the melt stabilizes the zirconium (IV) in the melt. As fluoride was added to the melt the zirconium (IV) was reduced at more and more negative potentials, indicating that the zirconium(IV) fluoride complex is more stable than the zirconium(IV) chloride complex. Additions of fluoride of four times, eight times, sixteen times, and thirty-two times the amount of zirconium in the melt were made. The reduction potential became more negative with each addition of fluoride. Also with each addition the melting point of the system increased. With additional fluoride the reduction potential of the zirconium(IV) may move negative enough so that the reduction reaction will be directly to zirconium metal. The melting point of the melt will have increased substantially before this point however.

The reaction is quasi-reversible at all fluoride concentrations studied. The diagnostic apparent n values obtained from the differential pulse polarograms become very close to two (2.04) as the fluoride concentration is increased. The polarographic and voltammetric waves taken in the solution with sixteen times as much fluoride as zirconium are less distorted than those obtained in solutions with less or no fluoride. It may be that additional fluoride would stabilize the zirconium(II) species in solution. If zirconium(II) were stable in solution that could account for the fact that good deposits of zirconium can be plated out of chloride-fluoride baths. Further experimentation would be required to determine what the reason is that zirconium can be deposited successfully out of

chloride-fluoride melts. It seems that either the fluoride stabilizes zirconium(IV) so that the deposition reaction is a four electron step, or the fluoride stabilizes zirconium(II) as a soluble species, which would account for the successful subsequent deposition reaction. The scans are shown in Figures 33 to 37 and the data are shown in Tables XVI to XXI.

No F⁻

F = 4 x [Zr]

E vs. Ag,AgCl
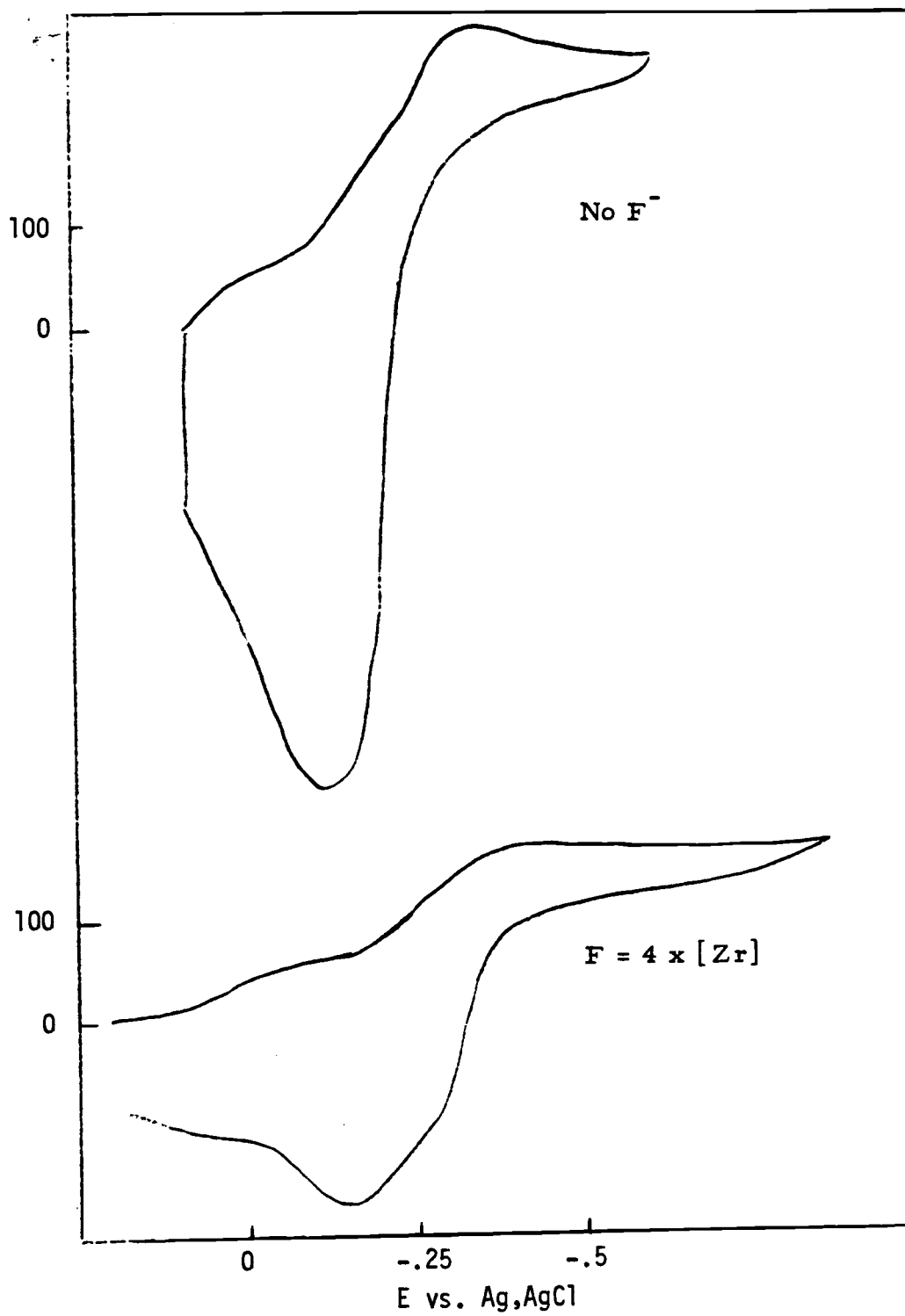
Figure 33.   Cyclic voltammograms.   200 mv/sec
[Zr] = 1.7x10⁻⁴

[F] = 8x[Zr]

[F] = 16x[Zr]

E vs. Ag,AgCl
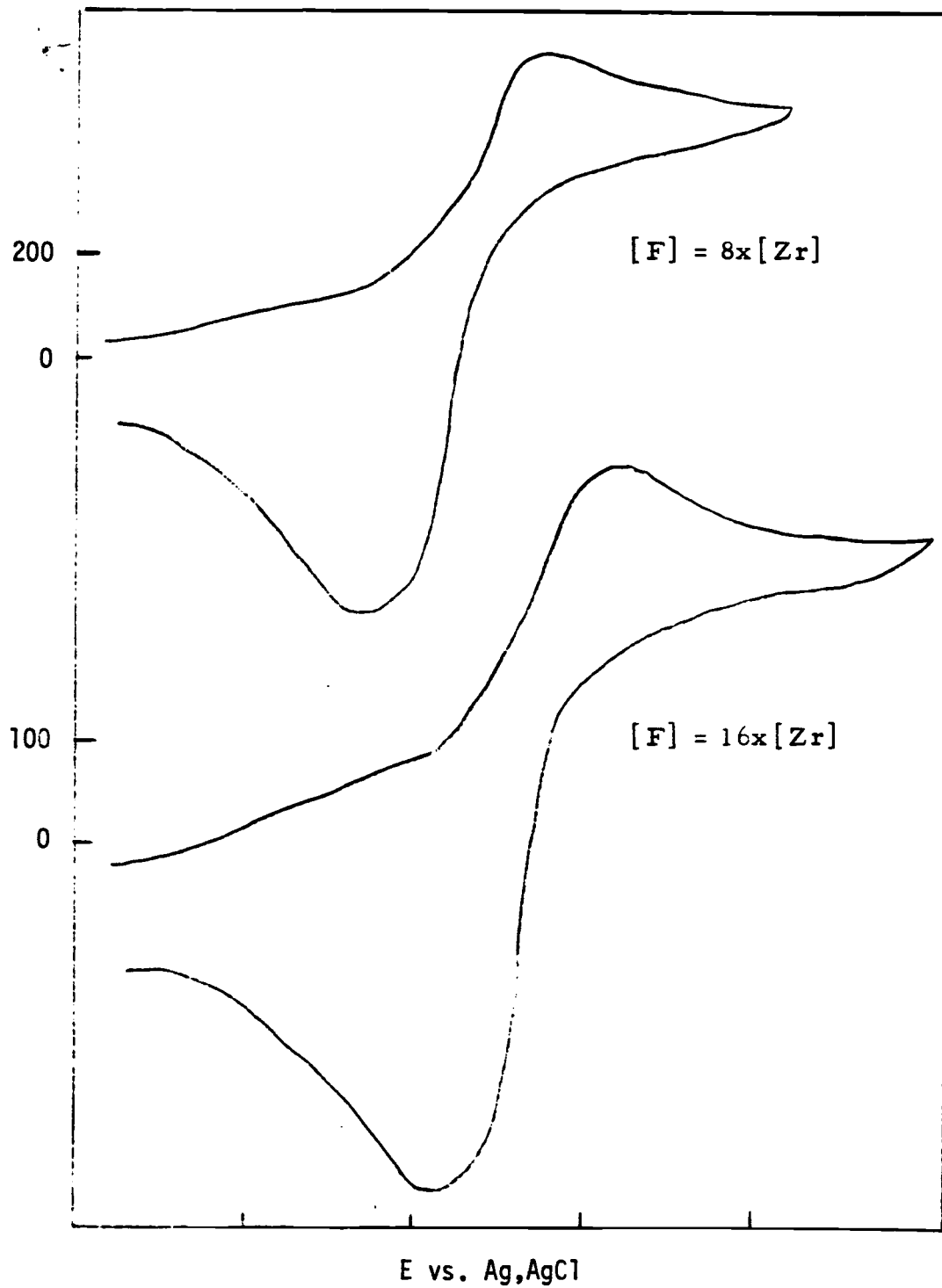
Figure 34. Cyclic voltammograms. 200 mv/sec
[Zr] = 1.7x10^{-4}
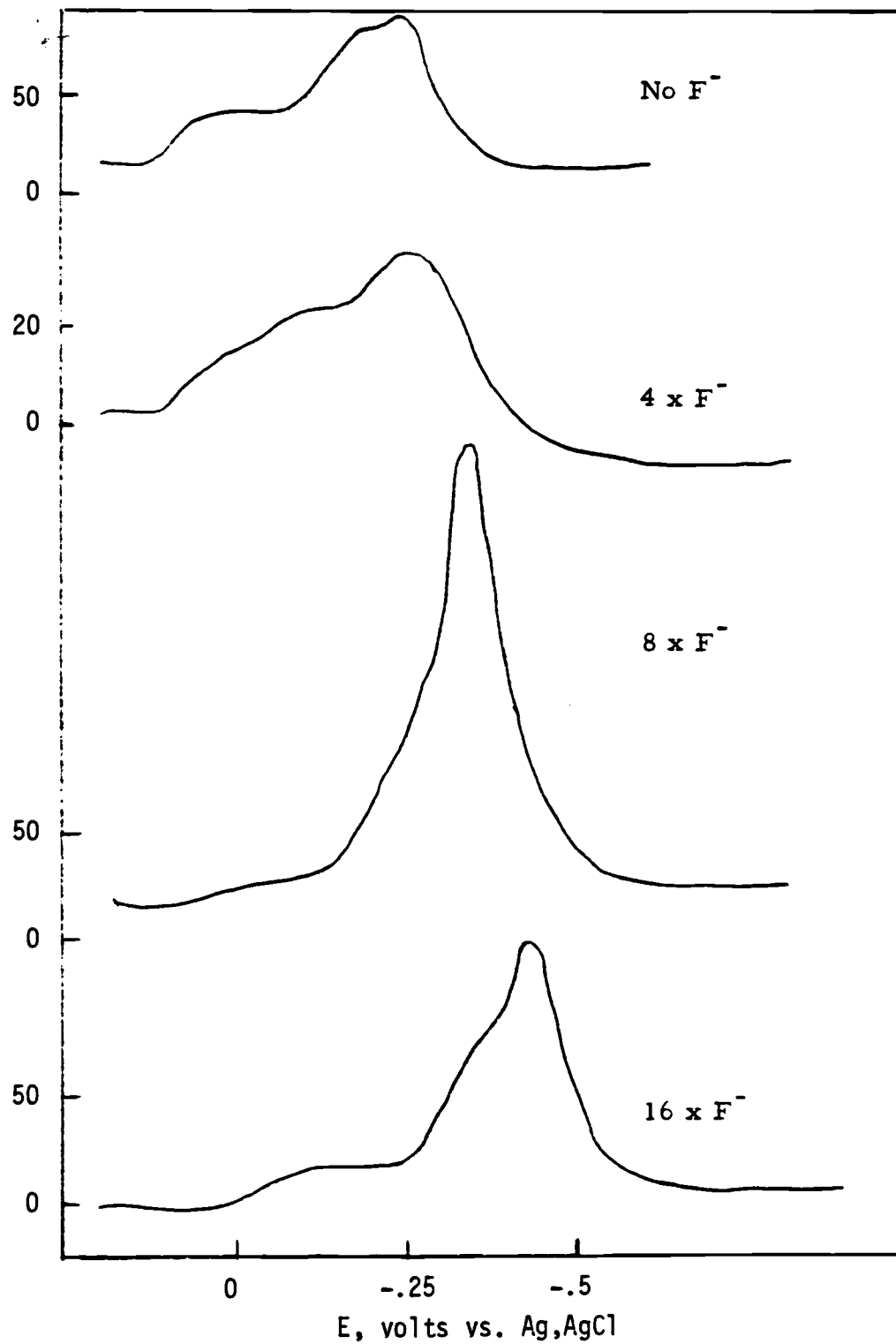
Figure 35. Differential pulse polarograms. 10 mv/sec
25 mv pulse height
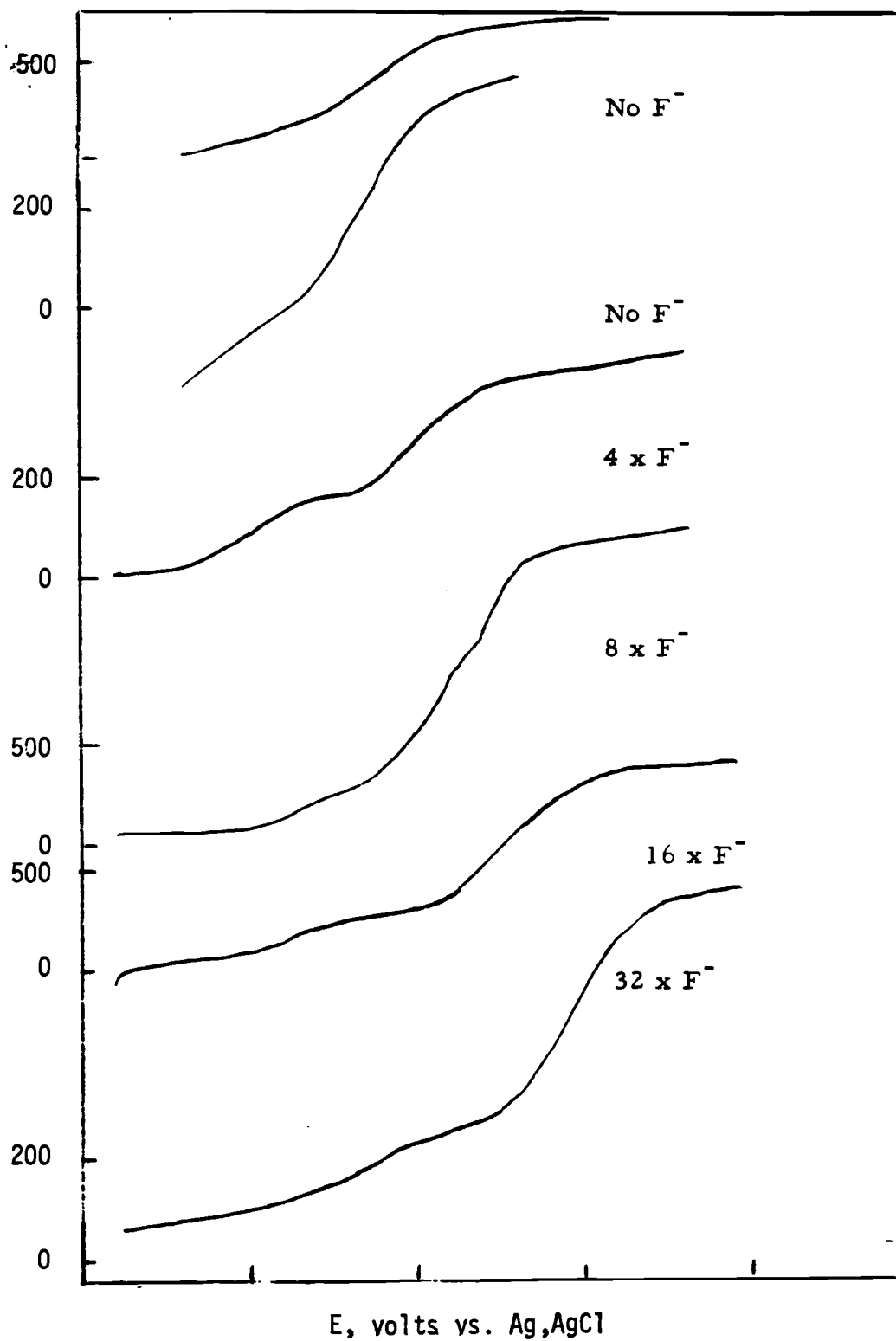
Figure 36. Normal pulse polarograms. 5 mv/sec
0.5 sec
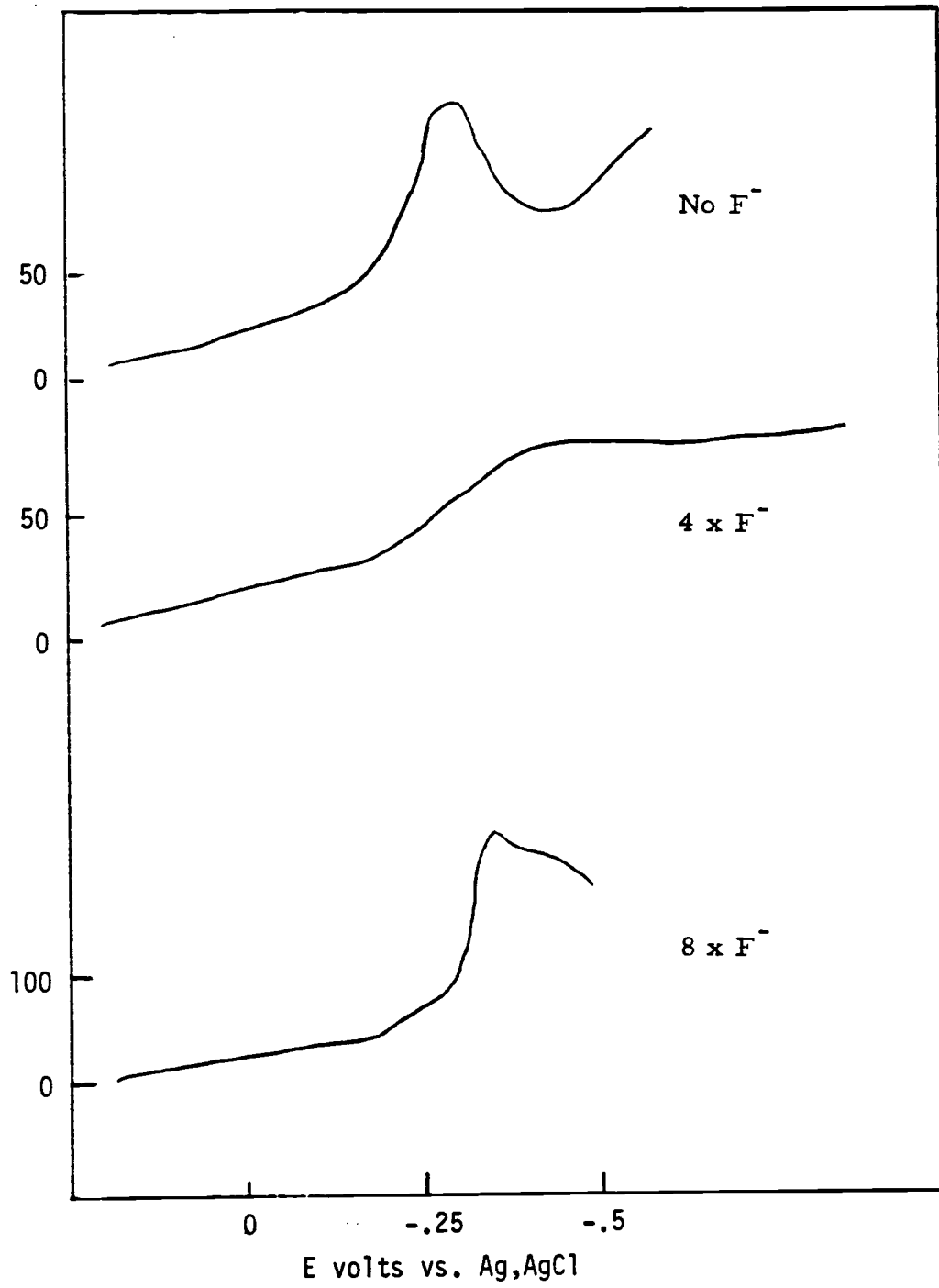
Figure 37. DC polarograms. 2 mv/sec

TABLE XVI. CYCLIC VOLTAMMETRY   TEMP. 1013K   200 mv/sec

Conc. F-	Conc. Zr^{4+}	E_{cp}, V	$E_{cp/2}$, V	E_{ap}, V	i_{cp}, μA	i_{ap}, μA
0	1.7×10^{-4}	-.350	-.212	-.100	300	450
4x[Zr]	1.7×10^{-4}	no peak	-.270	-.150	183	183
8x[Zr]	1.7×10^{-4}	-.435	-.330	-.160	600	507
16x[Zr]	1.7×10^{-4}	-.535	-.412	-.275	370	342

TABLE XVII. n VALUES FROM CYCLIC VOLTAMMOGRAMS   200 mv/sec

Conc. F-	$E_{cp}-E_{cp/2}$	"n"	$E_{cp}-E_{ap}$	"n"
0	.138	1.39	.250	0.77
4x[Zr]		- no cathodic peak -		
8x[Zr]	.105	1.82	.275	0.70
16x[Zr]	.123	1.56	.260	0.74

TABLE XVIII. DIFFERENTIAL PULSE POLAROGRAPHY   Conc. Zr = 1.7×10^{-4}

F- Conc.	Scan Rate	Pulse Height	E_p	$w\frac{1}{2}$	$w\frac{1}{4}$
No F-	10 mv/sec	25 mv	-.250	.185	.275
No F-	10	25	-.250	.175	.250
4x[Zr]	10	25	-.260	----	----
8x[Zr]	10	25	-.350	.090	.200
8x[Zr]	10	25	-.347	.107	.225
16x[Zr]	10	25	-.425	.145	.225
16x[Zr]	10	25	-.450	.140	.225

TABLE XIX. n VALUES FROM DIFFERENTIAL PULSE POLAROGRAPHY

F- Conc.	Scan Rate/ Pulse Ht.	$W_{1/2}$	"n"	$W_{1/4}$	"n"
No F-	10 / 25	.185	1.66	.275	1.67
No F-	10 / 25	.175	1.76	.250	1.84
8x[Zr]	10 / 25	.090	3.41	.200	2.30
8x[Zr]	10 / 25	.107	2.87	.225	2.04
16x[Zr]	10 / 25	.145	2.12	.225	2.04
16x[Zr]	10 / 25	.140	2.19	.225	2.04

TABLE XX.   NORMAL PULSE POLAROGRAPHY   Conc. Zr^{+4} = 1.7×10^{-4}

F- Conc.	Scan Rate	$E_{\frac{1}{2}}$, V	i_d, mA
No F-	5 mv/sec	-.187	.133
No F-	5 mv/sec	-.185	.317
4x[Zr]	5 mv/sec	-.005, -.260	.166, .233 (looks like two waves)
8x[Zr]	5 mv/sec	-.275	1.33
16x[Zr]	5 mv/sec	-.420	1.00
16x[Zr]	5 mv/sec	-.400	1.00
32x[Zr]	5 mv/sec	-.480	.917
32x[Zr]	5 mv/sec	-.500	.733

TABLE XXI. DC POLAROGRAPHY   Conc. Zr^{+4} = 1.7×10^{-4}

F- Conc.	Scan Rate	i_d, μA	$E_{\frac{1}{2}}$, V	$E_{cp/2}$, V
No F-	2 mv/sec	129	-.300	-.240
4x[Zr]	2 mv/sec	183	-.300	
8x[Zr]	2 mv/sec	237	-.352	-.325

Summary

The reduction of zirconium(IV) in fused equimolar NaCl-KCl occurs by a quasi-reversible two electron step according to the reaction:

$$Zr(IV) + 2e- \rightleftharpoons Zr(II) \tag{49}$$

The reaction has quite varied characteristics depending on the concentration of zirconium(IV). It is quasi-reversible between 2.5×10^{-5} and 1.9×10^{-4} mole fraction of zirconium, and presumably is above 1.9×10^{-4} mole fraction also. At concentrations approaching 2.5×10^{-5} mole fraction the deposition of zirconium dichloride is less, but still apparent. The deposition of zirconium dichloride complicates the measurements of formal potentials and n values.

Due to the quasi-reversibility and deposition the best that can be done is to obtain an estimate of the formal potential from all of the data available at each temperature.

The potential region that the formal potential values fall in is easy to determine from the polarographic curves. The region that the formal potentials fall in is quite close to that which Swaroop and Flengas report. It is quite far removed from the published values of Komarov, Smirnov, and Baraboshkin.

From these experiments it is plain that the reduction reaction of zirconium(IV) occurs at a much more positive potential than the studies by Komarov, Smirnov, and Baraboshkin have indicated. The potentials that Swaroop and Flengas published are close to the values obtained by this study, but the presence of zirconium(III) in the reduction scheme is not found. If the reduction scheme occured by two one

electron steps with identical formal potentials the polarographic waves would consist of a single wave with an n value of 1.47 (35, p. 172).

The n values found at low scan rates were larger than this value, indicating that the reaction is not a two step reaction. The deposition on the electrode is a strong indicator that zirconium(II) is the reaction product. With the n values that are the most reliable all being close to two, the reaction should be a two electron step.

The temperature dependance of the formal potential can only be estimated because of the complications encountered as the temperature is changed.

The formal potentials are shown in Table XXII.

TABLE XXII. Zr(IV, II) FORMAL POTENTIALS

Temperature	E^{o} vs Ag,AgCl	$E^{o'}$ vs Cl_2,Cl-
953K	-0.262	-1.316
973K	-0.228	-1.281
993K	-0.216	-1.269
1013K	-0.198	-1.251
1043K	-0.177	-1.229
1073K	-0.197	-1.249
1123K	-0.240	-1.292

The formal potential at 953K has a large degree of uncertainty. Observed values by the different techniques ranged from -0.215 V to -0.322 V vs the Ag,AgCl reference electrode. The values obtained at 973K, 993K, 1013K and 1043K are much more reliable and were more consistent. The values at 1073K and 1123K are doubtful.

The trend of increasingly negative formal potentials at and

above 1073K could be due to many reasons. The more probable reason is the complication due to deposition, low concentrations and high temperatures.

The formal potentials at 973K, 993K, 1013K and 1043K were used to determine an empirical equation relating the formal potential and the absolute temperature. The formal potential for the zirconium(IV), Zirconium(II) electrode reaction is:

$$E^{o'}_{Zr(IV,II)} = -2.012 + 7.5 \times 10^{-4}T \qquad (50)$$

To simplify comparing these results with those obtained by the Russians and the Canadians the standard electrode potentials determined at 1013K for the Zr(IV),Zr(II) electrode reaction are:

<div style="margin-left:2em">

Present work   -1.251 V vs Cl_2,Cl-

Canadians'   -1.494 V vs Cl_2,Cl-

Russians'   -2.011 V vs Cl_2,Cl-

</div>

However, comparisons of the values obtained are somewhat meaningless since the work done by both the Canadians and the Russians was predicated on the assumption the reactions involved are reversible. Potentiometric measurements require reversible reactions to obtain reliable formal potentials. The Canadians also assumed that Zr(III) would occur in the melt.

BIBLIOGRAPHY

1. Adams, Ralph N. Electrochemistry at Solid Electrodes. New York, Dekker, 1969.

2. Alabyshev, A. F., M. F. Lantratov, and A. G. Morachevskii. Reference Electrodes in Fused Salts, translated by Adam Peirperl. Washington, D. C., The Sigma Press, 1965.

3. Baboian, Robert, D. L. Hill, R. A. Bailey. Journal of the Electrochemical Society 112:1221-1224, (1965).

4. Barker, G. C. and A. W. Gardner. Z. Anal. Chem. 173, 79 (1960).

5. Baur, E. and Z. Ehrenberg. Elecktrokim 18:1002 (1912).

6. Blander, Milton. ed. "Molten Salt Chemistry". New York, Interscience Publishers, 1964.

7. Bockris, J. O'M, and A. K. N. Reddy. Modern Electrochemistry Vols. 1, 2. New York, Plenum Publishing Co., 2nd edition, 1976.

8. Burge, David E. Journal of Chem. Ed. 47:A81-A94 (1970).

9. Charlot, G. Selected Constants Oxidation-Reduction Potentials. New York, Paris, London, L. A., Pergamon Press, 1958.

10. Danner, G. and M. Ray. Electrochemica Acta 4:274, (1961).

11. Delahay, P. New Instrumental Methods in Electrochemistry; Theory, Instrumentation and Applications to Analytical and Physical Chemistry. New York, Interscience Publishers, 1954.

12. Dutrizac, J. E. and S. N. Flengas. "Pressure Temperature Measurements on Alkali and Alkaline Earth Complex Chlorides of Zirconium and Hafnium". Advances in Extractive Metallurgy Proc. Symp. Elsevier, Publishing Co., April, 1967.

13. Eon, C., C. Pommier, and J. C. Fondanaiche with collaboration by Fould, H. Bulletin de la Societe Chimique de France, 7:2574-2579 (1969).

14. Flengas, S. N. and T. R. Ingraham. Canadian Journal of Chemistry 35:1139-49 (1957).

15. Flengas, S. N. and T. R. Ingraham. Journal of American Electrochemical Society 106:714 (1959).

16. Fredericks, W. J., L. W. Shuerman and L. C. Lewis. An Investigation of Crystal Growth Processes. Final report Grant # AF-AFOSR-217-63 Project task 9762-02 January 31, 1966.

17. Hamer, W. J., M. S. Malmberg, and B. Rubin. Journal Electro-Chemical Society 103:8 (1956).

18. Hamby, D. C. and Allen B. Scott. Journal Electrochemical Society 115:704 (1968).

19. Heyrovsky, J. Chem. Listy 16:256 (1922).

20. Hills, G. J., L. Young, D. Inman, and J. O'M. Bockris. Ann. New York Acad. Sci. 79:803 (1960).

21. Janaf Thermochemical Tables. The Dow Chemical Company, Midland, Michigan.

22. Komarov, V. E., M. V. Smirnov, A. N. Baraboshkin. Trudy Inst. Electrokhim Akad. Nauk. SSR Ural' Filial Sverdlovsk 1:17 (1960).

23. Kudyakov, V. Ya and M. V. Smirnov. Trans. No. 6 Inst. Electrochem., Urals Branch USSR Academy of Sciences in Sverdlovsk (1965) translated by Consultants Bureau 227 W. 17th Street, New York, N. Y. 10011 (1966) p 15.

24. Kumins, Charles A. Anal. Chem., 19, 376 (1947).

25. Larson, E. M. and J. J. Leddy. Journal American Chemical Society 78:5983 (1956).

26. Laitinen, H. A., W. S. Ferguson, and R. N. Osteryoung. Journal of the Electrochemical Society 104:516-519 (1957).

27. Laitinen H. A. and C. H. Liu. Journal Amer. Chem. Soc. 80:1015 (1958).

28. Lister, R. L. and S. N. Flengas. Canadian Journal Chem. 42:1102 (1964).

29. Lister, R. L. and S. N. Flengas. Canadian Journal Chem. 43:2947 (1965).

30. Littlewood, R. Electrochemica Acta 13:270-278 (1961).

31. Maricle, D. L. and D. M. Hume. Journal of the Electrochemical Society 107:354-356.

32. Nicholson, R. S. and I. M. Shain. Anal Chem. 36:706 (1964).

33. Nicholson. R. S. Anal. Chem. 37:1351 (1965).

34. Parry, E. P. and R. A. Osteryoung. Analytical Chemistry 37(13):1634-1637 (1965).

35. Petcoff, D. G. Doctoral Dissertation. Corvallis, Oregon State University (1970).

36. Reinmuth, W. H. Analytical Chemistry 32:1891-2 (1960).

37. Reinmuth, W. H. Analytical Chemistry 33:1793-1794 (1961).

38. Sakakura, T. Denki Kagaku 34(9):780 (1966)(Japan).

39. Sawyer, D. T. and J. L. Roberts. Experimental Electrochemistry for Chemists. New York, John Wiley and Sons, 1974.

40. Senderoff and Brenner. Journal Electrochem. Soc. 101:31 (1954).

41. Smirnov, M. V. and V. Ya Kudyakov. Zashchita. Metal. i Oksidnye Pokrytiya, Korroziya Metal. i Issled. v obl. Elektrokhim. Akad. Nauk SSSR, otd. Obshch. i Tekhn. Khim., Sb. Statei p257 (1965) (Russ.)

42. Smirnov, M. V. and V. Ya Kudykov. Tr. Inst. Elektrokhim Akad. Nauk SSSR, Ural. Filial, 12:55 (1969) (Russ.)

43. Struss, A. W. and J. D. Corbett. Inorgan. Chem. 8:227 (1969).

44. Struss, A. W. and J. D. Corbett. Inorgan. Chem. 9:1373 (1970).

45. Sundheim, B. R. Fused Salts. New York, McGraw Hill Inc., 1964.

46. Suzuki, Tadashi J. Electrochem (Japan), 39:864 (1971).

47. Swaroop, B. and S. N. Flengas. Canadian Journal Chem. 42:1495 (1964).

48. Swaroop, B. and S. N. Flengas. Canadian Journal Chem. 43:2115 (1965).

49. Swaroop, B. and S. N. Flengas. Canadian Journal Chem. 44(2):199 (1966).

50. Turnbull, A. G. and J. A. Watts. Australian Journal Chem. 16:947 (1963).

51. Yang, L., and R. G. Hudson. Trans. AIME 215:589 (1959).

52. Yang, L., R. G. Hudson, and Chien-Yeh Chien. Phys. Chem. of Process Met. Part II. INST Sci. Publ., New York, 1961.

APPENDIX

Voltage Stepping Coulometry

In addition to the polarographic experiments a coulometric technique was developed to try to measure $E^{o\prime}$ values. Because of the deposition of the product and the large volatility of Zr(IV) the technique was not useful for this system. It would be useful for a system in which both reactant and product are soluble and non-volatile. It may be yet used for the zirconium(IV) system by employing very low concentrations and very fast electrolysis times. The technique is known as voltage stepping coulometry.

In this technique the potential of the working electrode, in a coulometric system, is started more positive than the expected reaction and is then scanned across the potentials at which the reaction will occur in a series of voltage steps. At each voltage step the coulombs are accumulated until the background rate is achieved. The background accumulation is then subtracted, and the resultant coulombs due to the reaction recorded. The sum of the coulombs from the step plus all previous steps is recorded. A wave results if the sums are plotted versus potential. The potential at Q equal to $Q_{max/2}$ is the standard electrode potential.

The equation relating the potential and the accumulated coulombs is derived by assuming only the oxidized species to be present at the start of the experiment, and inserting expressions relating the accumulated coulombs to the oxidized and reduced species concentrations into the Nerst expression.

$$[Ox] = [Ox_{Init}] - Q/nF \text{ Volume}$$

$$Mol_{Ox} = Mol_{OxInit} - Q_A/nF$$

$$[Red] = Q_A nF \text{ Volume}$$

$$Mol_{red} = Q_A/nF$$

$$E = E^o + \frac{RT}{nF}\ln \frac{Mol_{oxinit} - Q_A/nf}{Q_A/nF} \tag{51}$$

The initial number of moles of the oxidized species can be related to the final observed coulombs by the appropriate n value.

$$Mol_{ox} = Q_{total}/nF \tag{52}$$

therefore:

$$E = E^o + RT/nF \log\left(\frac{Q_T/nF - Q_A/nF}{Q_A/nF}\right) \tag{53}$$

cancelling:

$$E = E^o + RT/nF \log[(Q_T/Q_A) - 1] \tag{54}$$

At the potential where the accumulated coulombs equals exactly half of the total final coulombs Q_T/Q_A becomes two and the log term goes to zero, leaving E equal to E^o.

The method was tested on aqueous Fe^{+2}, Fe^{+3} systems and yielded reasonable results. The graph of total coulombs versus potential for a solution of Fe^{+3} in 0.5 M H_2SO_4 is shown in Figure 38. The formal potential from this curve is +0.669 V. The literature value (Charlot) is +0.68 V.
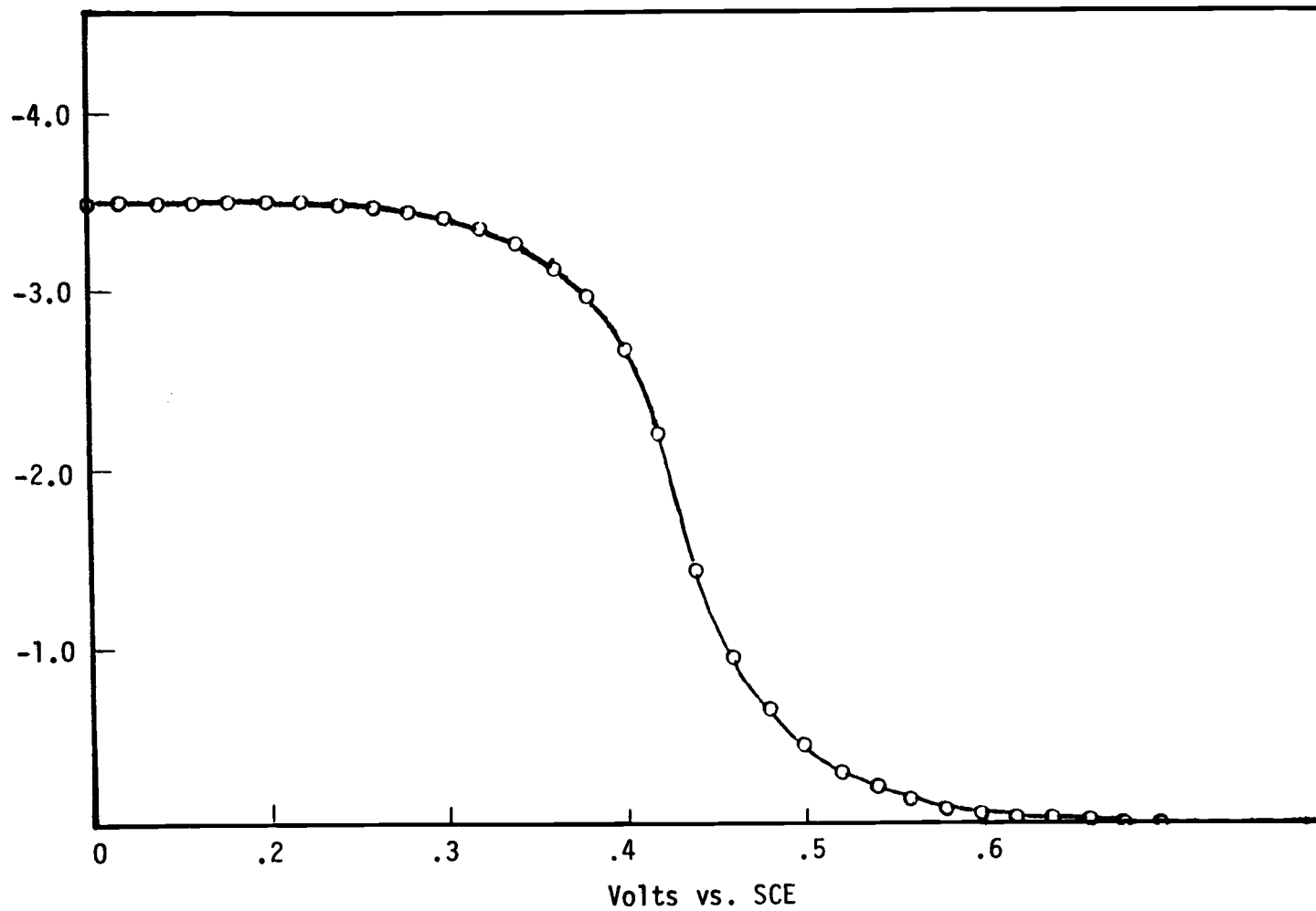
Figure 38. Stepping Coulemetric curve Fe in 0.5 M H_2SO_4
$E_{\frac{1}{2}}$ = 0.669 Volts vs. SHE

Experimental Procedure

The experiments were carried out with the PAR potentiostat and coulometer and a PDP 11/20 computer. The cell used is shown in Figure 39. The reference electrode used was a commercial SCE, the counter electrode a piece of platinum gauze and the working electrode a star-shaped platinum gauze tube. The solution of 3×10^{-4} molar Fe^{+3} in 0.5 M H_2SO_4 was vigorously stirred by bubbling with N^2.

The PAR coulometer and potentiostat were directly interfaced with our PDP 11/20 computer. The program used performed several functions. It applied the potential to the cell through the digital to analog converter and the external potential input to the potentiostat. The potential is easily changed by changing the digital number in the digital to analog converter. The program changes the potential each time the potential needs to be stepped. The program collects the number of coulombs from the coulometer every three seconds, and processes the numbers so that the rate of accumulation is determined. The potential is stepped to a new potential each time the coulomb accumulation has become constant. The number of volts stepped each time is selected at the start of the program. The initial and final potentials are also selected at the start of each experiment. The program halts the experiment and plots a graph of the sum of the coulombs versus potential.

The program consists of two related parts. First a binary program which converts a series of BCD numbers stored at a given location (hereafter known as LOCAT) to a binary integer to be stored at another location in core. Second, using this external

Cross Section

Glass Frits

2 way Valve

Nitrogen

Suction Flask

Platinum
Working
Electrode
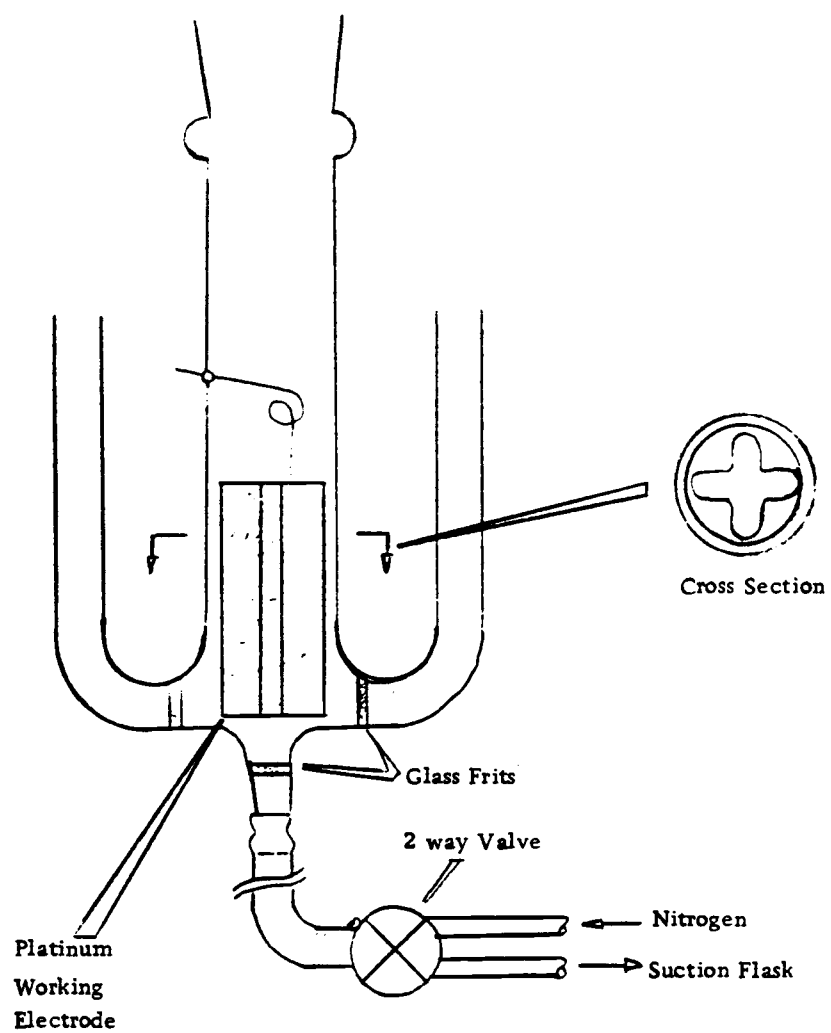
Figure 39. Cell for aqueous voltage stepping coulometry.

function, two other small machine language programs, and a BASIC program, the computer is programmed to control the coulometric experiment using the PAR coulometer. It accumulates data, makes decisions concerning this data, and sets the cell potentials.

EXF (110., LOCAT, DIGITS) BCD to Binary Conversion

This external function's BASIC format (PAL 11 BASIC) is as shown above. LOCAT is the first location in core of the BCD sequence to be converted.

DIGITS is the number of BCD numbers to be converted. The address is in octyl notation, and the digits in decimal notation. This program assumes that four BCD numbers are stored at each word location in core. The first four BCD numbers are converted to a binary integer and the binary integer stored at location 37510_8. Any remaining BCD numbers are then converted and stored at location 37512_8. The program has space saved at locations 37516_8 and 37520_8 for the BCD numbers. Any other location in core could also be used. The program will convert two, four, six or eight BCD numbers. The program is stored starting at location 37110_8, going to 37330_8, then jumping to 37500_8 and ending at 37530_8. The program skips from 37330_8 to 37500_8 to jump around the BASIC software multiply routine.

This routine works as follows: the program reads and saves the location and number of the BCD digits. It then places an ASCII semicolon in location Stor +4 to indicate the end of the ASCII string. The first BCD number is then converted by clearing all but the last four bits of the first BCD word. An octyl 60 is then added to this number, converting it to an ASCII number of the same value. This is stored as a byte in location Stor +3. The BCD word is again called,

and this time four Roll Rights are performed to bring the second BCD number into the first four bits. Again the higher bits are cleared, 60_8 added, and the ASCII number stored at Stor +2. A Swap Bytes instruction alters the BCD word, and the above routine is again called, with the next two ASCII numbers stored at Stor +1 and Stor. The subroutine ATOI (ASCII to Integer) is then called and the ASCII string is converted into a binary integer, and the value stored at location 37510_8. If there are any further BCD numbers, Locat is incremented to point at the next word location in core, and the above routine carried out, storing the integer at location 37512_8. These integers may then be used by a machine language program, or called by an external function and used by a BASIC routine.

Machine Language Programs

Two other small machine language programs are also used. One is stored starting at 60000_8 and the other at 61000_8. The first resets the coulometer to zero, outputs a selected voltage on the digital to analog converter, and starts the clock. The second waits for n (10 currently) clock interrupts, and then collects BCD data from locations 167774_8 and 167764_8. These locations are the external digital inputs. The computer freezes the display of the PAR as it does this. The PAR is connected to locations 167774_8 and 167764_8. The BASIC program is designed to collect the coulomb data and to do logical operations on it. It also increments the voltage in the digital to analog converter each time the accumulation of coulombs from 167774_8 reaches a constant rate.

At this point it also uses the time and final rate to determine the background, and subtracts this from the final accumulation. When the voltage reaches the input final potential the experiment is ended.
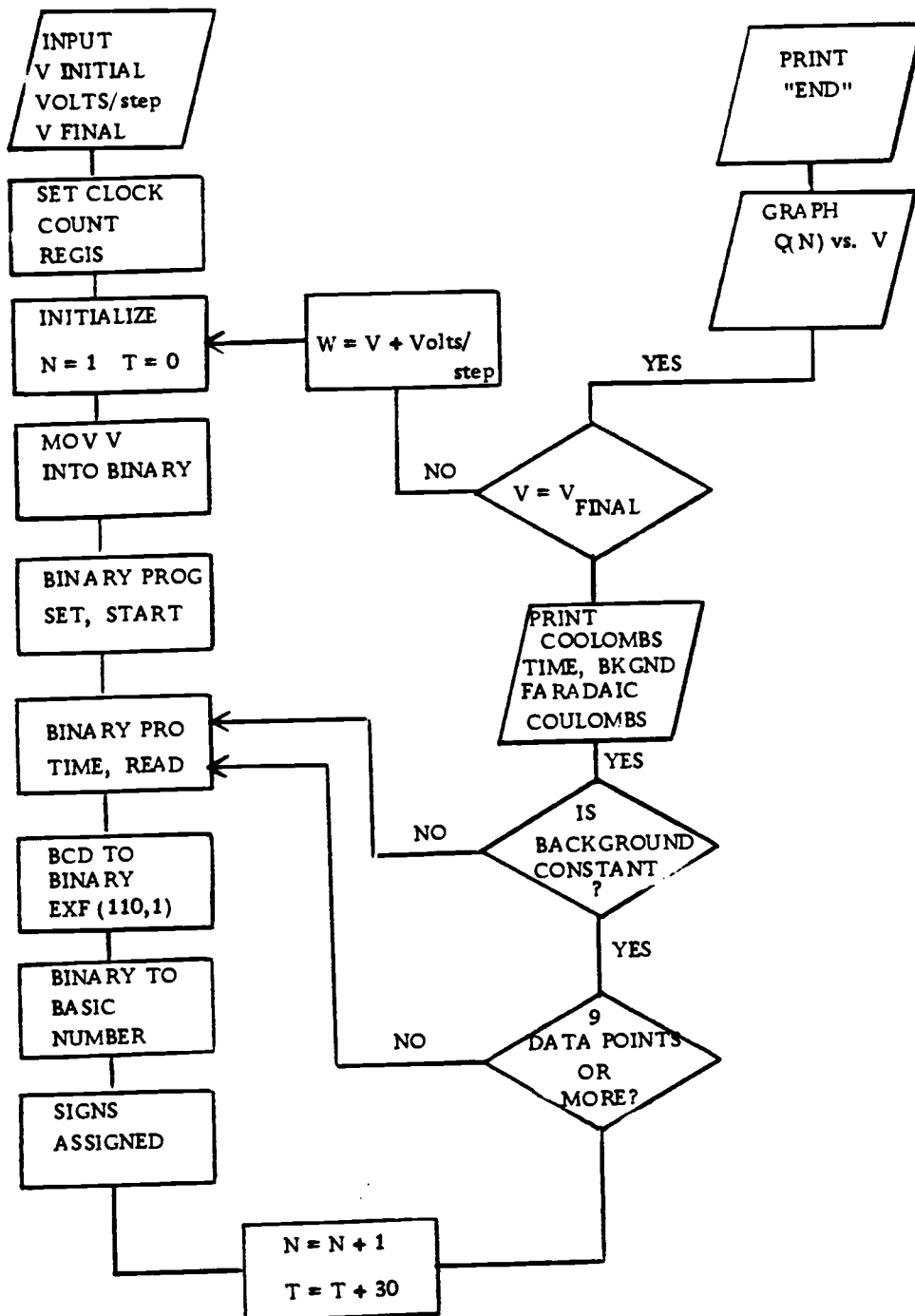
Figure 40. Basic program flow diagram.
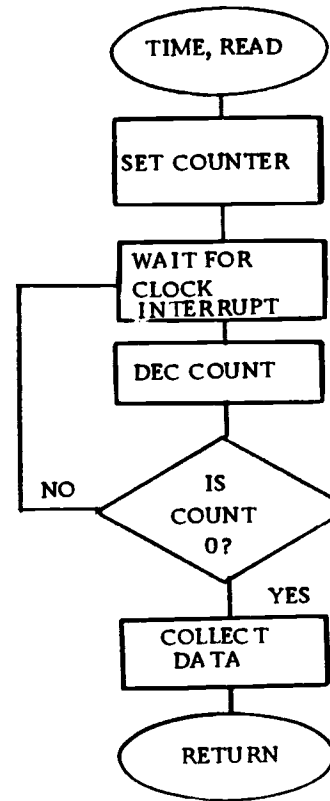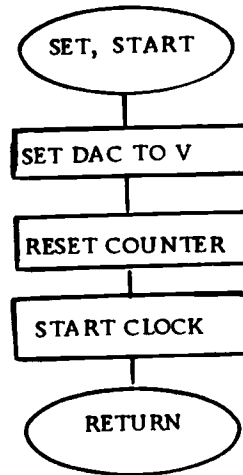
Figure 41. Binary programs.

BASIC PROGRAM

```
10 DIM Q (255),C(100),E(100),X(10),A(10),B(10)
20 PRINT "INITIAL POTENTIAL";: INPUT V
30 PRINT "VOLTS/STEP";: INPUT V1
40 PRINT "FINAL POTENTIAL";: INPUT V2
45 PRINT "TOTAL COUL","TIME","BACKGND COUL","FARADAIC COUL"
50 LET D=1 : LET E=0
60 LET V=(V-V1)*2048/2
70 LET V1=V1*2048/2
80 LET V2=V2*2048/2
90 LET F=EXF(9,172542,30000)
100 LET V=V+V1
101 LET N=1 : LET T=0
110 LET G=EXF(9,60026,V)
120 LET G=EXF(999,60000)
121 LET H=EXF(999,61000)
125 LET L=EXF(110,37516,6)
130 LET Q=EXF(80,37510,1,X)
135 LET G=EXF(80,37512,1,A)
136 LET U=EXF(80,167764,1,B)
137 IF B<0 GOTO 140
138 LET X=X*(-1)
139 GOTO 141
140 LET B=B+32650
141 IF B>15 GOTO 150
142 LET A=A*(-1)
150 LET Q(N)=X*10+(A-3)
155 PRINT Q(N)
160 LET T=T+30
165 LET N=N+1
170 IF N<9 GOTO 121
180 LET J=0
190 FOR I=0TO5
200 LET S=(Q(N-I-1)-Q(N-I-2))-(Q(N-I-2)-Q(N-I-3))
```

```
210 IF S<=0 THEN LET J=J+1
220 NEXT I
230 IF J<=4 GOTO 254
250 GOTO 121
254 LET N=N-1
255 LET P1=(Q(N)-Q(N-2))/60
256 LET P2=(Q(N)-Q(N-3))/90
257 LET P3=(Q(N)-Q(N-1))/30
258 LET P=(P1+P2+P3)/3
260 PRINT Q(N),T,T*P,Q(N)-T*P
270 LET C(D)=Q(N)
280 LET E(D)=E(D-1)+C(D)
290 LET D=D+1
300 IF ABS(V)<ABS(V2) GOTO 100
310 LET X=35/E(D-1)
320 FOR K=1 TO D-1
330 FOR I=0 TO X*E(K)
340 PRINT "";
350 NEXT I
360 PRINT"."
370 NEXT K
380 PRINT V1*2/2048'"VOLTS/LINE"
390 PRINT "END"
400 END
```

MACHINE LANGUAGE PROGRAMS

```
        . = 60000
        MOV # 172540,R2
        MOV # 176760,R2
        BIC # 2,@#DBRO
        BIS # 3,@#DBRO
        MOV # 0,(R3)
        MOV # 113,(R2)
        RTS PC

        . = 104
        .WORD CLK, 340
        . = 61000
        MOV # 10.,R1
        MOV # LOCAT, R2
TIME:   WAIT
        DEC R1
        BNE TIME
        BIC # 1,1766772
        MOV @# 176774, (R2)+
        MOV @# 176764, (R2)
        RTS PC
CLK:    RTI
```

EXTERNAL FUNCTION 110 in its form as it is on the computer can
be found in the book with the PDP-11 computer.